Concentrating PFAS waste streams

generated during drinking water treatment

MSc Thesis

Joséphine Annabelle van Ruiten

Delft University of Technology

TU Delft

Concentrating PFAS waste streams

generated during drinking water treatment

by

Joséphine Annabelle van Ruiten

Daily supervisor:	Dr. Ing. Kim Maren Lompe
Assessment committee:	Dr. Ing. Kim Maren Lompe, Dr. ir. Bas Heijman, Prof. dr. ir. Jan Peter van der Hoek and Dr. ir. Mar D.M. Palmeros Parada
Project Duration:	November 2022 - August 2023
Faculty:	Faculty of Civil Engineering, Delft

Cover:
The-
BrockenI-
naGlory

TU Delft

Preface

First of all, I would like to express my gratitude to the entire graduation committee for allowing me to research this topic. I am driven to work towards a pollution-free world and hence felt a great motivation throughout this entire project to perform my utmost best. Chemical pollution is silently destroying aquatic systems. Since it occurs below the water's surface, people are not confronted directly with the continuous destruction it is causing, which results in a reduced awareness of this problem. These chemicals not only harm the environment, but also have an an adverse effect on human health. These are mostly long-term and come to light when it is already too late. During the past 100 years, there has been an ongoing cycle of the production and prohibition of chemicals. This must be stopped by following the REACH protocols strictly.

I want to acknowledge my daily supervisor, Dr. Ir. Kim Lompe. Not only for the endless support and good advice but also for her enthusiasm and making the past few months very interesting and pleasant. I would also like to credit Dr. Ir. Bas Heijmans for his advice, great help, and for consistently being approachable. Moreover, I want to thank Prof. Dr. Ir. Jan Peter van Der Hoek for his valuable feedback and guidance and the drinking water company Waternet for making this research financially possible. Next, I am thankful to Dr. ir, Mar Palmeros Parada for our interesting discussions and her valuable feedback.

Additionally, I am grateful to the drinking water companies for giving me information about their treatment plants, sharing their data, and allowing me to take samples to perform my research, and also to the people of Waterlab at the Tu delft, Armand and Jasper especially, for aiding me to find my way in the lab.

Further, I am appreciative to my university friends for the continuous support and the shared moments of joy that enriched this period. Last but not least, I would like to express my heartfelt appreciation to my family and friends for providing me with a solid foundation of strength and encouragement.

Joséphine Annabelle van Ruiten
Delft, August 2023

Abstract

Globally, drinking water sources are polluted with poly- and perfluoroalkyl substances (PFAS). The toxicity and persistent properties of these industrial chemicals raised concerns about environmental and public health. As a result, drinking water companies are removing PFAS from drinking water using separation technologies. Anion exchange and nanofiltration membranes have been proven to be effective drinking water treatment methods for the removal of PFAS. However, these drinking water technologies produce large volumes of PFAS-containing waste streams, which poses new challenges for the drinking water industry. To prevent toxic PFAS from re-entering the environment, these waste streams must be treated. This can be done by PFAS destruction, however, due to the large volumes of the waste streams, this is very expensive and energy-intensive. Therefore, concentrating the drinking water waste streams before destruction is desired. This research examined existing PFAS-concentration technologies and compared their PFAS removal efficiency, volume reduction, and cost-effectiveness in concentrating the PFAS waste streams produced during drinking water treatment. These waste streams include the concentrate of nanofiltration and the brine from anion exchange. The analysed concentration technologies are foam fractionation, adsorption of PFAS onto DEXSORB+ and all-silica BEA zeolites, and nanofiltration.

Foam fractionation removes PFAS from the waste stream by injecting air bubbles. Two laboratory setups were made for the injection mechanism of the air bubbles. First, by passing pressurized air through an air stone, and second, by adding pressurized water (i.e. white water) to the waste stream. The adsorbents were tested in the laboratory by conducting equilibrium batch experiments with different adsorbent dosages. The laboratory experiments were performed on both drinking water waste streams. The performance of concentrating the anion exchange brine solution with nanofiltration membranes was evaluated with the use of IMS Design models, as it is already known that nanofiltration membranes remove more than 90% of the PFAS when the molecular weight cutoff of the membrane is below 270 Daltons.

Foam fractionation, with the use of pressurized air, and with the addition of a cationic surfactant, performed the best for the treatment of the nanofiltration concentrate with respect to the volume reduction and the PFAS removal efficiency. This technology was able to remove 76% of the total sum of PFAS (∑PFAS) while reducing the waste volume by 93.8%. DEXSORB+ and all-silica BEA zeolites removed 65%, and 62% of the ∑PFAS from the concentrate and achieved a volume reduction of 79%. For the anion exchange brine solution, nanofiltration performed best, removing more than 90% of the PFAS while reducing the waste volume by 90%. DEXSORB+ removed 62% of the ∑PFAS from the brine and adsorbed short-chain PFAS more efficiently compared to the other adsorbent. The better uptake of the short-chain PFAS is due to the cationic molecule added to the cross-linker of the DEXSORB+, which enhances short-chain PFAS removal due to the electrostatic interaction between the anionic head of the PFAS and this cationic element in the cross-linkers. All-silica BEA zeolite achieved a removal efficiency of 36% from the brine. Both adsorbents reduced the waste stream volume by 79%.

Foam fractionation removed less PFAS from the brine solution than from the nanofiltration concentrate, which can be because no surfactant was used for the brine solution as already 210 milliliters of foam was created out of one liter of the anion exchange waste stream. The adsorbents' removal efficiencies of PFAS from the nanofiltration concentrate were also higher than from the anion exchange brine solution. It was found that PFAS is removed less effectively with decreasing chain length due to its reduced hydrophobicity and hence higher solubility in water. Furthermore, PFAS with a sulfonic acid head were removed better than PFAS with a carboxylic acid head. This is because sulfonic acid is a more polar acid, which generally enhances the removal.

Separating PFAS from drinking water appeared to be more economically favorable with IX than NF. IX generated a waste volume equivalent to 0.5% of the incoming flow, which is substantially smaller

than the waste stream produced during drinking water production with NF, which is 20% of the influent flow. As a result, the concentration costs per volume of drinking water produced were significantly lower for the IX brine than for the NF concentrate. Concentrating the IX brine was the least expensive with FF. Nonetheless, this technology did not effectively reduce the waste volume or remove PFAS from the brine. DEXSORB+ was found to be more cost-effective for the IX brine treatment and removed more than all-silica BEA zeolite, which was the most expensive concentration technology. Nanofiltration reduced the waste volume of the IX brine the best while achieving the highest ∑PFAS removal efficiency. Despite that, this method was estimated to be more expensive. For the NF concentrate treatment, DEXSORB+ was found to be the least expensive concentration technology. Yet, foam fractionation achieved higher PFAS removal and higher volume reduction and was ranked second best based on its cost-effectiveness.

Overall, it was concluded that the removal efficiency, volume reduction, and cost-effectiveness of the different concentration technologies depends on the types of PFAS and other constituents present in the waste stream and the PFAS standards that must be reached.

Contents

List of Figures

List of Tables

Nomenclature

Abbreviations

Abbreviation	Definition
AC	Activated Carbon
AER	Anion Exchange Resins
DAF	Dissolved air flotation
CD	Cyclodextrin
DOC	Dissolved organic carbon
DWD	Drinking Water Directive
ECHA	European Chemical Agency
EFSA	European Food Safety Authority
EPA	Environmental Protection Agency
FF	Foam Fractionation
HDPE	High Dense Polypropylene
GAC	Granular Activated Carbon
IC	Ion Chromatography
IX	Ion Exchange
NF	Nanofiltration
NOM	Natural Organic Matter
MWCO	Molecular Weight Cut Off
PEQ	PFOA Equivalent concentration
PFAS	Poly- and perfluoroalkyl substances
PFSA	PFAS with sulfonic acid head
PFCA	PFAS with carboxylic acid head
PFAA	Perfluoroalkyl acids
REACH	Registration, Evaluation, Authorization and Restriction of Chemical
RIVM	Dutch National Institute for Public Health and the Environment
RPF	Relative Potency Factors
RO	Reverse Osmosis
TOC	Total organic carbon
TWI	Tolerable Weekly Intake
WTP	Water Treatment Plant
WWTP	Waste Water Treatment Plant
UV	Ultraviolet
∑PFAS	Sum of PFAS

Symbols

Symbol	Definition	Unit
$MWCO$	Molecular weight cut-off	[Da]
C_f	Enrichment factor	[-]
E_f	Enrichment factor	[-]
EC	Electrical conductivity	[mS/cm]
$EBCT$	empty bed contact time	[h]
$\%_{foam}$	Collected foam fraction	[%]
Q_f	foam flow	[m^3/h]
Q_w	waste flow	[m^3/h]
T_c	contact time	[min]
V	volume	[m^3]
Q_{air}	air flow	[m^3/h]
m_A	adsorbent mass	[kg]
ρ_B	bed density	[kg/m^3]
q	loading	[mg/g]
x	mass of adsorbed pollutant	[mg]
m	mass of adsorbent	[g]
C_0	initial concentration	[mg/L]
C_e	equilibrium concentration	[mg/L]
m	mass of adsorbent in the batch	[mg/L]
K_F	Freundlich constant	[$(ng/mg) \cdot (L/ng)^n$]
n	Freundlich adsorption intensity factor	[-]
ΔV	Achieved volume reduction	[%]
RE(%)	Removal efficiency	[%]

1

Introduction

Per- and polyfluoroalkyl substances (PFAS) have emerged as a pressing concern after extensive use over the past 40 years. Recent findings by the Dutch National Institute for Public Health and the Environment (RIVM) indicate that Dutch people ingest higher levels of PFAS through drinking water and food than the health-based limit set by the European Food and Safety Authority (EFSA).

PFAS is a collective name for certain non-degradable, synthetic substances that are harmful to plants, animals, and humans [1]. These substances are characterized by a chain of linked carbon and fluorine atoms, with the carbon-fluorine bond being the strongest bond known in organic chemistry, requiring 536 kJ/mol of energy to break [2][3]. The presence of these bonds, along with the PFAS chain's hydrophobicity and the functional groups' electronegativity, imparts heat, oil, and water resistance to PFAS molecules, making them extremely difficult to degrade [4] [5]. Exposure to PFAS poses serious health risks, including liver and kidney cancer, infertility, developmental issues in fetuses and children, and negative impacts on the immune and endocrine systems [6].

Conventional drinking water treatment plants are unable to efficiently remove PFAS from water. Thus, the implementation of new technologies is required [7]. Consequently, the drinking water industry needs to urgently address this problem. Nanofiltration membranes and anion exchange resins have proven effective in separating PFAS from drinking water [8] [9] and mitigating its harmful effects on human health. However, these solutions present a new challenge: the generation of highly concentrated PFAS-containing waste streams. Currently, these waste streams are discharged back into the environment, causing adverse effects on the environment and perpetuating the destructive PFAS cycle.

To break this cycle, the separated PFAS must be effectively eliminated. Various destruction technologies have been researched, but they are often expensive, energy-intensive, and chemical-intensive, particularly when dealing with large volumes and high flow rates [2][10][11]. Therefore, it is preferred to employ relatively low-cost technologies for further concentrating the PFAS waste before the final step of PFAS elimination [2]. While multiple concentration technologies exist for PFAS removal, they are relatively novel, and a comprehensive comparison is lacking. Additionally, their performance on the complex PFAS-containing waste streams generated during drinking water treatment and their efficacy in the treatment line encompassing PFAS separation, concentration, and destruction remains unclear. Promising concentration technologies for PFAS include foam fractionation, nanofiltration and adsorption on cyclodextrins or synthetic zeolites. Foam fractionation utilizes the attachment of PFAS to the air-water interface of air bubbles to separate them from aqueous solutions. Cyclodextrins and zeolites are novel adsorbent materials used in water treatment, capable of adsorbing PFAS onto their surfaces. Nanofiltration, a well-known treatment method, concentrates PFAS in the concentrate stream through size exclusion.

The main objective of this research is to compare different technologies for concentrating PFAS waste streams generated during drinking water treatment from nanofiltration membranes (NF) and anion exchange resins (IX) based on their costs, PFAS removal efficiency, and volume reduction. Additionally,

this study aims to assess and compare the effects of these different waste streams on the performance of concentration technologies. To achieve this objective, three sub-objectives have been defined.

Firstly, it is necessary to characterize the waste streams generated during the PFAS separation process using NF and IX in drinking water treatment. Understanding the specific characteristics of these waste streams is important, as they have the potential to impact the performance of concentration technologies. The second objective is to determine the volume reduction and PFAS removal efficiency achievable through known PFAS waste stream concentration technologies. This will be accomplished through different laboratory testing and the utilization of existing modelling software. The final objective is to determine and compare the costs of these technologies. Therefore, the aim is to estimate the associated costs involved in concentrating the different PFAS-containing waste streams. By considering the economic aspects, this research aims to identify and recommend cost-effective solutions for reducing the volume of PFAS waste streams before the final step of PFAS destruction.

The main research question:
What are cost-effective technologies for concentrating the PFAS waste produced during drinking water treatment with nanofiltration membranes (NF) and anion exchange (IX)?

The subquestions are:
1. What are the characteristics of waste generated through the use of NF and IX in the process of removing PFAS from drinking water?
3. Which waste volume reduction of NF and IX waste streams can be achieved by known PFAS concentration technologies?
4. Which costs are associated with the PFAS waste volume concentration for waste generated by NF and IX?

In the second chapter, the theoretical background information for this research is presented, this includes an explanation of what PFAS is and a discussion of various PFAS separation, concentration, and destruction technologies. The methodology followed during this research is described in chapter three. Chapter four presents the results obtained from the research, which will be further discussed in chapter five. Next, chapter six concludes the study by providing recommendations and highlighting the implications of the findings for water companies. This is followed by recommendations in chapter seven, identifying areas that require further investigation. Finally, in chapter 8, a reflection on this research is given.

2

Theoretical background

2.1. What is there to know about the "forever" chemical PFAS

2.1.1. The infinite journey of PFAS

Per- and polyfluoroalkyl substances are molecules that contain a carbon chain in which hydrogen (H) atoms are entirely or partly replaced by fluorine (F) atoms. The carbon-fluorine bond is the strongest bond known in organic chemistry and hence very difficult to degrade [4] [5]. They are heat, oil, and water resistant and therefore added to a variety of products such as firefighting foam, non-stick cookware, water-resistant fabrics, cosmetics, household products, food packaging, dental floss, and much more.

These anthropogenic chemicals are in circulation since 1950 [13] and enter our environment via various routes, see Figure 2.1. The main sources are fire fighting foams, industrial sites that discharge their waste to the surface water, landfill leachate, and wastewater treatment plants (WWTPs): wastewater is contaminated with PFAS from consumer products or industrial waste which can not be efficiently removed by traditional WWTPs [14][15][7]. The Belgian company Indaver, which manages the waste of industries and municipalities, is one of many Belgian companies with a permit to discharge PFAS directly to the surface water [15]. This permit allows a total discharge of 29000 ng/L for the sum of four different types of PFAS ($\sum$ PFOS, PFOA, PFNA, PFHxS) until 2026. Due to the ongoing PFAS pollution and the fact that these substances hardly break down, PFAS are ubiquitously detected in the environment.

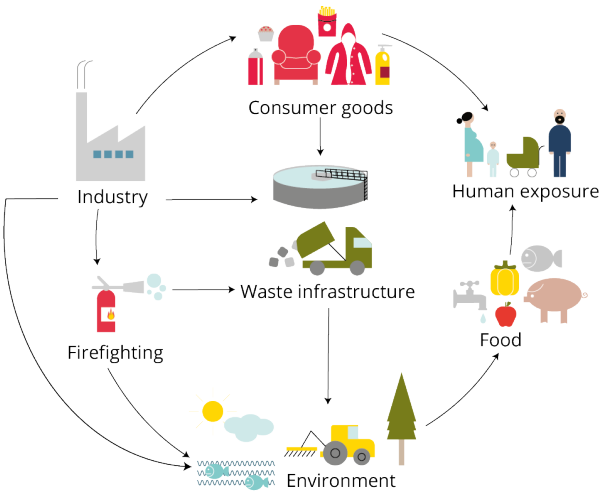

Figure 2.1: Pathways that lead to human PFAS exposure [12].

There is a great number of PFAS exposure pathways to humans. These sources are food, contaminated drinking water, the indoor environment (dust, air), and consumer goods [16][12]. Some PFAS are highly soluble in water, leading to their accumulation in rivers, groundwater, oceans, and hence the drinking water resources [16]. Furthermore, according to the European Chemicals Agency (ECHA), some PFAS can accumulate in living organisms [6] and in this way, PFAS can enter the food chain [17]. Especially the marine food chain due to PFAS accumulation in the ocean [16]. The median PFAS content in fish tested by the US EPA between 2013 and 2015 was 11,800 ng/kg [18], which is approximately 2,600 times higher than the allowed limit of 4.4 ng/L in water, which was set up by the RIVM. PFAS also enters the food chain through commonly used insecticides [19]. S. Lasee et al. (2022) de-

tected that, in the US, 6 out of the 10 tested insecticide formulates contained PFOS (3.92-19.2 mg/kg) [19]. According to the ECHA, various studies in the EU have shown that the average blood serum concentration of PFOA in people in the EU is 3.5 ng/ml [20]. In 2022, the RIVM found that the Dutch people are ingesting more PFAS through food products and water than the provisional health-based guideline [21]. Therefore, water companies start removing PFAS from drinking water and above that also want to prevent re-contamination of the environment with PFAS.

2.1.2. Classification and properties

PFAS is a term that refers to a group of man-made chemicals that contain fluorinated carbon atoms. Currently, more than 4700 unique PFAS are in use [22] [9]. It is important to understand how they are classified. All PFAS are synthetic and difficult to break down. There are two main groups of PFAS: polymers and non-polymers. Polymers are molecules that exist out of a repeating pattern of multiple identical smaller molecules (monomers) [23]. This group is divided into three subgroups: side-chain fluorinated polymers, polymeric perfluoropolyethers, and fluoropolymers [24]. Non-polymer PFAS are most commonly detected in the environment, in humans, and in biota [23] and hence obtain more attention within this research. There are two subgroups within the non-polymer group: poly- and perfluoroalkyl compounds. Polyfluoroalkyl compounds only have partially fluorinated carbon chains while perfluoroalkyl compounds have fully fluorinated carbon chains [22]. Some polyfluorinated substances are 'precursors', these polyfluorinated substances can transform into PFAAs which are a group of perfluorinated compounds as can be seen in Figure 2.2. These are more persistent forms of PFAS. PFAAs are also referred to as 'terminal PFAS' because no further degradation products will be formed under environmental conditions [23].

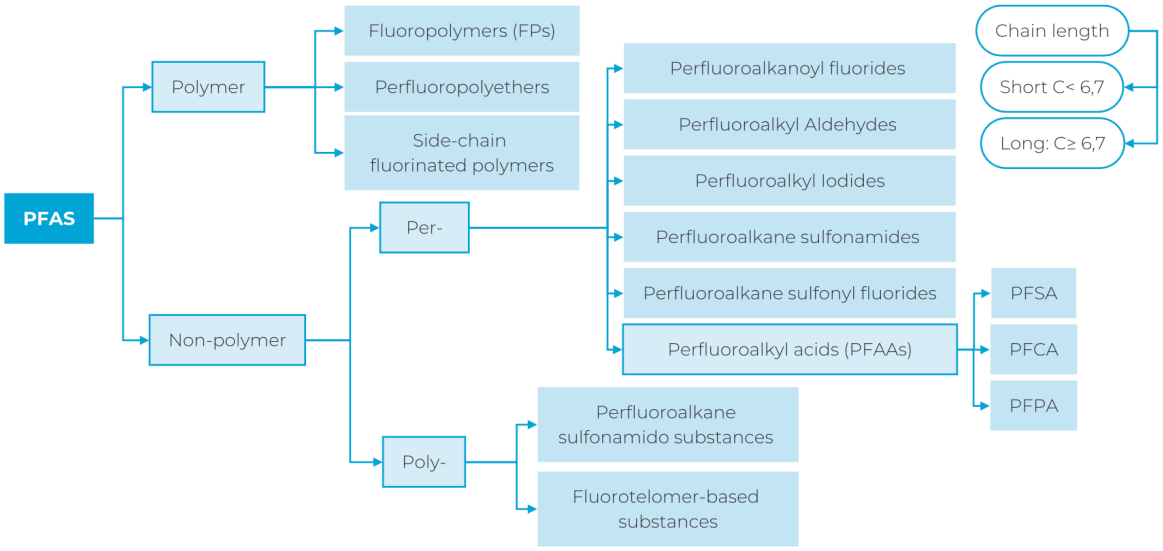

Figure 2.2: Classification of PFAS - figure made by author

The perfluoroalkyl substances are divided into six subgroups of which perfluoroalkyl acids (PFAAs) is the largest group. PFAAs can be divided again into three groups distinguished by the functional group of the PFAS: sulfonate (PFSA), carboxyl (PFCA), and phosphate (PFPA), as can be seen in Figure 2.3. The sulfonic acid group (PFSA) is a stronger and more polar acid compared to the carboxyl group (PFCA) [10]. The PFSA group includes the well-known PFAS: perfluorooctane sulfonic acid (PFOS) and perfluorohexane sulfonic acid (PFHxS) also referred to as C8 PFSA and C6 PFSA, respectively. PFCA group includes the well-known PFAS: perfluorooctanoic acid (PFOA) and perfluorononanoic acid (PFNA), also known as C8 PFCA and C9 PFCA, respectively. PFOA and PFOS are the most commonly detected types of PFAS.

It is important to note the distinction between ”long” and ”short” chain PFAS. This is based on the length of the fluorinated carbon chain. Only for PFCA, PFSA, and their precursors, a distinction is made. Long-chain refers to [23]:

- PFCAs: seven or more carbons are perfluorinated (C≥7)
- PFSAs: six or more carbons are perfluorinated (C≥6)

Short-chain refers to [23]:

- PFCAs: less than seven carbons are perfluorinated (C<7)
- PFSAs: less than six carbons are perfluorinated (C<6)

PFAS owns its stability due to the C-F bonds. Therefore, the longer the chain, the more chemically and thermally stable the PFAS is [25][22]. However, other factors may also influence the stability of PFAS, such as oxygen bridge bonds, and cyclic or branched forms [22]. The chain of the PFAS is nonpolar and thus water-repellent. A longer PFAS chain also leads to a higher hydrophobicity. Short-chain PFAS have greater mobility as the aqueous solubility increases with decreasing hydrophobicity [25]. At pH levels relevant to water treatment, most PFAS heads are anionic [8]. Hence, the head is hydrophilic. This makes the PFAS amphiphilic.

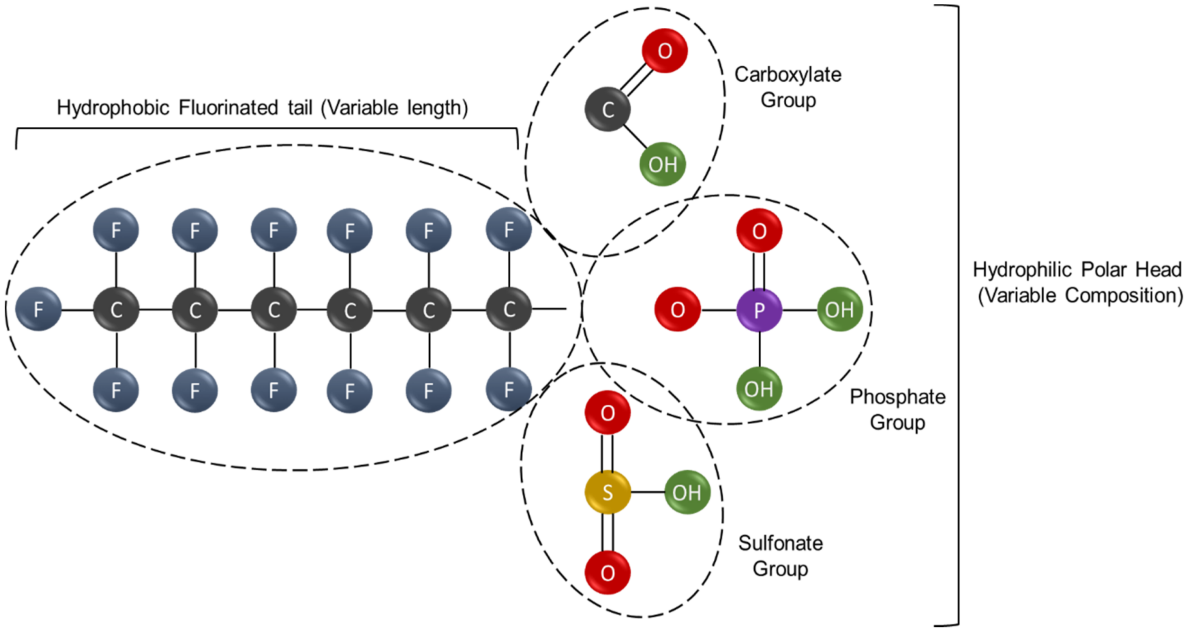

Figure 2.3: Properties of PFAS [26]

In the 1950s, DuPont and 3M introduced PFAS on the global market. In 2015, the first generation of PFAS: PFOA, and PFOS, were voluntarily phased out by its major producers under the 2010/15 PFOA Stewardship Program because of concerns related to bioaccumulation and toxicity [27]. As a result, DuPont began producing GenX in the early 2010s as a substitute for PFOA. GenX is the tradename of the chemical compound hexafluoropropylene oxide (HFPO) dimer acid and its ammonium salt. 3M replaced PFOS (C8) with perfluorobutanesulfonic acid PFBS (C4). However, the EPA found that GenX is hazardous at much lower levels of exposure than PFOA and PFOS [28]. Furthermore, ECHA has recognised PFBS and GenX as substances of very high concern (SVHC) [29]. The presence of these specific PFAS substitutes in the environment is expected to increase over the coming years. The SVHC identification was based on their persistence, mobility, and toxicity.

2.1.3. Environmental and human health impact of PFAS

The concerns about the impact of PFAS on human health and the environment have grown in recent years. Studies have linked exposure to certain types of PFAS to a range of adverse health effects, such as immune system dysfunction, interference with placental function, induce oxidative stress, altered thyroid function, liver dysfunction, irregularities in lipid and insulin metabolism, renal disease, negative impacts on reproduction and development, including low birth weight and delayed development in infants and children, as well as increased risk of cancer [30] [31]. PFAS has also been associated with declines in fertility and fecundability. Studies have shown that the combined effects of PFAS exposure are linked to a 30% to 40% lower chance of becoming pregnant within one year and delivering a living baby. The persistent nature of PFAS is attributed to its chemical structure, which makes it resistant to degradation in the human body. As a result, PFAS can accumulate over time. The estimated half-life of PFOA and PFOS in humans is approximately 3.5 and 4.8 years, respectively [32].

Also in the environment, PFAS do not break down easily and hence, PFAS accumulate in water, soil, and wildlife over time. Studies have shown that PFAS is found in water sources, including groundwater and surface water, as well as in the soil and air. The halftime of PFOS and PFOA in water (at 25 degrees Celsius) is 41 and 92 years, respectively [33]. The presence of marine PFAS pollutants can have harmful impacts on gas exchange and disrupt the ocean's carbon cycle. This can contribute to an increase in greenhouse gas emissions, ultimately affecting global warming and climate change [34]. PFAS negatively affects the growth and photosynthesis of phytoplankton, the development, and reproduction of zooplankton, marine biological processes, and the overall storage of carbon in oceans [34]. Phytoplankton utilizes sunlight, carbon dioxide, water, and nutrients to generate oxygen and nutrients for other organisms via the process of photosynthesis [35]. Phytoplankton is responsible for producing up to 50% of the oxygen we breathe [35]. According to a NASA study, the number of Diatoms, the largest species of phytoplankton, has been declining worldwide at a rate of 1% per year from 1998 to 2012 [36].

2.1.4. PFAS regulations

European Drinking Water Directive

Since January 2021, a new European Drinking Water Directive (DWD) has come into force. This DWD also addresses the human intake of PFAS. By January 2026, Member States must have implemented the necessary steps to ensure that water intended for human consumption complies with one or both PFAS parametric values of the DWD. This directive states two maximum concentrations of PFAS. The first is a maximum concentration of 100 ng/L for the "Sum of PFAS". The "Sum of PFAS" is a group of 20 types of PFAS[1] that have, according to the DWD, a risk in connection to human drinking water consumption. The second is a maximum concentration of 500 ng/L of "PFAS total", which involves all PFAS. According to an initial assessment of the RIVM, Dutch drinking water concentrations are lower than both these parameter values [37].

European Food Safety Authority

After the DWD was made in 2021, new scientific data about human health risks became available which led to the new advice to lower the concentrations even more. The European Food Safety Authority (EFSA) has published a health-based limit value, the so-called 'Tolerable Weekly Intake (TWI)', for the sum of four different types of PFAS ($PFAS_4$ = PFOS, PFOA, PFNA, PFHxS) which is 4.4 ng/kg body weight per week [37] [38]. This is the total quantity of $PFAS_4$ that a human can ingest safely during their entire live [39].

RIVM, Netherlands

The TWI value of the EFSA is used by the RIVM to calculate the drinking water guideline value. Three factors were taken into consideration when determining this value. First, people are also exposed to PFAS via other sources such as food, air, and consumer products. The RIVM used the starting point of the World Health Organisation which estimates that 20% of human PFAS ingestion comes from drinking water. Secondly, it is assumed that a person with a weight of 70 kg consumes two liters of drinking water a day. Third, the advice of RIVM is to consider a larger group of PFAS and not just

[1] PFCA (perfluoro carboxylic acid) and PFSA (perfluoro sulphonic acids), both with chain length 4 to 13.

Table 2.1: Relative Potency Factors of the 23 different PFAS types (RIVM, 2021) and their carbon chain length.

PFAS	Carbon chain	RPF	PFAS	Carbon chain	RPF
PFBS	C4	0.001	PFDA	C10	10
PFPeS	C5	0.6	PFUnDA	C11	4
PFHxS	C6	0.6	PFDoDA	C12	3
PFHpS	C7	2	PFTrDA	C13	3
PFOS	C8	2	PFTeDA	C14	0.3
PFDS	C10	2	PFHxDA	C16	0.02
PFBA	C4	0.05	PFODA	C18	0.02
PFPeA	C5	0.05	GenX	C6	0.06
PFHxA	C6	0.01	ADONA	C6	0.03
PFHpA	C7	1	6:2 FTOH	C8	0.02
PFOA	C8	1	8:2 FTOH	C10	0.04
PFNA	C9	10			

$PFAS_4$ from EFSA. Therefore, the RIVM compared the toxicity of 23 individual types of PFAS to PFOA and expressed this in PFOA equivalent concentrations (PEQ). The 'Relative Potency Factors (RPFs)' are used to quantify the relative potencies of different types of PFAS concerning an effect and can be used to express combined exposures of multiple PFAS in terms of the exposure value of the chosen index substance which is PFOA. The RPF method recognizes that the different PFAS are not all equal. The RPF method also takes into account the possibility that multiple PFAS may cause an effect and considers a maximum of 23 PFAS instead of 4, therefore the risk of health effects is less likely to be underestimated. RPF lies between 0.001 and 10 which means the 23 different types of PFAS can be 1000 times less toxic and 10 times more toxic than PFOA. The relative potency factors of the 23 different types of PFAS are given in table 1. Finally, the RIVM decided on a drinking water guideline of 4.4 ng PEQ/L [37] [38].

The RIVM has also established **surface water quality standards** for the concentration of PFOA, PFOS, and GenX. This action was taken in response to the EFSA's findings, which indicated that these substances are more toxic than previously thought. These standards are risk limits, with the set values being 0.3 ng/L for PFOA, 10 pg/L for PFOS, and 10 ng/L for GenX [40].

Denmark, Sweden, and Germany

In 2021, the Danish Environmental Protection Agency established maximum levels for several PFAS in drinking water, food, and consumer products. The maximum level for drinking water is 2 ng $PFAS_4$ /L for four different types of PFAS [41]. The Swedish National Food Agency set the drinking water limit to 4 ng/L for $PFAS_4$ and lower than 100 ng/L for $PFAS_{21}$ which includes: C_{4-13} PFSAs, C_{3-13} PFCAs, and 6:2 FTS. The new German Drinking Water Regulations must enter into force in Germany by January 2023 at the latest. This regulation specifies two limit values. First, the total of 20 different types of PFAS (C_{4-13} of PFSAs and PFCAs) should be less than 0.1 µg/L. Second, the total PFAS-4 concentration, which includes PFOA, PFOS, PFNA, and PFHxS, should be less than 0.02 µg/L.

Table 2.2: PFAS concentration standards per country in drinking water.

Guidelines and regulations per region			
Region	Concentration	Unit	Types of PFAS
EU DWD	100	ng/L for "Sum of PFAS"	PFCA and PFSA: C4-13
EU DWD	400	ng/L for "Total PFAS"	The total of all PFAS
RIVM	4.4	ng PEQ/L	PFOA equivalent concentration
Sweden	4	ng/L for $PFAS_4$	PFOS, PFOA, PFNA, PFHxS
Denmark	2	ng/L for $PFAS_4$	PFOS, PFOA, PFNA, PFHxS
Germany	100	ng/L for sum of PFAS	PFCA and PFSA: C4-13
Germany	20	ng/L for $PFAS_4$	PFOA, PFOS, PFNA, PFHxS.

The PFAS concentration standards in drinking water differ between countries. An overview of the different guidelines is given in table 2.2. It is important to note that the treatment cost of removing PFAS from drinking water largely depends on the treatment goals, which are mostly based on governmental guidelines [2].

REACH, European Union

Every year, thousands of new chemicals are coming onto the market. Typically, the health effects of a chemical are only researched after they are already on the market. REACH (Registration, Evaluation, Authorization, and Restriction of Chemicals) was established by the European Union in 2007 to ensure chemicals will be tested before entering the market [42]. It is a European regulation on the production and trade of chemical substances. The aim is to protect European citizens against the toxic chemicals in various products, such as PFAS. In a recent experiment, more than 300 chemicals were found in human bodies that were previously absent in the bodies of our grandparents [43]. REACH describes what companies and governments must adhere to [44]. It states that chemicals must be tested and registered in advance before a substance can be put on the market [45]. However, the chemical industry did not agree with this plan and therefore started lobbying with the European Commission [46]. Lobbyists tried to convince the Commission that it would lead to an increase in unemployment in Europe because REACH would mean an end to the chemical industry in the EU [46]. REACH planned to test all chemicals that are circulating in the EU, for environmental and health risks [47]. According to the EU inventory, there are about 100,000 chemical products worldwide [48]. Yet, instead of 100,000 products, fewer than 30,000 substances were included in the REACH dossier [6]. This means there are around 70,000 products in circulation without being tested and are therefore potentially dangerous. This also led to the fact that the human and environmental health risks of PFAS remained unknown to the public until now.

Researchers at the University of California San Francisco analysed previously undisclosed industry documents and found evidence that the chemical industry had knowledge of the harmful health effects resulting from exposure to PFAS and actively suppressed this information [49]. PhD. prof. Tracey J. Woodruff states that these documents are evidence that the chemical industry knew about the PFAS dangers and failed to let this known to the public, regulators, and even their own employees [49]. If REACH was followed correctly, regulations against PFAS might be made earlier.

From February 2023 onwards, 16 years later than the establishment of REACH, perfluorinated carboxylic acids with chain length nine to fourteen (C9-14 PFCAs), their salts and precursors are restricted in the European Union. This restriction was proposed by the German and Swedish authorities. Furthermore, Norway has proposed a restriction on PFHxS (C6, PFSA), its salts and related substances. Next, Germany has proposed a further restriction for PFHxA (C6, PFCA), its salts and related substances. The European Commission together with the EU countries will decide on the restriction for these substances in due course. Finally, the national authorities of Germany, Denmark, the Netherlands, Norway and Sweden are proposing a restriction that covers a wide range of PFAS uses. These countries submitted their proposal in January 2023. ECHA's scientific committees will now evaluate this proposal.

2.1.5. Dutch water quality

A study conducted by the EFSA concluded that parts of the European population exceed the PFAS tolerable weekly intake (TWI) [50]. Also in the Netherlands, the RIVM found that the Dutch people ingest more PFAS than the health-based limit value of 4.4 ng/kg body weight per week derived by EFSA [37]. The mean lower bound exposure, which reflects the most optimistic assumptions, was estimated by the RIVM to be 5.9 ng PEQ/kg body weight per week through food and drinking water produced from surface water [51]. It is important to note that the contribution of PFAS ingestion is greater from food than from drinking water (more than 70%) [38][51]. WHO estimated that 20% of ingested PFAS comes from the consumption of drinking water.

Between 2015 and 2021, 53% of all Dutch drinking water samples made of surface water exceeded the Dutch drinking water guideline when only the EFSA-4 PFAS (PFOA, PFOS, PFNA, PFHxS) were included [37]. When considering all PFAS types, this value increases to 57%. 8% of the drinking water

samples made from surface water exceed a concentration of 22 ng PEQ/L [37]. Dutch drinking water which is produced from surface water contributes 30 to 37% of the EFSA TWI. This is a larger contribution to the EFSA TWI than the estimated 20% according to WHO guidelines [38]. In Dutch surface water, PFNA, PFUnDa, PFDA, PFDoDA, PFOA, and PFOS are mainly present [51].

2.2. PFAS separation technologies

2.2.1. Granular activated carbon (GAC)

GAC is a possible treatment method for the removal of PFAS from water. Activated carbon (AC) is an effective adsorbent for the removal of organic micropollutants (OMP) because it is a highly porous material and hence it provides a large surface area for adsorption [52]. AC is made from organic materials with high carbon contents such as wood, coconut shells, and lignite [52]. The carbon adsorbs all non-water-soluble organic substances from the water onto its solid matrix [53]. As a result, the removal of PFAS occurs through the adsorption of the hydrophobic fluorinated chain of the PFAS onto the GAC [53], and hence the longer the fluorinated chain the better the PFAS will be removed from the water. The operating time of the GAC filters influences the PFAS removal efficiency. Recently installed GAC filters with low loading[2] can achieve removal efficiencies of 92 to 100% for five frequently detected types of PFAS [54]. However, the sorption affinity of short-chain PFAS is notably lower and thus leads to a lower removal efficiency [55][56]. Furthermore, GAC will also adsorb other hydrophobic compounds, such as natural organic matter (NOM), which can lead to competition for adsorption sites. NOM is always present in surface water, and mostly at concentrations in the mg/L range while PFAS are present in much lower concentrations (ng/L range). NOM is taken up by the GAC and takes away the adsorption sites for PFAS. After a period of time, PFAS breakthrough occurs and thus the desired water quality is no longer achieved and the GAC filter must be reactivated. This limits the lifetime of the GAC filter. Regeneration and reuse of GAC are energy-intensive and expensive (0.73€/kg) [2] and hence, the drinking water treatment goals have a significant impact on the operation costs of GAC. A Swedish study conducted by N. Belkouteb et al. (2020) showed that the annual operating costs for treating drinking water with GAC would increase by 31.4% if a maximum ∑PFAS concentration of 90 ng/L in drinking water is reduced to 10 ng/L [54]. When the treatment goal is 10 ng/L, the unit costs for GAC ranged from 0.08-0.10 € per m^3 of water treated for $PFAS_{11}$[3] [54]. The high cost and energy intensity of GAC reactivation and reuse is one of the reasons that drinking water treatment companies consider using other PFAS separation methods.

The waste generated from GAC treatment is PFAS-laden GAC [5], which can be either reactivated, disposed of, or incinerated. Reactivating GAC involves heating it to high temperatures, which volatilizes and destroys the adsorbed contaminants and restores the GAC to a near-virgin state for reuse [57]. However, this process may also make larger portions of the PFAS volatile and emit them into the air [53]. The reactivation process requires heating the spent AC to temperatures between 500-900 degrees Celsius, which may not fully restore its performance and can also degrade its pore structure and surface chemistry [58] [5]. No PFAS residuals are left on the GAC when the temperature was 700-1000 degrees Celsius [59]. Furthermore, reactivation of GAC cannot create a liquid waste stream that can be further treated. Finally, it is not feasible to perform reactivation on-site, leading to high transportation costs. Disposing of AC by landfilling is not recommended, as it can release PFAS into the environment. Leachate, which is the water that passes through or comes into contact with solid waste in a landfill, can carry PFAS into the surrounding soil and water, polluting the environment. Additionally, the GAC will not be re-used, which is less sustainable. Finally, incinerating the PFAS-laden GAC can release harmful contaminants such as fluorinated greenhouse gases, incomplete combustion products, and PFAS-containing ash into the air [60] and is therefore also not recommended.

[2] 63 operation days old and 5725 Bed Volumes (BV) treated for groundwater

[3] PFBA, PFPeA, PFHxA, PFHpA, PFOA, PFNA, PFDA and PFBS, PFHxS, PFOS and 6:2 FTSA

2.2.2. Anion exchange (IX)

IX using strong base anion resins has been shown to be an effective drinking water treatment technology for removing PFAS from water by numerous pilot and full-scale studies [8] [61]. The anion exchange resins are made from a highly porous and polymeric material [52]. This method separates PFAS from water by exchanging the negatively charged PFAS ions in the water with negatively charged ions on the resin surface (Cl^-, OH^-, HCO_3^-), as illustrated in Figure 2.4. Since most PFAS are negatively charged (anionic) at the relevant pH level for water treatment, anionic IX is a good choice for the removal of PFAS from water [62]. IX is more effective in eliminating short-chain PFAS compared to GAC [8] and the overall removal of PFAS is more effective [63]. Additionally, IX has better adsorption capacities, requires shorter contact times, and has a longer bed lifetime compared to GAC [64] [2] [65]. Likewise to GAC, PFAS competes with NOM and anions for sorption sites. The concentration of dissolved organic matter (DOC) and inorganic anions influences the lifetime of IX resins [62]. Nevertheless, research conducted by Franke et al. (2021) showed that PFAS adsorption appears to occur independently of the adsorption of major anions, despite the greater anion concentration [9]. From this, it can be concluded that the affinity of PFAS for IX resins is higher than that of most other anions.

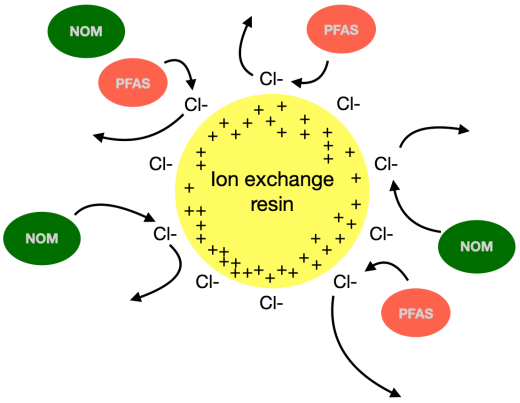

Figure 2.4: Working principle of anion exchange. PFAS exchanged with Cl-. NOM in competition with PFAS

There are two ways to use Anion Exchange Resins. First, without regeneration. The IX resins will be incinerated or landfilled once the PFAS adsorption capacity is reached [66]. Incinerating the IX resins after a single use is costly and can increase the environmental impact of the overall process and landfilling it will return the PFAS into the environment. Secondly, there are resins that can be regenerated, which is more sustainable. Anionic IX resins can be regenerated on-site, using brine solutions which are highly concentrated salt solutions [66]. In a study conducted by Dixit et al., effective recovery of PFAS from the resins was achieved (>85%) when a volume of 10 BV sodium chloride brine solution is used (10% NaCl) with a contact time of two hours [62]. After regeneration, resins can be reused as they are restored to their ionic form. The regeneration efficiency for PFOA and PFOS can be 90% [67]. However, this process creates a brine solution with high concentrations of PFAS, which is difficult to treat [66]. When IX is used for the removal of NOM, approximately 3000 times more clean water than regenerate is produced [68]. The characteristics of the brine vary widely and depend on the target contaminants removed during the treatment cycle and the operational conditions [69]. However, after one single regeneration, the pH is around 7-8 and the electrical conductivity is high (100 mS/cm). Furthermore, the study conducted by Liu et al (2021) showed that the reuse of the brine for regeneration can be possible in some situations [69]. A treatment plant located in the Netherlands successfully showed that reuse of the brine is possible for five regeneration cycles before disposal of the brine is required. This can reduce the waste volume significantly. There are limited and costly brine management options [68]. Currently, the generated waste stream is transported off-site for landfilling, incineration or pumped into the underground. However, incineration can emit PFAS in ash into the air [60], and landfilling and discharging the waste will return the PFAS into the environment.

2.2.3. Nanofiltration (NF)

NF is often used for treating water contaminated with micropollutants, including PFAS. The separation of PFAS using NF is mainly based on size exclusion, and the effectiveness, therefore, depends on the molecular cut-off point of the membrane [9]. NF membranes with a molecular weight cutoff (MWCO) of 270 Da or lower generally achieve high PFAS rejections (>90%) [9]. In table 2.3, the molecular weight (MW) of different types of PFAS are stated. PFAS with a higher MW than the MWCO will be separated more effectively than lower MW PFAS.

Table 2.3: Molecular weight of commonly detected PFAS [70]

type	PFBA	PFPeA	PFHxA	PFHpA	PFOA	PFBS	PFHxS	PFOS	GenX
MW [g/mol]	213.03	263.04	313.04	363.05	413.06	299.09	399.10	499.12	357.7

Different types of NF membranes are available, and the specific surface characteristics of the membrane material can cause chemical interactions between the PFAS and the membrane, further enhancing the removal of PFAS. The different retention mechanisms of the membrane are steric hindrance due to MWCO and pore size, electrostatic interactions due to membrane charge, and hydrophobic interactions due to hydrophobicity [71]. An advantage of using NF is that it can help achieve more water quality targets by separating other impurities, which is especially important given the expected increase in the production and emission of man-made chemicals [9], micro- and nano plastics, and pharmaceuticals in the future. This will increase the pressure on drinking water sources, and therefore new regulations might require the removal of these chemicals from water [9]. For this reason, separation based on size exclusion may out-compete adsorption processes. However, the downsides of NF are that it requires high energy input [2] and may suffer from scaling and fouling of the membranes. NF generates a waste stream that consists of 10-20% of the incoming water with 5-10 times greater PFAS concentrations [72]. Therefore, it is necessary to evaluate economically feasible treatment options to handle this waste stream [9] [72].

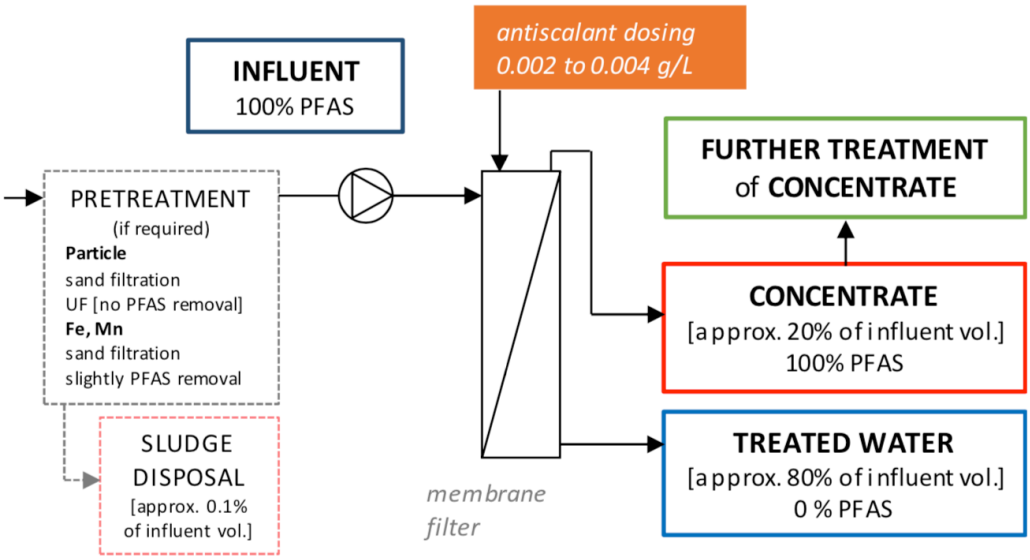

Figure 2.5: Nanofiltration performance and flow diagram [53].

2.3. Techniques for concentrating PFAS-containing waste streams

2.3.1. Foam fractionation

Foam fractionation (FF) is a technique used to separate amphiphilic species from aqueous solutions by utilizing air bubbles [74]. FF has demonstrated high effectiveness in removing PFAS from contaminated water [75]. In this process, fine air bubbles are injected into the influent water, causing PFAS molecules to adsorb to the air-liquid interface of the rising bubbles due to their amphiphilic properties, as illustrated in Figure 2.6. This reduces the Gibbs free energy of the system [74] and increases the stability of the bubbles as it reduces the surface tension of the air bubble [76]. Consequently, a foam is formed on the liquid's surface, and the PFAS-containing foam, referred to as the foamate, is removed from the treated water, which is referred to as retentate [77]. FF is considered a cost-effective and sustainable method since it does not require chemical reagents or adsorbent media [74]. However, energy is needed for aeration, and specific techniques for aeration and foam collection are necessary. Research conducted on contaminated raw leachate water demonstrated an overall PFAS removal efficiency of approximately 60%, with removal rates exceeding 90% for long-chain PFAS and less than 30% for short-chain PFAS [75]. Short-chain PFAS are less amphiphilic and more soluble in water and hence have worse removal efficiencies compared to long-chain PFAS [75]. Higher removal efficiencies could be achieved by increasing the airflow rate, enhancing ionic strength, a larger collected foam fraction, and the addition of a thickener [56] [72] [75]. According to McCleaf et al. (2023), collecting the foam continuously may increase the PFAS removal [72]. The exact volume and concentration of the foamate depend on the type of FF setup and influent water. Robey et al. (2020) found that for landfill leachate, approximately 22% of the initial waste volume ends up in the foamate, and most of the PFAS removal occurs in the first 14% of volume removed [11]. McCleaf et al. (2021) found for landfill leachate that 83% of the PFAS was captured in 10% foam. In the study of McCleaf et al. (2023), who used FF on NF concentrate, the volume reduction was approximately 10% [72]. Wang et al. found that the use of a two-stage FF resulted in a smaller waste volume compared to a single-stage FF [56]. In table 2.4, the interfacial adsorption coefficients (µm) of different types of PFAS to the water-air interface are given [78]. From this table, it can be concluded that PFSA have higher adsorption coefficients than PFCA, and long-chain PFAS higher adsorption coefficients than short-chain PFAS.

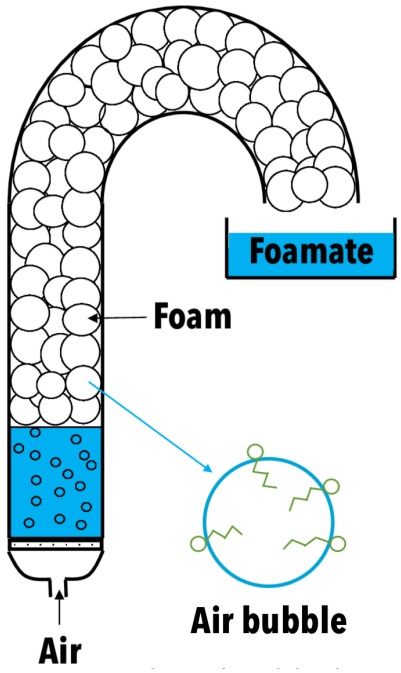

Figure 2.6: Foam fractionation PFAS removal mechanism [73]

Table 2.4: Interfacial Adsorption coefficient for commonly detected PFAS to water-air interface [78].

Type	PFBA	PFPeA	PFHxA	PFHpA	PFOA	PFNA	PFDA	PFBS	PFHxS	PFHpS	PFOS
	C4 PFCA	C5 PFCA	C6 PFCA	C7 PFCA	C8 PFCA	C9 PFCA	C10 PFCA	C4 PFSA	C6 PFSA	C7 PFSA	C8 PFSA
K [µm]	0.0172	0.0584	0.220	0.576	2.32	9.34	37.2	0.178	0.972	5.14	23.0

Important process variables, according to a study by Smith et al. (2022), include the contact time T_c (min), collected foam fraction $\%_{foam}$ (%), airflow Q_{air} (L/min), and air-to-feed ratio (AR) [75]. $\%_{foam}$ can be calculated using equation 2.1, where the volume of the foam V_f is divided by the total initial volume V_i. Meng et al. (2018) found that for the performance of the FF system, the aeration time is one of the most influential variables [79]. Smith states that the aeration time should be greater than 20 minutes and that increasing the airflow Q_{air} cannot compensate for shorter contact times T_c.

It is important to note that these process variables are highly dependent on the inlet concentrations, and these recommendations are specifically for landfill leachate [75]. Smith et al. (2022) found that dissolved organic matter (DOC), iron, and aluminium were enriched in the foam [75].

$$\%_{foam} = V_f / V_i \tag{2.1}$$

The size of the air bubbles can significantly impact the PFAS removal efficiency. Studies have found that increasing the adsorption surface area can lead to greater recoveries [77][80]. One approach to achieve this is by generating smaller air bubbles within the waste stream, such as using pressurised water (i.e. white water), which is already employed in the drinking water industry and referred to as dissolved air flotation (DAF). Furthermore, lower gas flow rates result in longer residence times for the air bubbles. Both smaller bubble sizes and lower gas flow rates provide additional contact time and surface area for PFAS adsorption onto the bubbles, thereby facilitating the removal process.

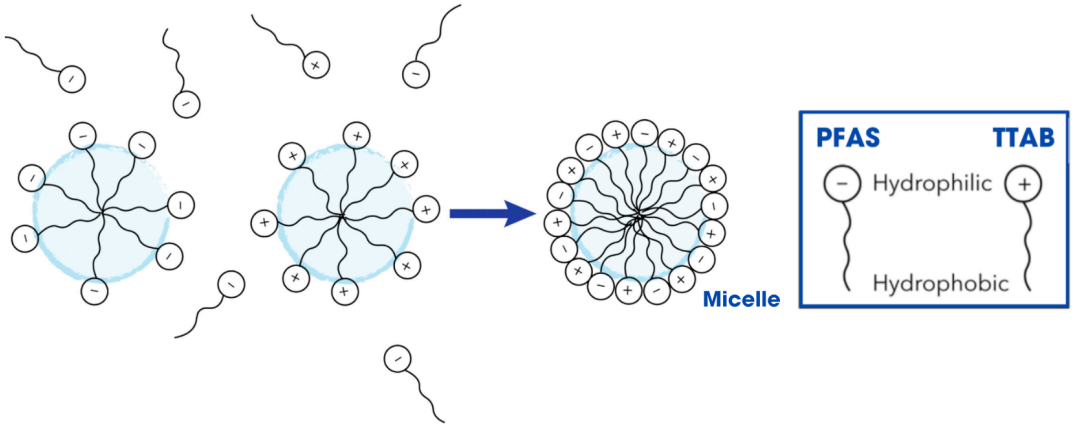

Figure 2.7: Cationic surfactant TTAB and its electrostatic interaction with PFAS [81]

The PFAS concentrations in the waste streams might not be sufficient to form foam by itself. Hence, the addition of a surfactant might be required to enhance the foamability of the waste streams and the stability of the foam [72]. A cationic surfactant improves the PFAS removal the greatest compared to anionic, non-ionic, and zwitterionic surfactants [82] [81] [83]. This is mainly due to the electrostatic interaction between the head groups of the cationic surfactant and anionic PFAS head [82], as can be seen in Figure 2.7.

2.3.2. Zeolites

Originally, zeolites are naturally occurring aluminosilicate composites [84] [85]. Currently, also different types of zeolites are manufactured synthetically, which requires chemicals and energy. These crystalline solids have symmetrical structural units that form networks of pores and channels, which give them a high surface area, size and shape selectivity for contaminants, and unique surface chemistry [86]. As a result, zeolites exhibit a unique reaction and adsorption selectivity [87]. Zeolites separate PFAS from water through ion exchange and adsorption. The effectiveness of zeolites in removing PFAS from a liquid waste stream depends on several factors, including the type of zeolite used, the concentration and type of PFAS in the liquid, and the pH of the liquid. Two major factors that determine the adsorption behaviour of zeolites are their porosity and hydrophobicity [86]. Zeolites come in a variety of pore sizes and distributions, with hundreds of natural and synthetic variants discovered [86]. The pore size is a limiting factor, as it determines the size of compounds that can be adsorbed into the pores and channels of the zeolite. Molecules with similar pore sizes are increasingly adsorbed to the zeolite due to the strength and frequency of van der Waals forces of attraction [86]. The hydrophobicity of the zeolite depends on the silica-to-aluminum atoms ratio (SAR) in their structure. A higher SAR indicates a more hydrophobic zeolite [86]. After the zeolites have become saturated, they may need to be regenerated, which can be done through thermal desorption. Natural zeolites are abundant, inexpensive and ecological [84]. Nevertheless, synthetic zeolites are expensive compared to natural zeolites.

A study conducted by Van den Bergh et al. (2020) found that the synthetically manufactured, all-silica BEA (Beta) zeolite is a highly selective and high-capacity adsorbent for removing PFOA and PFOS from water and is not influenced by the presence of organic competitors [10]. When zeolites are not all-silica and have a lower SAR, they contain more aluminium, which is a negatively charged ion and thus repels the anionic heads of the PFAS. Hence, it is preferable to have the highest possible SAR. The perfluorinated chains of the PFAS are situated in the hydrophobic, straight channels of the BEA zeolite [10]. Important to note is that the synthesis of all-silica BEA zeolite was done using fluoride as the mineralizing agent [10].

2.3.3. Cyclodextrins

Cyclodextrin (CD) polymers are a class of adsorbents known for their rapid removal of various chemicals from water [65]. CDs are naturally occurring cyclic oligosaccharides typically composed of 6-8 monosaccharides [88] [89]. CDs have a torus-like form with multiple hydroxyl (OH) groups at each end, enabling them to encapsulate hydrophobic compounds while remaining soluble in water [88]. This cup-like structure of CDs, with a non-polar interior, facilitates the interaction between the hydrophobic PFAS chain and the inner part of the CD molecules leading to PFAS removal [90] [53]. CD-based adsorbents are created by linking CD molecules together to form porous polymers. Cross-linking allows the addition of functional groups, enhancing the adsorbent's ability to remove PFAS [53]. Research has shown that installing positively charged units on CD polymers improves their binding with anionic PFAS, including short-chain PFAS [91]. Several studies have demonstrated promising results in terms of rapid and efficient regeneration of CD polymer adsorbents, enabling their reuse [58] [92] [65]. During regeneration, a solvent is typically used to desorb contaminants from the CD polymer. The regeneration efficiency depends on the solubility of the specific contaminant in the solvent used [93].

Among CD-based adsorbents, β-CDP (β: 7 monosaccharides) has shown promising performance for PFAS sequestration [91]. A type of $\beta-$CD known as DEXSORB+ has demonstrated exceptional performance in removing anionic PFAS from the water while resisting fouling [95]. DEXSORB+ has uniform 0.78 nm cups and a positively charged surface which provides high selectivity for PFAS while it prevents fouling of natural organic matter (NOM) and other constituents by size-exclusion, as can be seen in Figure 2.8 [94] [95] [96]. This enables DEXSORB+ to maintain its capacity and performance across different water matrices, including drinking water, wastewater, leachate, and membrane concentrates [94]. The $\beta-CD$ molecules in DEXSORB+ are connected using tetrafluoroterephthalonitrile (TFN) crosslinkers and an additional positively charged quaternary ammonium (QA) molecule, see Figure 2.9. QA makes the DEXSORB+ permanently positively charged. TFN is a fluorinated compound with acute toxicity if swallowed, as well as potential skin and eye irritation and respiratory irritation [97].

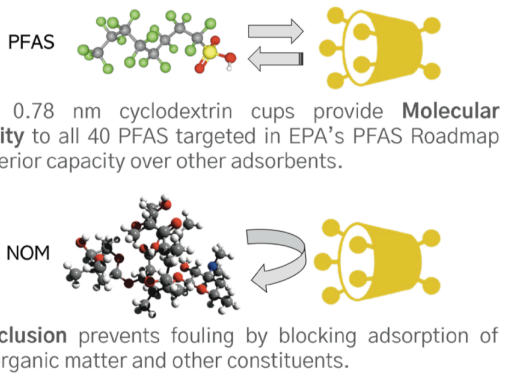

Figure 2.8: DEXSORB - molecular selectivity and size-exclusion. Source: Cyclopure [94]

DEXSORB+ has a significantly higher water treatment capacity compared to GAC, treating 25 times more water volume with the same amount of media [94]. The recovery of PFAS from DEXSORB+ can be done on-site using an ethanol mixture at room temperature, which is an important advantage of DEXSORB+. It can be concluded that the waste stream produced by DEXSORB+ is an ethanol-water mixture containing PFAS, that must be treated further [90]. When regeneration is no longer feasible, the CD polymers must be disposed of.

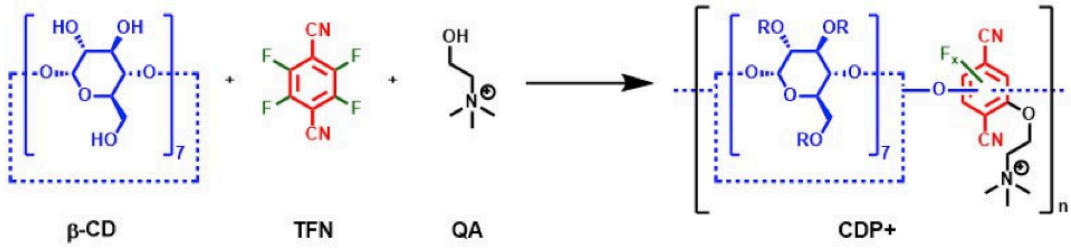

Figure 2.9: Synthesis of DEXSORB+ . It has a permanently positively charged surface due to the addition of the low-molecular-weight quaternary ammonium (QA) compound. Tetrafluoroterephthalonitrile (TFN) is used for cross-linking. [95].

2.3.4. Membranes

Membrane filtration can also be used to concentrate the IX waste stream. It has been found that membranes will reject more than 90% of PFAS when the MWCO is smaller than 270 Da [9]. The MWCO range of NF is 200-10,000 Da, while for RO the MWCO is smaller than 200 Da. Thus, NF is preferred over RO for further waste concentration, as NF can remove PFAS while requiring less energy. A study conducted by Korak et al. showed that NF can be used to decrease the waste brine volume by 70% and that re-use of the permeate was possible as brine for the next regeneration of the IX resins [98].

2.4. PFAS destruction and mineralization techniques

Incineration is the destruction/mineralization of a compound with the use of high temperatures [99]. Above 700 degrees Celsius, efficient mineralization of PFOA and PFOS to fluoride ions (>80%) occurs, along with nearly complete PFOA and PFOS decomposition (>99.9%) [100]. However, incineration of PFAS can emit harmful combustion by-products into the air: fluorinated greenhouse gasses, products of incomplete combustion, and remaining PFAS in ash [60]. A study conducted by Liu et al. (2021) showed that leachate, fly ash, and bottom ash from waste incineration plants are important PFAS vectors to the environment [7]. The emission of products of incomplete combustion is difficult to investigate because the required measurement methods for the characterization of fluorinated and mixed halogenated organic compounds are lacking [101]. More research into this method is needed because it is unclear how successful incinerating is at destroying PFAS compounds [101]. Incineration happens off-site and therefore requires transportation of the waste. It also requires fuel and is energy-intensive. This makes this whole process expensive.

Chemical oxidation reduces non-biodegradable compounds by using oxidation reagents such as hydrogen peroxide, ozone, persulfate, and chlorine dioxide [102]. Chemical oxidation processes that are only based on OH• radicals cannot break the C-F bonds that are present in PFAS [85]. However, degradation of PFAS can be achieved when OH• radicals are combined with other radicals. A study conducted by Dombrowski et al. (2018) concluded that heat-activated persulfate is the best PFAS degrading oxidation technique [103]. At pH 2, predominant SO_4^-• radicals degrade 89.9% of PFOA [85]. A disadvantage is that heat-activated persulfate has the highest energy demand compared to other available physicochemical treatment techniques[4] [104]. Another disadvantage is that activated persulphate does not support complete mineralization [105]. For ozone-based systems, PFAS removal was proven. A study conducted by Dai et al. (2019) showed that a combined UV and ozone treatment removes 73% of the PFAS at a residence time of 20 minutes [106]. No study was able to confirm destruction through mass balance and analysis of byproducts [107]. An unknown mass of PFAS cannot be identified; thus, it is unknown how much oxidative destruction takes place [103]. There are concerns that shorter chains of PFAAs are formed [105]. In case oxidation techniques are used to degrade PFAS, it is important to examine if toxic degradation products are formed [108].

Sonochemical degradation is a treatment method that emits sonic waves into the liquid [107]. The propagation of the waves results in cavitation: micro/nano bubbles are formed which is followed by their

[4]Chemical oxidation processes using heat-activated persulfate, electrochemical oxidation, ultrasonication (US), reductive chemical processes using ZVI, advanced reduction processes, and plasma-based technology.

implosion. This causes high local temperatures and pyrolysis: the formation of hydroxyl radicals (OH•), hydrogen (H), and oxygen (O) atoms [109]. These radicals and the localized thermal treatment promote the degradation of PFAS. Multiple studies have shown that sonochemical degradation degrades and defluorinates more than 90% of PFOA and PFOS [107]. The costs of this technique are moderate [85]. 100 to 300 Watt-hour of energy is required to obtain one liter of treated water [85]. This method is only tested on a laboratory scale and more research must be conducted on its effect on other types of PFAS. From the perspective of large-scale applications, hazardous intermediates and/or products may be produced during this cavitation process [110]. Thus, it is important to further investigate this PFAS degradation mechanism and perform toxicological research on the degradation intermediates and products [110].

Biodegradation of PFAS is another technique that requires further investigation. To treat or remove toxic chemicals with the use of aerobic treatment; 10 to 15 days of residence time are required (Clean Water Wave CIC) [111]. Pure cultures of microorganisms could biodegrade PFAS over the course of weeks or months in controlled laboratory environments [5]. Biodegradation has a lower investment cost and is less disruptive to the soil and water environment compared to physical and chemical methods [112]. However, this treatment method might require a great amount of time as the degradation process is very slow. Furthermore, conflicting reports exist about microbial degradation of PFAS [107] and thus further research is required.

Ball-Milling is another researched PFAS destruction method. This mechanochemical process mixes PFAS and co-reagents, such as potassium hydroxide (KOH), with metal balls at high velocities for PFAS destruction [113]. This method destroys ≥99% PFOA, PFOS, PFBS, and GenX. Additionally, the fluoride is almost completely recovered (≥99%), and hence full mineralization of PFAS into inorganic salts takes place [114].

Electrochemical oxidation (EC), also known as anodic oxidation, uses electrical currents to oxidize pollutants that are present in the water [115]. EC is an advanced oxidation process (AOP) [116]. Bench-scale studies have shown successful EC degradation and defluorination of PFCA, PFSA, and polyfluorinated compounds [104]. EC requires less energy than incineration [115]. Like other destruction technologies, this method has the potential to generate harmful by-products and might not destroy some PFAS [104]. Furthermore, electrodes can contain toxic heavy metals, and thus, these heavy metals may be released into the environment [104]. Electrodes have relatively high costs [104]. Most tests that were conducted use a control waste stream[5], while real waste streams might give different results. Studies have observed decreases in the parent compounds, but total PFAS destruction has not yet been verified [115] and thus, further research is required.

Photochemical oxidation uses ultraviolet (UV) irradiation together with chemical oxidation to accelerate the oxidation reactions between the contaminants and the free radicals [104]. When UV is used alone 16.8% of PFAS is removed [106]. When UV is combined with ozone the removal of PFAS increases to 73% [106]. A comparative assessment of different technologies[6] conducted by Nzeribe et al. (2019) concluded that photochemical oxidation was the most ineffective method to degrade and defluorinate PFAS [104]. It was shown to have the longest treatment time with high energy demands, resulting in the highest total costs [105].

Plasma degradation is a technique that generates reactive oxygen and nitrogen species in the water. Only water, air, and electricity are used to create plasma-activated water (PAW). The electricity is used to bring ambient air into the plasma phase. Then, the plasma-activated air is brought into contact with water. Finally, the reactive nitrogen and oxygen dissolve into the water creating PAW [117]. For the degradation of PFAS argon gas (instead of air) can be used. The PFAS will adsorb onto the gas-water interface of the formed argon gas bubble. The PFAS are then destroyed by plasma that is generated at the interface [118] [104]. Fast degradation of long-chain PFAS is achieved however, for short-chain PFAS the degradation can be more slowly [119]. According to a study that induced non-thermal plasma

[5] Clean water spiked with PFAS.

[6] Chemical oxidation processes using heat-activated persulfate, electrochemical oxidation, ultrasonication (US), reductive chemical processes using ZVI, advanced reduction processes, and plasma-based technology.

degradation, 90% of PFOA compounds are degraded after 60 minutes of treatment [120]. Preliminary research on the by-products conducted by Stratton et al. (2017) showed that about 10% of PFOA and PFOS are converted to shorter-chain perfluoroalkyl acids (PFAAs) [121]. Also, Khan et al. (2022) analysed that most PFAS are completely degraded during treatment and not only transformed into short-chain PFAS compounds [120]. The limitations of non-thermal plasma are the significantly high costs and high energy use [105]

Chemical reduction processes involve either direct electron transfer or the generation of free radicals to treat and degrade contamination [104]. **Zero-Valent Iron (ZVI)** is a type of chemically reducing agent. The contaminants adsorb onto the ZVI surface, where these compounds degrade into less toxic or non-toxic compounds. This is followed by the desorption and thus release of byproducts into the water. These are the steps in the removal of contaminants by ZVI [122]. This technology is feasible for most PFAS degradation [107] and reduced 86.8% of PFHS within 6 hours [85]. A disadvantage of this method is the cost of zerovalent iron [85].

Nzeribe et al. (2019) compared the effectiveness of available physicochemical treatment techniques for PFAS destruction. The comparison was based on their rate, cost, energy use, and their ability to degrade and defluorinate PFAS. The research showed the following order (from most to least efficient): electrochemical oxidation > ARPs > plasma > sonolysis > heat-activated persulfate > photochemical oxidation [104]. Nevertheless, toxic degradation byproducts are often reported during PFAS degradation: fluoroform (CF3H) a chemical compound with a high global warming potential, perchlorate, lead, bromate, halogenated hydrocarbons, trichloroethane (TCA), short-chain PFAS and other harmful by-products [104] [60] [105] [123]. As long as destruction methods form byproducts that are toxic or harmful to the environment these methods can not be used to eliminate PFAS. Hence, detailed studies on the toxicology of PFAS breakdown products are required [85] and complete mineralization should be confirmed with the use of a fluoride mass balance or other means [104]. Ball-milling was the only destruction method where complete mineralization of PFAS into organic salts was proven. The destruction of PFAS is the final step in ending the PFAS cycle. However, PFAS destruction lies outside the scope of this research, and only a literature review was conducted.

2.5. PFAS treatment line

PFAS can be removed from drinking water by using nanofiltration membranes and anion exchange reactors. However, these PFAS separation techniques yield significant quantities of highly concentrated PFAS-containing waste streams. NF generates a PFAS-containing concentrate and IX a PFAS-containing brine solution during drinking water production. These waste streams should not be discharged without further treatment due to the environmental and public health impacts of PFAS. Consequently, it is essential to eliminate PFAS from these waste streams. This can be done by PFAS destruction, but this is generally an energy-intensive and costly treatment step. A cost- and energy-saving solution involves concentrating the waste streams before destruction. During this research, the concentration of these drinking water waste streams, with different concentration technologies, will be further investigated. An overview of the intended treatment sequence for PFAS separation, concentration and destruction is presented in Figure 2.10. The waste from granular activated carbon is not included in this research as reactivation of GAC can not lead to a liquid waste stream.

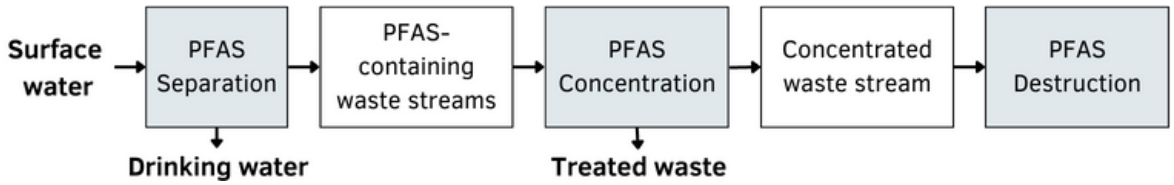

Figure 2.10: PFAS treatment line: PFAS separation, concentration, and destruction

3 Methodology

3.1. Drinking water waste streams

3.1.1. Analysis of PFAS separation technologies

First, the PFAS mass and volumetric balances of water treatment technologies that separate PFAS from drinking water were made. The two technologies considered were anion exchange (IX) and nanofiltration (NF) membranes. Both generate a highly concentrated PFAS-containing waste stream. To establish these balances, data obtained from drinking water companies were compiled. This information was used to determine the PFAS removal efficiencies of these technologies, as well as the proportion of waste stream volume generated relative to the influent volume. The mass and volumetric balances of PFAS separation with GAC were not included in this study because GAC is considered not sustainable for the removal of PFAS [2] and because no liquid waste stream is formed [5].

3.1.2. Sampling of waste streams

The waste stream samples were collected from two different drinking water companies in the Netherlands, where NF and IX technologies are employed for producing drinking water from surface water sources. The IX brine solution was collected on the 1st of March from a full-scale treatment plant. The influent water comes from a large reservoir, where the water stays for approximately nine weeks. Here, air is injected to avoid stratification, and to reduce the growth of algae. Caustic soda is added to remove calcium, and hence soften the water. Then, the water passes through drum screens to remove larger particles that might clog up the system further downstream. Hereafter, the water enters the anion exchange suspended plug flow reactors. After the required contact time, the used resins are removed from the treated water using lamella separators and regenerated in the regeneration vessel. The regeneration solution is re-used five times before discharging as waste. A sample of the waste stream generated after five regeneration cycles was collected. This is called the IX brine solution. In Figure 3.1, a schematic overview of this treatment line is shown.

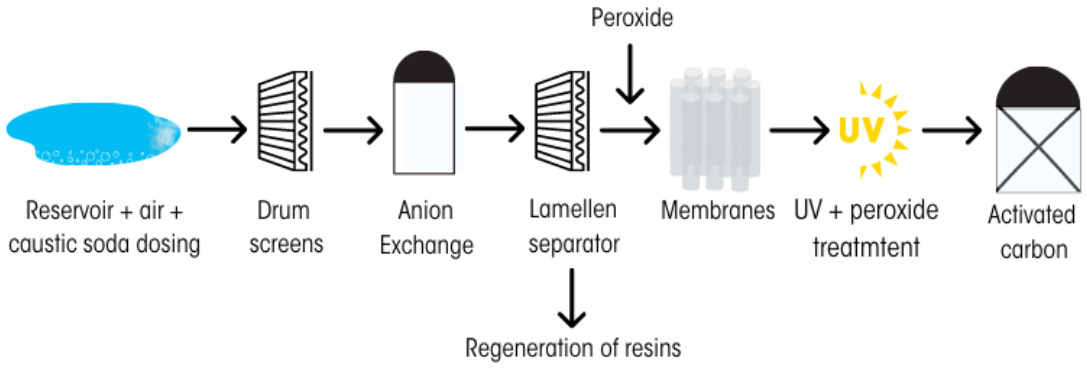

Figure 3.1: The different treatment steps before and after the anion exchange reactor.

The sample of the NF membrane concentrate was collected from a pilot plant on the 24th of February, 2023. The treatment steps before the NF membranes in this specific treatment line are microfilters for the removal of larger particles, iron dosage to create iron flocs which are removed during the following step, which is floatation, active coal filters (GAC), and finally the water passes through the NF membranes. The different treatment steps and the sequence of this treatment line are shown in Figure 3.2. The NF waste stream, called the NF concentrate, was collected. The IX brine solution and NF concentrate were collected in 10-liter HDPE cans and stored in a fridge at 5.6 degrees Celsius. The different

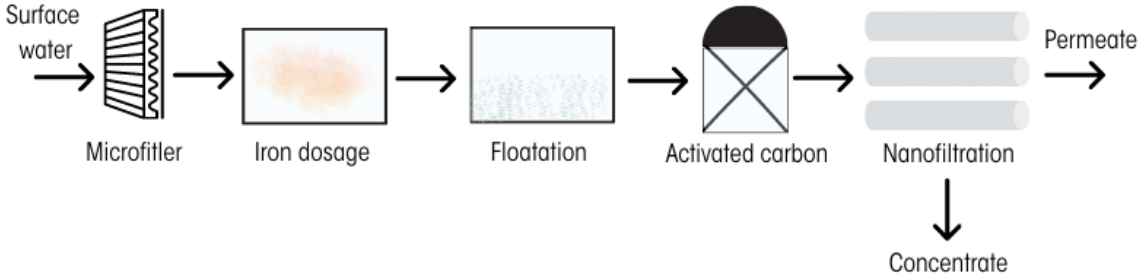

Figure 3.2: The different treatment steps before the nanofiltration membranes.

characteristics of the PFAS-containing waste streams from NF membranes and IX were measured, namely the PFAS, TOC and ion concentrations, pH and electric conductivity (EC).

3.2. Testing of the concentration technologies

The second sub-goal was to determine the volume reduction (ΔV) (eq.3.1) and the different PFAS removal efficiencies ($RE(\%)$) (eq.3.2) that could be achieved with the known PFAS concentration technologies for the two different types of drinking water waste streams (NF and IX). During this research, four concentration technologies were investigated; foam fractionation (FF), adsorption on DEXSORB+ (CD) and all-silica BEA zeolites (ZEO), and nanofiltration (NF). The performance of FF, CD, and ZEO was evaluated in the laboratory, whilst NF was modelled using IMS Design software.

$$\Delta V = \frac{V_w}{V_0} \tag{3.1}$$

$$RE(\%) = \frac{c_0 - c_e}{c_0} \cdot 100 \tag{3.2}$$

With:

- V_w: Volume of concentrated waste (= regenerant volume for adsorbents)
- V_0: Initial volume
- c_e: Effluent concentration
- c_0: Initial concentration

3.2.1. Adsorbents

The adsorbents DEXSORB+ (Cyclopure Inc.), a type of cyclodextrin, and All-Silica BEA zeolites were tested in the laboratory using batch reactors. The adsorption loading of PFAS on the adsorbents was analysed, and a regeneration process was performed to determine the achieved volume reduction, the PFAS enrichment factors, and the desorption capacity. To enhance kinetics while maintaining the characteristics of the granules, the granules were crushed into a powder form for these tests, as this form is more commonly used on an industrial scale. The tests were performed on the earlier collected NF and IX waste samples.

Adsorption tests

The first step involved crushing the DEXSORB+ and all-silica BEA zeolites and passing them through a 75 µm sieve. Then, the sieved material was mixed with ultra-pure water (UPW) to create adsorbent suspensions. The concentrations of the adsorbent suspensions were one g/L for DEXSORB+ and two g/L for all-silica BEA zeolites. First, these suspensions were mixed with a vortex mixer for 30 seconds, then sonicated for three minutes, and finally mixed for 30 minutes on the magnetic stirrer. During the sonification process, sound energy is applied to agitate particles. These steps were performed to ensure that small aggregates were fragmented and that the adsorbent concentration of the suspension was distributed equally. Next, 100 mL of the PFAS-containing waste stream samples (c_0) were added to 250 mL glass bottles. The suspensions were kept on the magnetic stirrer before dosing to make sure it was thoroughly mixed. These adsorbent suspensions were then added to the bottle reactors using a pipette to achieve the predetermined adsorbent dosages (m). The bulk density of zeolites is 600-800 kg/m^3 and 400 kg/m^3 for DEXSORB+ [124][94]. Therefore, it was decided to dose twice as much zeolite as DEXSORB+. The dosages were 10, 50, and 100 mg/L for DEXSORB+ and 20, 100, and 200 mg/L for all-silica BEA zeolites. The bottles were mixed for 24 hours using a magnetic stirrer. After these 24 hours, the adsorption media was separated from the water through vacuum filtration. A glass filter holder was placed on a joint flask with a side arm. That was then connected to a vacuum source. A 47 mm glass fibre filter paper was placed between the glass filter holder and the flask. When the vacuum source was opened, the water passed through the glass microfiber filter paper (Whatmann D = 47mm, pore size = 0.7µm. CAT No.1825-047), separating the adsorbent from the liquid. This filter paper was selected because Chandramouli et al. (2015) found that glass fibre filter paper has a negligible effect on the PFAS because there was minimal adsorption of PFAS on the filter paper [125]. The filtered water (c_e) was stored in HDPE bottles for later PFAS analysis. Hereafter, the flask was rinsed with ethanol and then cleaned with ultra-pure water (UPW). After which, the following samples could be filtered.

Regeneration tests

The regeneration tests were performed for the highest adsorbent dosages for DEXSORB+ and all-silica BEA zeolites (100 mg/L and 200 mg/L, respectively) and each treated waste stream. For regeneration, a solution of ethanol and water in a ratio of 2:1, supplemented with 0.5 g/L potassium sulfate, was used. The glass fibre filter paper (Whatmann D = 47mm, pore size = 0.7µm. CAT No.1825-047), used for separating the water stream from the adsorbent, was placed again in the glass filter holder. The vacuum source was closed, and 7 mL of the regeneration mixture was added to the glass filter in the filter holder. The regeneration mixture passed through the filter paper in approximately 25 minutes. This process was repeated three times, thus using a total regeneration time of 75 minutes and a total regeneration volume of 21 mL. The regeneration solution was collected in a 100 mL HDPE bottle and then diluted with 79 mL of ultra-pure water (UPW) to reach the minimum sample volume required for PFAS analysis.

After the samples were analysed, the regeneration efficiency was determined. This was done by first calculating the total mass of PFAS adsorbed (M_{Ads}) onto the adsorbents with equation 3.3 and the total mass of desorbed PFAS (M_{Des}), with equation 3.4, where c_r is the concentration of PFAS in the regeneration solution and V_r the volume of the regeneration solution. The regeneration efficiency ($R_{\%}$) was then calculated by dividing the total mass desorbed from the adsorbent by the total mass initially adsorbed onto the adsorbent, equation 3.5.

$$M_{Ads} = (c_0 - c_e) \cdot V_0 \tag{3.3}$$

$$M_{Des} = c_r \cdot V_r \tag{3.4}$$

$$R_{\%} = \frac{M_{Des}}{M_{Ads}} \tag{3.5}$$

Isotherms

The equilibrium loadings for the different dosages were determined for both adsorbents. Equilibrium represents the system's final state, where the adsorbate's concentration in the water remains constant, indicating that adsorption is equal to desorption. Using this information, the equilibrium loading of PFAS on the adsorbent, denoted as q_e (mg/g), can be determined. It represents the mass of adsorbed

pollutant, adsorbate, (x) per unit mass adsorbent (m), also known as the dosage. This relationship is described by equation 3.6.

$$q_e = x/m \tag{3.6}$$

$$x = c_o - c_e \tag{3.7}$$

The mass of adsorbed pollutant, x, can be calculated using equation 3.7, where c_0 (mg/L) represents the initial concentration of PFAS in the waste streams and c_e (mg/L) is the concentration at equilibrium. The initial PFAS concentrations, c_o, were determined during the first phase of the research when characterising the waste streams. The final PFAS concentrations, c_e, were measured in the filtered water after 24 hours of contact time.

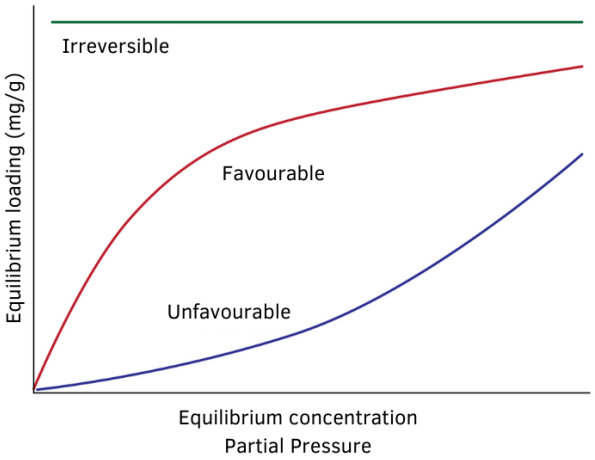

Figure 3.3: The favorable adsorption isotherm: a large amount of adsorption at low partial pressure. Unfavorable adsorption: high partial pressure is required to achieve high adsorption. [126]

The experimental results at equilibrium are presented in isotherm graphs (q_e over c_e). To describe the relationship between the concentration of the solute adsorbed onto the adsorbent surface and the concentration in the water, the Freundlich equation 3.8 was employed in this research. The Freundlich constant K_F is also known as the capacity factor $((ng/mg)\cdot(L/ng)^n)$. n represents the adsorption intensity. If n < 1, favorable adsorption occurs, and when n > 1, there is unfavorable adsorption. Favourable adsorption represents a large amount of adsorption at low partial pressure, while unfavourable adsorption requires high partial pressure, hence adsorbate concentration, to achieve higher adsorption loading. This relation is shown in Figure 3.3.

$$q_e = K_F \cdot c_e^n \tag{3.8}$$

$$logq_e = logK_F + n \cdot logc_e$$

3.2.2. Foam Fractionation

Air stone

FF experiments were conducted in batch mode, in the laboratory to asses its efficiency in treating the two waste stream types, namely NF and IX. The experimental setup is schematically illustrated on the left side in Figure 3.4. 1,000 mL of NF or IX waste stream was added into a 2,000 mL glass column (with diameter = 83.5 mm, height = 565 mm). To create tiny air bubbles in the waste stream, adjustable pressurised air from the laboratory's pressure line was passed through an air stone (with diameter = 20 mm, height = 30 mm from Uniclife - nano air pumps) and placed at the bottom of the column. The airflow rate was measured with an airflow meter and maintained at a constant value of 0.95 L/min. A magnetic stirrer was used to mix the air bubbles throughout the entire surface of the column. If no foam was generated for a particular waste stream, a cationic surfactant (TTAB) was added. The surfactant was dissolved in the wastewater by mixing it with the magnetic stirrer for 5 minutes before introducing the air into the system. Once the surfactant was dissolved in the liquid, air bubbles were introduced. S.J. Smith et al. (2022) demonstrated that decreasing the contact time below 20 minutes decreased the total PFAS removal efficiency [75]. Therefore, a contact time of 20 minutes was chosen for these experiments. The foam formed on the water surface was collected using a vacuum pump. The collected foam fraction was specific to each waste stream as the volume of foam produced varied for each waste stream. The final collected foamate was determined by measuring the volume of collapsed foam produced. The foamate and retentate samples were stored in HDPE sampling bottles for further analysis. After each test run, the column and vacuum pump were cleaned using tap water and rinsed with demi water. The air stone was cleaned by rinsing it with demi water and blowing pressurised air through it for one minute.

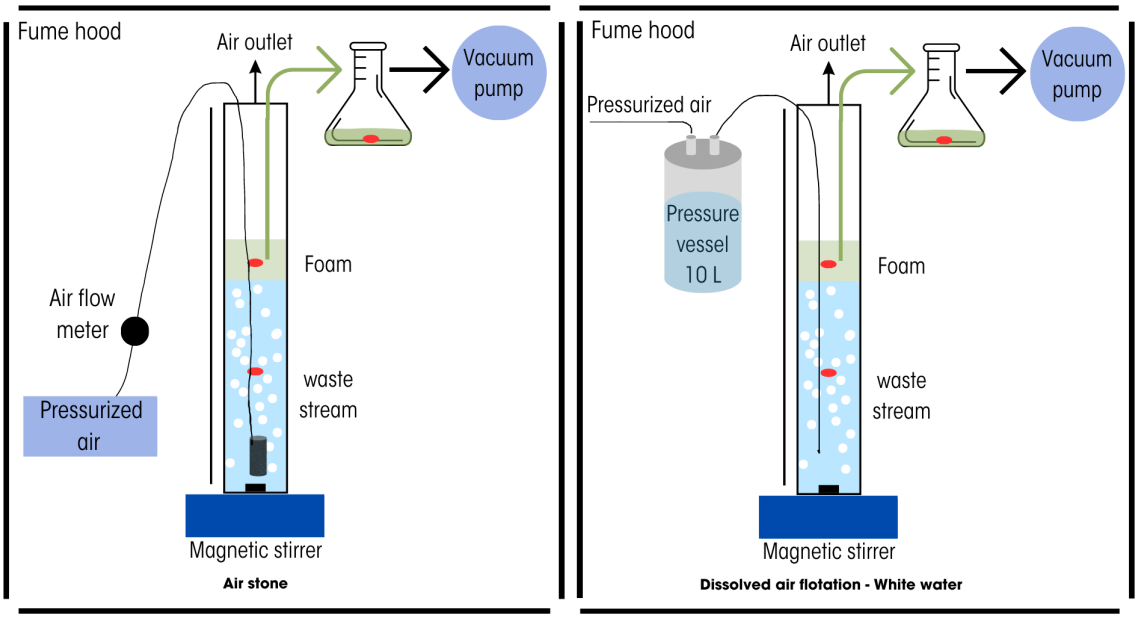

Figure 3.4: Foam fractionation laboratory setups at Waterlab Tu Delft. Left: air bubbles created by passing pressurised air through an air stone. Right: air bubbles created by dosing pressurised water (DAF). Red dots represent the collected samples: the foamate and the treated water (i.e. retentate)

Dissolved air flotation

To research the effect of the air bubble size, a dissolved air flotation (DAF) setup was used in the second FF setup. The DAF test was only conducted on the NF waste stream. White water was introduced in the system which led to the formation of tiny air bubbles. The sealed pressure vessel was filled with 5 liters of tap water. The pressure regulator, located in front of the inlet of the pressure vessel, regulates the amount of air introduced into the vessel (5 bar) [127]. The pressure inside the vessel accumulated, after which the vessel was closed. Hereafter, the vessel was stirred manually for 5 minutes and put aside for 12 hours to ensure that all the water inside the vessel was equally pressurised and the gas concentration in the water reached its equilibrium state [127]. Then, the outlet valve was opened and the pressurised water was introduced into the column, filled with NF concentrate. The pressurised water is from now on referred to as **white water**. As the white water returned to normal atmospheric pressure, the air was released from the white water in the form of tiny air bubbles. 65 mL (13%) of white water was added to the 500 mL NF waste stream. The magnetic stirrer was used to mix and maintain the air bubbles in the column for approximately two minutes. After these two minutes, the magnetic stirrer was stopped and the formed foam layer on the water surface was collected with a vacuum pump. The foamate and retentate were stored in HDPE bottles for further analysis by HWL and the achieved volume reduction was measured. It is important to note that for this specific setup, the waste stream is diluted with the dosed white water. The volume reduction of the DAF setup was based on the initial volume, without dilution, and the volume of the foam after the white water was added. After each test run, the column and vacuum pump were cleaned using tap water and then rinsed with demi water.

The airflow in the FF setup generated by white water was estimated using Henry's law, equation 3.9. The dissolved air concentration in this specific situation was estimated using solubility data. At a temperature of 15 degrees Celsius and for atmospheric pressure, the approximate solubility of air in water is 25.9 mg/(L·atm) (Edzwald, 2007). This solubility value, also known as Henry's law solubility constant (K_h), was used to calculate the dissolved air concentration in the pressurised white water by multiplying this value with the pressure (P, [bar]) of the water. This led to approximately 0.13 g/L of dissolved air in the white water.

$$C_{air} = Kh \cdot P \tag{3.9}$$

$$Q = V/\Delta t \tag{3.10}$$

This air concentration in the white water could be multiplied by the white water flow, which was determined by equation 3.10 to calculate the airflow rate. The amount of volume (V) entering the column per time interval (Δt). For this specific setup, the white water flow was 20 mL/s. This led to an airflow rate of 2.6 mg air per second.

Surfactant

During these experiments, a surfactant was utilized when no or very unstable foam was formed without a surfactant. The selected surfactant was tetradecyltrimethylammonium bromide (TTAB). This is a cationic surfactant with a carbon chain length of C14. The dosage depended on the required concentration required for foam formation. TTAB is acute and chronic hazardous to the aquatic environment, and there is no data about its persistence and degradability [128].

Table 3.1: Tetradecyltrimethylammonium bromide (TTAB) :molecular formula, classification, toxicity, and biodegradability.

Name	Molecular formula	Classification	Toxic	biodegradability
TTAB	$C_{17}H_{38}N\bullet Br$	Cationic	Very toxic to aquatic life	No data

Mass balance and enrichment factor

The mass balance was calculated for the foam fractionation setup using Equation 3.11. The equation divides the mass of PFAS in the foam (M_{foam}) and the mass of PFAS in the effluent (M_e) by the initial PFAS mass in the influent (M_0). Additionally, the enrichment factor E_f was calculated, representing the enrichment of PFAS in the foam concentration (c_{foam}) compared to the initial PFAS concentration in the untreated water (c_0). This is calculated using Equation 3.12.

$$\frac{M_{foam} + M_e}{M_0} \tag{3.11}$$

$$E_f = \frac{c_{foam}}{c_0} \tag{3.12}$$

3.2.3. Nanofiltration

The laboratory testing did not include the concentration of the drinking waste streams using NF membranes since it was already established that NF effectively removes more than 90% of PFAS when the molecular weight cut-off (MWCO) is smaller than 270 Da [9]. Instead, the Hydranautics Integrated Membrane System (IMS) Design software was utilised to model and predict the performance of the NF membrane. IMS Design allows for the specification of the chemical composition of the feed water, enabling analysis of the NF membrane's performance for both the IX and NF waste streams. The characteristics of the feed flow stream were determined in the previous step through the characterization of the drinking water waste streams. These were used as input for the model. The software allowed for making an NF design that is feasible to treat the specific incoming waste stream, including the number of treatment trains, and stages, as well as the required energy and chemical dosing. Furthermore, the model took into consideration the desired recovery rate and the plant's permeate flow production. If any exceeded design parameters were indicated, the design should be adapted until no parameters were exceeded. Additionally, the model provided predictions for the characteristics of the concentrated waste, including ion concentrations, total organic carbon (TOC), and pH.

3.3. Analytical methods

For the PFAS analyses, 100 mL samples were sent in HDPE bottles to Het Waterlaboratorium (HWL). HWL employs liquid chromatography and mass spectrometry to identify and quantify various types of PFAS present in the samples. HWL can measure 25 different PFAS compounds, these are given in table 3.2. In the table also the detection limits of the individual PFAS types are given. For the analysis of the concentration technologies, the type of PFAS plays an important role in the removal efficiency and effectiveness of the different technologies. For the representation of the results, the PFAS are grouped per chain length and functional group.

- Short chain PFCA: PFBA, PFPeA, PFHxA
- Long chain PFCA: PFHpA, PFOA, PFNA, PFDA. PDUdA, PFDoA, PDTrDa
- Short chain PFSA: PFBS, PFPeS
- Long chain PFSA: PFHxS, PFHpS, PFOS, PFNS, PFDS. PDUdS, PFDoS, PDTrD
- Others: 6:2 FTS, DONA, GenX, 9Cl-PF3ONS, 11Cl-PF3OUdS

Ion chromatography was used to measure the ions present in the waste streams. This method can measure the concentrations of the major anions, such as fluoride, chloride, nitrate, and sulfate, as well as the major cations, such as sodium, ammonium, potassium, calcium, and magnesium. The signal produced by each ion specie is measured using a conductivity detector. These signals are then plotted in the MagIC Net Software. Each signal peak represents a specific type of ion and its respective concentration. The dissolved organic matter (DOC) was measured using a TOC analyser after filtration through 0.45 µm filters (Whatman Spartan 30/0.45RC Rinse filter). This analyser operates by combusting the samples, heating them to 680 degrees Celsius in the presence of oxygen and a platinum catalyst. The resulting carbon dioxide produced from the combustion process is then detected using an infrared gas analyser (NDIR). This is the total carbon (TC). Next, the inorganic carbon (IC) in the sample is measured through a process called sparging. Sparging converts the IC into carbon dioxide, which can be measured again using the NDIR device. Finally, the TOC concentration is calculated by subtracting the IC from the TC.

Table 3.2: PFAS substances that can be measured by HWL. Chain length and abbreviation, full name, and detection limit.

Abbreviation	Substance name	Detection limit [ng/L]
C4 PFBA	Perfluorobutanoic acid	0.2
C4 PFBS	Perfluorobutanesulfonic acid	0.2
C5 PFPeA	Perfluoropentanoic acid	0.2
C5 PFPeS	Perfluoropentanesulfonic acid	0.2
C6 PFHxA	Perfluorohexanoic acid	0.2
C6 PFHxS	Perfluorohexanesulfonic acid	0.2
C7 PFHpA	Perfluoroheptanoic acid	0.2
C7 PFHpS	Perfluoroheptanesulfonic acid	0.2
C8 PFOA	Perfluorooctanoic acid	0.5
C8 PFOS	Perfluorooctanesulfonic acid	0.2
C9 PFNA	Perfluorononanoic acid	0.5
C9 PFNS	Perfluorooctanesulfonic acid	0.2
C10 PFDA	Perfluorodecanoic acid	0.5
C10 PFDS	Perfluorodecane sulfonic acid	0.2
C11 PFUdA	Perfluoroundecanoic acid	0.5
C11 PFUdS	Perfluoroundecanesulfonic acid	0.2
C12 PFDoA	Perfluorododecanoic acid	0.5
C12 PFDoS	Perfluorododecanesulfonic acid	0.2
C13 PFTrDA	Perfluorotridecanoic acid	1
C13 PFTrDS	Perfluorotridecanesulfonic acid	2
6:2 FTS	6:2 Fluorotelomer sulfonate	0.5
11Cl-PF3OUdS	11-Chloroperfluoroundecanesulfonic acid	1
9Cl-PF3ONS	9-Chloroperfluorononanesulfonic acid	0.2
DONA	4,8-dioxa-3H-perfluornonaanzuur	0.2
GenX	2,3,3,3-tetrafluor-2-(heptafluorpropoxy)propanoaat	0.2

3.4. Economic feasibility study of concentration technologies

The estimated costs for treating the drinking water waste streams were expressed in euros per cubic meter of drinking water produced. It was assumed that both PFAS separation technologies should have the capacity to produce 70 million cubic meters of drinking water per year. This volume of water is produced annually at the treatment line of Leiduin by the company Waternet [129]. The flow of the generated drinking water waste streams was determined with the data obtained from the drinking water companies.

3.4.1. Adsorption filters

The cost estimations for treating the drinking water waste streams using DEXSORB+ and all-silica BEA zeolite adsorbents were based on the utilisation of adsorption filters. Adsorption filters are well-suited for the application of granular adsorbents, which is the recommended form for these adsorbents in the drinking water industry. Cyclopure, the company that introduced DEXSORB+ to the market, states that granules appear to be the most promising form of DEXSORB+ for water treatment applications [53].

The key design parameters for the adsorption filters include the empty bed contact time (EBCT), filter velocity, and contamination loading rate. The EBCT determines the dimensions of the adsorption filter and influences the breakthrough time. The breakthrough time is the moment that the effluent quality of the target compound is no longer reached. At this point the adsorbent is saturated and no more adsorption of PFAS on the adsorbent can take place. When a breakthrough occurs, regeneration of the filter bed is necessary to restore the adsorbents capacity to adsorb PFAS. This is done by desorbing the PFAS from the adsorbent surface. Regeneration is a critical factor that affects the operational costs of the filter, making the breakthrough time of PFAS an important parameter for cost estimation. The Equilibrium Column Model (ECM) was employed to determine the breakthrough time. This model only requires isotherm data as input which was found by conducting the previously mentioned laboratory tests. While this model simplifies the real situation by neglecting the influence of dispersion and adsorption kinetics on the shape of the breakthrough curve (BTC), as can be seen in Figure 3.5, it can still predict the ideal breakthrough time and estimate the maximum service life of the adsorption filter [130]. As can be seen in Figure 3.5, the breakthrough time is probably overestimated with the Equilibrium Column Model (ECM).

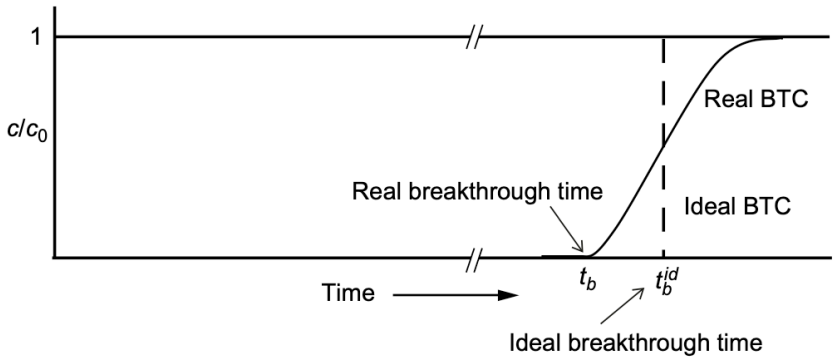

Figure 3.5: The ideal breakthrough curve compared to the real breakthrough curve through the adsorber bed. [130]

The breakthrough time varies for every type of PFAS and thus, for every type of influent water matrix. The bed lifetime for the estimation of the costs will be based on the most dominant type of PFAS present in the influent of the adsorbent filters for which a favorable isotherm was found. Hence, it is determined by the results from the characterisation of the drinking water waste streams and the obtained Freundlich parameters.

To calculate the ideal breakthrough time t_b^{id} for a single adsorbate, the following equation is used [130]:

$$t_b^{id} = \frac{q_e \cdot m_A}{Q \cdot c_0} \tag{3.13}$$

$$m_A = V * \rho_B \tag{3.14}$$

With:

- m_A: Adsorbent mass [kg]
- Q: Volumetric flow rate [m^3/h]
- c_0: PFAS inlet concentration [ng/L]
- q_e: Equilibrium loading for specific inlet concentration [m=ng/mg]
- V: Adsorber volume [m^3]
- ρ_B: Bed density [kg/m^3]

The construction costs also play a significant factor in the overall costs of the installation. The required dimensions of the adsorption filters are determined by the assumed Empty Bed Contact Time (EBCT) and the fixed volume flow (Q). A smaller reactor volume (V) means a shorter EBCT and a longer EBCT can be achieved by increasing the column size. Equation 3.15 is used to determine the volume of the reactor.

$$EBCT = \frac{V}{Q} = \frac{h \cdot (\frac{d}{2})^2 \cdot \pi}{v \cdot (\frac{d}{2})^2 \cdot \pi} = \frac{h}{v}$$

$$V = EBCT \cdot Q \tag{3.15}$$

With:

- d: Diameter [m]
- h: Height [m]
- v: Velocity [m/h]

A larger filter column is required to achieve longer EBCT, which means higher construction costs. However, the EBCT also influences the breakthrough time. A shorter EBCT accelerates the breakthrough time, and hence, leads to earlier regeneration requirements, increasing the operational costs. The economical optimal EBCT should be found to predict the lowest possible overall cost. This was done by creating a Python model (given in Appendix D) that plotted the construction, regeneration, and overall costs over the EBCT.

DEXSORB+

Based on data from rapid small-scale column tests (RSSCT), an EBCT of three to ten minutes is sufficient for high PFAS removal using DEXSORB+ [131]. Cyclopure states that 3-bed volumes (BV) of regeneration solution are required to desorb PFAS. The regeneration process can be conducted on-site. The cost of one kilogram of DEXSORB+ is 15 €/kg [53]. The regeneration solution, which consists of a mixture of ethanol, water, and potassium sulfate, also contributes significantly to the costs. Ethanol is commercially available at a price of approximately €2000 per cubic meter (Spain, 2023) [132]. Potassium sulfate costs around €0.45 per kilogram (2018, Netherlands) [133]. The cost of clean water for drinking water companies is assumed to be €2.5 per cubic meter. It is important to note that these prices may vary depending on the market, region, and time.

All-Silica BEA Zeolites

It was already found by Zeolites can be regenerated thermally to desorb PFAS from its surface [10]. During this research regeneration with the use of the regenerant employed by Cyclopure for DEXSORB+ was tested in the laboratory. The cost estimation of all-silica BEA zeolite regeneration was based on the usage of the same regeneration mixture and volume as used for DEXSORB+. Based on the European market price (2021), high-silica BEA zeolites cost 47€/kg. It was assumed for the cost estimation that the price of all-silica BEA zeolites is approximately the same.

3.4.2. Foam fractionation

The cost estimation for the FF treatment was based on data obtained from Envytech, a company in Sweden specialising in Surface Active Foam Fractionation (SAFF) for the removal of PFAS from contaminated waters. SAFF is a process that only requires air and electricity, where the foam is collected using a passive spill-over weir and an active vacuum system. Envytech's SAFF system consists of multiple fractionation steps, where the PFAS concentrate from the first stage undergoes further fractionation in the second stage to achieve higher concentrations [134]. Envytech does not add a surfactant. However, it might was found, during this research, that adding a surfactant was necessary for treating the examined drinking water waste streams. This would increase the costs.

According to Envytech pre-treatment is usually not required, except for cases involving the removal of larger suspended particles, where a lamella separator can be employed. The operating costs of SAFF are mainly affected by the energy requirement, which ranges between 0.4-0.7 kWh/m^3 treated water [134]. Service costs associated with SAFF treatment plans are minimal since all pumps, valves, and sensors can be connected to a digital monitoring and logging program that tracks operational and power data [134].

A paper by CONCAWE, which investigated the performance of water treatment systems for PFAS removal, estimated an energy usage of approximately 0.1 kWh/m^3 treated water [53]. This suggests that there may be variations in energy consumption depending on the specific system and influent water. For the estimation of the capital costs of the FF system, it was assumed that the price was similar to that of DAF. The costs of DAF, including the capital and operation costs, were estimated with the 'Kostenstandaard' website. In case it was required to dose a surfactant, the operation costs would increase. The cost of TTAB surfactant was determined to be €7/kg according to a reference [135].

3.4.3. Nanofiltration

The cost estimation of NF was based on the results from the IMS Design model. For the operational expenditure the chemical requirements, power requirements, replacement costs, and maintenance costs were considered. The capital costs were based on the design parameters determined with the IMS Design, such as the number of stages and elements and membrane type.

4

Results

4.1. Characterization of the drinking water waste stream

Figure 4.1 demonstrates the different types of PFAS present in the sampled NF and IX drinking water waste streams. The PFAS concentrations of each PFAS type individually and the corresponding PFOA equivalent concentration (PEQ) are given for both waste streams. From the first diagram, it can be seen that PFOA (C8) is the most dominant PFAS type in the NF concentrate, and it is also the primary contributor to the PFOA equivalent concentration. The ∑PFAS concentration in the collected NF concentrate sample was 304 ng/L. The PFOA equivalent concentration for the NF concentrate is 152 ng PEQ/L. The IX brine solution volume is 0.5% of the total water treated by the IX reactors. The brine waste stream from IX primarily contains short-chained PFAS, namely PFPeA (C5) and PFBS (C4). However, these PFAS types do not make a significant contribution to the PFOA equivalent concentration. The predominant PFAS types in terms of PFOA equivalent concentration are PFHpA (C7), PFOA (C8), and PFOS (C8). Furthermore, the ∑PFAS concentration in the IX brine solution is 172 ng/L. The PFOA equivalent concentration in the IX brine solution is 37 ng PEQ/L. In Table 4.1, the ∑PFAS and PFOA equivalent concentrations of the NF and IX waste streams are given.

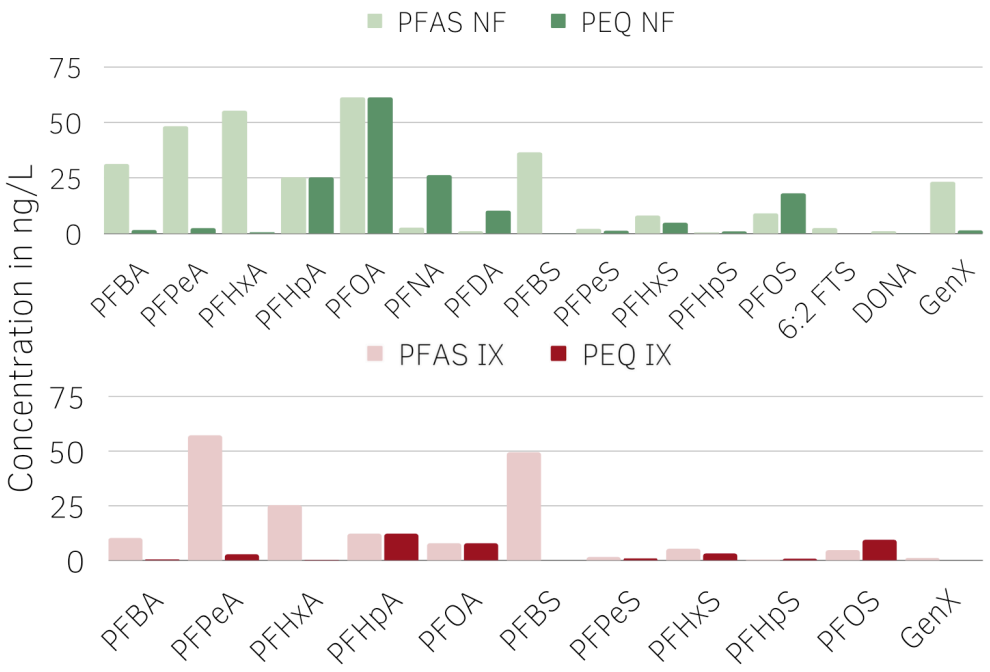

Figure 4.1: PFAS and PFOA equivalent concentrations [ng/L] in NF and IX waste streams. PFAS measurements were conducted by HWL on collected waste stream samples. PEQ is determined with relative potency factors (RPFs).

Table 4.1: Measured ∑PFAS concentration and PFOA equivalent concentrations (PEQ) in the nanofiltration and anion exchange waste streams.

	∑PFAS [ng/L]	∑PFOA eq. [ng PEQ/L]
NF concentrate	304	152
IX brine solution	172	37

The flow of the NF concentrate corresponds to 20% of the incoming flow, as can be seen in Table 4.2. Therefore, when 70 million cubic meters of water is produced, 17.5 million cubic meters of drinking water waste stream is generated. For the IX reactor, the volume of the IX brine corresponds to 0.5% of the incoming flow. Hence, 350 thousand cubic meters of the PFAS-containing brine solution is generated when 70 million cubic meters of drinking water is produced.

Table 4.2: The portion of waste stream volume generated relative to the influent volume with drinking water treatment technologies nanofiltration and anion exchange when 70 million cubic meters of drinking water is produced.

	Waste stream generated per drinking water produced	Flow of waste stream
NF concentrate	20%	17.5 million m^3/year
IX brine solution	0.5%	350 thousand m^3/year

In Table 4.3, the chemical composition of the waste streams is provided. The regeneration of IX resins with a brine solution results in elevated ion concentrations, particularly sodium, chloride, and sulfate. Consequently, the ionic strength and electrical conductivity of the IX brine are high, 914 mol/m^3 and 20,900 µS/cm, respectively. The dissolved organic carbon present in the regeneration solution is 358 mg/L.

In contrast, the NF concentrate contains fewer ions, resulting in lower electrical conductivity and ionic strength. Analysis of the collected NF concentrate sample showed that the main ions present in the NF waste stream are chloride, sulfate, magnesium, calcium, and sodium. The calculated ionic strength of the NF concentrate is 26 mol/m³, and the concentration of dissolved organic carbon in the NF concentrate sample was 21.8 mg/L.

Table 4.3: Chemical composition of the NF concentrate and IX brine solution.

Parameter [unit]	IX brine solution	NF concentrate
DOC (mg/L)	358	22
pH	9.05	8.7
Electrical conductivity (µS/cm)	20,900	1472
Potassium (mg/L)	3.4	5.6
Magnesium (mg/L)	< 1	42.4
Calcium (mg/L)	< 1	202
Sodium (mg/L)	5,951	101
Fluorine (mg/L)	0.51	0.54
Chlorine (mg/L)	2,026	81
Bromine (mg/L)	10	< 1
Sulfate (mg/L)	7,122	400
Nitrate and nitrite (mg/L)	75.7	9.96
Phosphate (mg/L)	39	< 1
Ionic strength (mol/m³)	914	26

4.2. Laboratory results concentration technologies

4.2.1. PFAS removal efficiency

Nanofiltration concentrate

The initial PFAS concentration of the drinking water waste stream per PFAS group is shown in Figure 4.2 (1), as well as the concentration achieved after 24 hours of treatment with 10, 50, and 100 mg/L of DEXSORB+. When 100 mg/L of DEXSORB+ was used to concentrate the NF waste stream, it removed 66% of the ∑PFAS. Long-chain PFAS removal efficiencies were higher than short-chain PFAS removal efficiencies. With 93% and 99% removal for long-chain PFCA and long-chain PFSA, respectively, compared to 46% and 87% removal for short-chain PFCA and short-chain PFSA, respectively. Considering the toxicity of each individual PFAS type, the removal efficiency of PFOA equivalent concentrations (∑PEQ) was 94%.

Figure 4.2 (2) depicts the removal of PFAS using all-silica BEA zeolite. The overall removal efficiency for ∑PFAS with 200 mg/L all-silica BEA zeolites was 62%. When PFOA equivalent concentrations were taken into account, the PEQ removal efficiency reached 97%. This was the highest achieved PEQ removal among the tested technologies. The high PFOA equivalent removal was primarily due to the effective removal of long-chain PFAS, with 99% removal of PFCA and PFSA. Short-chain PFAS removal efficiency was lower, at 52% and 28% for PFCA and PFSA, respectively.

The removal of the various PFAS groups with FF is shown in 4.2 (3). To generate foam on the surface of the NF concentrate during treatment with FF, a surfactant was added. The TTAB surfactant was used at a dosage of 1.4 mg/L, resulting in the formation of a stable foam layer. The ∑PFAS removal efficiency was 76%, which was the highest ∑PFAS removal achieved by the laboratory-tested technologies for the NF concentrate. Short-chain PFCA was removed by 47%, short-chain PFSA by 96%, long-chain PFCA by 96%, and long-chain PFSA by 99%. For the PFOA equivalent concentrations, the removal efficiency was 93%.

Compared to FF, DAF required a much higher concentration of surfactant to form stable foam, specifically 36 mg/L. DAF removed the smallest fraction of PFAS from the NF concentrate, removing only 50% of ∑PFAS and reducing PFOA equivalent concentration by 75%. According to Figure 4.3 (7), long-chain PFCA and PFSA were removed more effectively, by 68% and 93%, respectively, while short-chain PFAS were removed less, by 28% for PFCA and 64% for PFSA.

Anion exchange brine Solution

As can be seen in 4.2 (4), when DEXSORB+ was utilised to treat IX brine solution, the PFAS concentration increases from the second to third dosage. This could be the result of an analytical or experimental error. Therefore, the concentrations of the second dose are taken into account to determine the PFAS removal efficiencies. When dosed at 50 mg/L, DEXSORB+ had a ∑PFAS removal efficiency of 62%. This was the most efficient removal efficiency of the three technologies tested in the laboratory for the IX waste stream. Short-chain PFCA and PFSA were removed by 55% and 72%, respectively. Long-chain PFAS removal efficiencies were 69% for PFCA and 97% for PFSA. The PFOA equivalent concentration was reduced by 79%.

The removal efficiency of 200 mg/L all-silica BEA zeolites from the IX waste stream was 35.8%. This low efficiency was primarily due to the poor removal of short-chain PFAS, as shown in Figure 4.2 (5), with only 28% and 20% removal for PFCA and PFSA, respectively. Long-chain PFCA and PFSA were removed more effectively, with 84% and 99% removal, respectively. Nevertheless, all-silica BEA zeolites demonstrated the highest removal efficiency for PFOA equivalents, reaching 82.5%, due to its higher removal effectiveness towards long-chain PFAS.

Since treating the IX brine solution with FF did not necessitate the use of a surfactant to achieve stable foam, no surfactant was used. The removal of the various PFAS groups after using FF is given in 4.2 (6). The removal efficiency of the ∑PFAS was 29%, which was the lowest achieved removal of the three tested technologies in the laboratory. Again, short-chain PFAS had a lower removal efficiency of 13% for PFCA and 38% for PFSA. The removal efficiency of long-chain PFCA and PFSA was 43.9%

and 99.0%, respectively. The removal efficiency of PFOA equivalent concentrations was 61%.

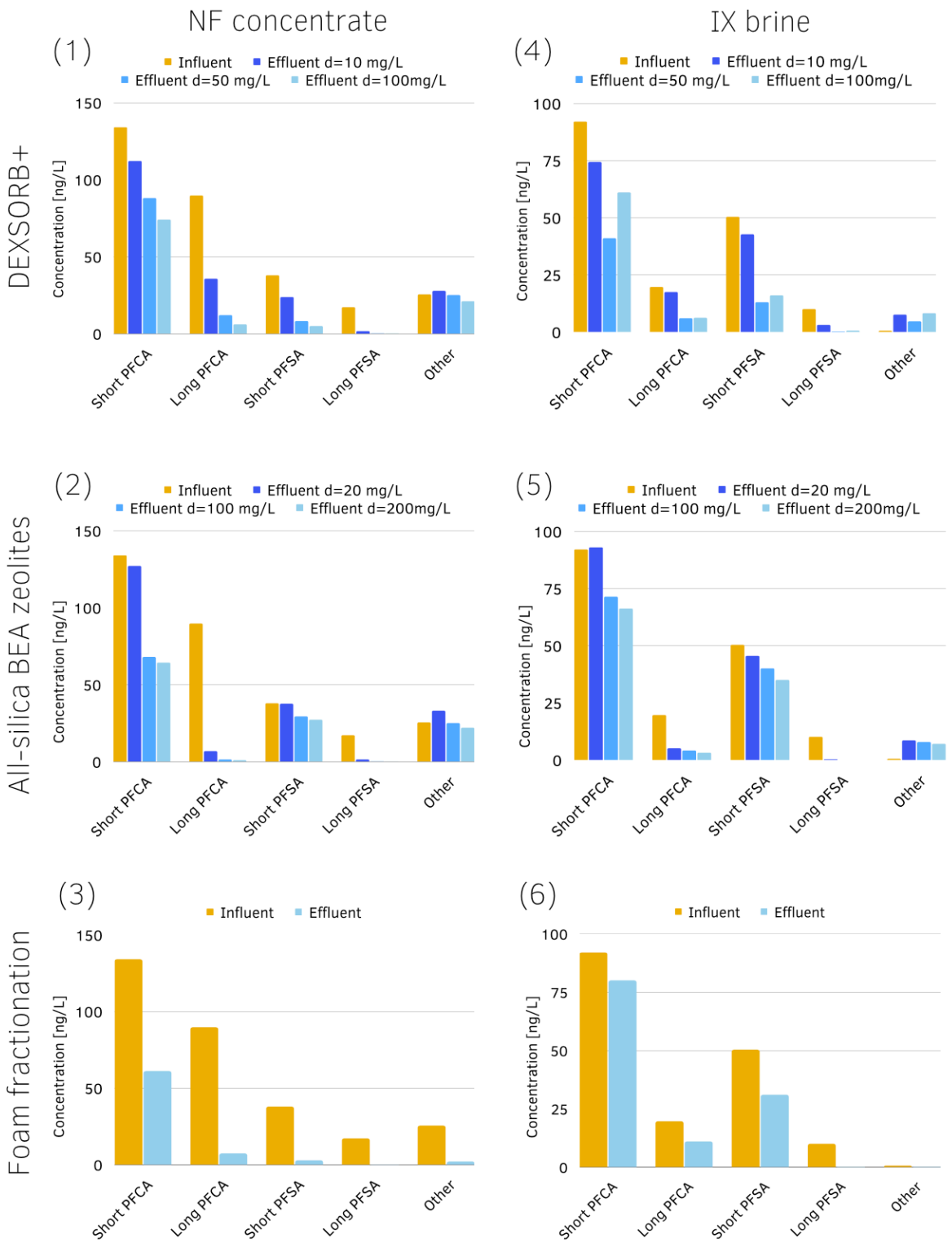

Figure 4.2: Outcomes of the laboratory tests. Influent concentration (NF and IX waste streams) and effluent concentrations after treatment of the waste streams with different concentration technologies for various PFAS groups [ng/L]. NF concentrate treated with (1) DEXSORB+, (2) all-silica BEA zeolite, (3) Foam Fractionation. IX brine solution treated with (4) DEXSORB+, (5) all-silica-BEA zeolite (6) Foam fractionation.

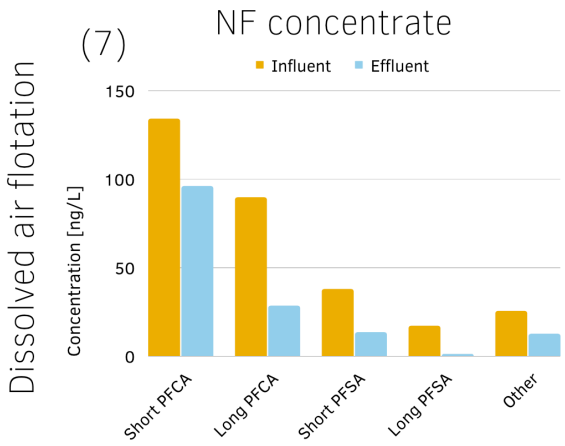

Figure 4.3: Outcomes of the laboratory tests. Influent concentration (NF waste streams) and effluent concentrations after treatment of the waste stream for various PFAS groups [ng/L]. NF concentrate treated with (7) Dissolved Air Flotation.

Treated waste stream	Concentration technology	∑PFAS RE (%)	PEQ RE (%)
NF concentrate	DEX, 100 mg/L	66	94
NF concentrate	ZEO, 200 mg/L	62	97
NF concentrate	FF	76	93
NF concentrate	DAF	50	75
IX brine	DEX, 50 mg/L	62	79
IX brine	ZEO, 200 mg/L	35	83
IX brine	FF	29	61

Table 4.4: ∑PFAS and PEQ removal efficiency (RE) achieved with concentration technologies for the two different waste streams, NF concentrate and IX brine.

For the PFAS group defined as 'other', which includes 6:2 FTS, DONA, and GenX, the concentrations increased after DEXSORB+ and all-silica BEA zeolites treatment, as can be seen in Figure 4.2. This can be due to an analytical or experimental error or due to leakage of PFAS from the used materials and equipment in the laboratory. Therefore the removal efficiencies were determined by the concentration in the waste stream after the first dose. There was no increase in concentration for this group of PFAS (6:2 FTS, DONA, and GenX) when FF and DAF were used. The PFAS concentrations and removal efficiencies for each individual PFAS type after each concentration technology can be found in appendix E.

4.2.2. Volume reduction

Table 4.5 presents the achieved volume reductions in the laboratory. For the adsorbents, the volume reduction was determined based on the volume of the regenerant solution employed for the laboratory regeneration experiments of the adsorbents. Consequently, the volume reduction was identical for both the adsorbents and both the NF concentrate and IX brine solution. A 21 mL mixture of ethanol and water (2:1) with a potassium sulfate concentration of 0.5 g/L was used to desorb the PFAS and regenerate the adsorbents, resulting in a volume reduction of 79%. In laboratory conditions, FF achieved a volume reduction of 93.8% for the NF concentrate. However, when FF was applied to the IX brine solution, a volume reduction of only 79% was achieved. Lastly, the volume reduction accomplished with DAF (pressurised water) on the NF concentrate was similar as with the FF setup (pressurised air), at 94.1%.

Treated waste stream	Concentration technology	Volume reduction (%)
NF concentrate	DEX	79
NF concentrate	ZEO	79
NF concentrate	FF	93.8
NF concentrate	DAF	94.1
IX brine	DEX	79
IX brine	ZEO	79
IX brine	FF	79.5

Table 4.5: The achieved volume reduction. The volume reduction of the adsorbents was based on the volume of regeneration solution used in the laboratory for the desorption of the PFAS.

4.2.3. PFAS Mass balances foam fractionation

The PFAS mass balances for the foam fractionation and dissolved air flotation laboratory batch experiments are shown in Figure 4.4. The mass balance was closed with 77% for the NF concentrate treated with FF and the addition of 1.4 mg/L surfactant (1), meaning 23% less ∑PFAS was measured in the foamate than was removed from the NF waste stream. The mass balance was closed with 89% when the IX brine solution was treated without the addition of a surfactant (2). For the laboratory setup with pressurised water (i.e. white water), DAF (3) had a mass balance closure of 78%, indicating that 22% of the ∑PFAS was missing. The surfactant dose was 36 mg/L in this setup and +/- 13% pressurised water was dosed.

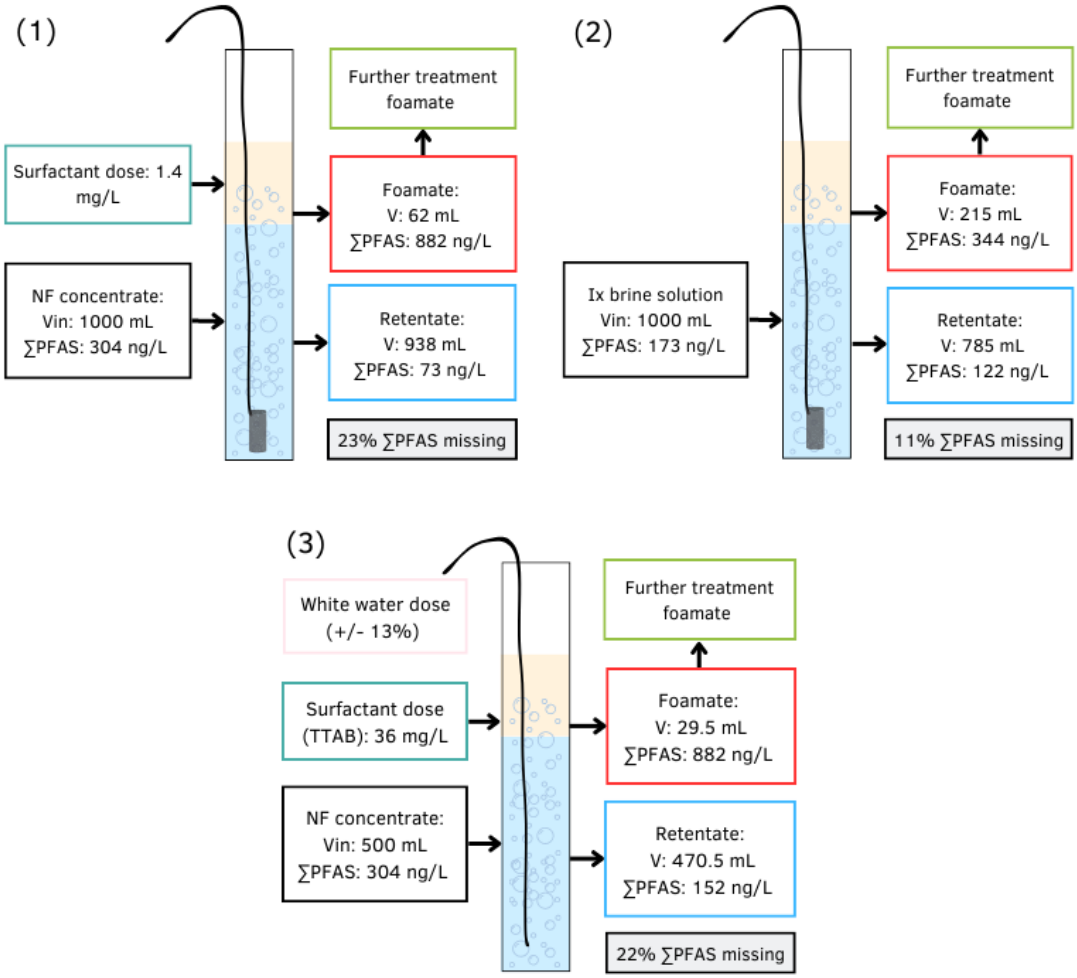

Figure 4.4: Mass balances for (1) FF treating the NF concentrate, (2) FF treating the IX brine solution, and (3) DAF treating the NF concentrate.

Furthermore, the enrichment factors of the ∑PFAS were calculated using these mass balances and are stated in table 4.6. The enrichment factor of the ∑PFAS in the foam for the NF concentrate treated with FF was 8.8. For the NF concentrate treatment with DAF, the enrichment factor of ∑PFAS in the foam was 2.9. For the IX brine solution, the FF concentration technology achieved a ∑PFAS enrichment factor of two in the foam.

Treated waste stream	Concentration technology	Enrichment factor (-)
NF concentrate	FF	8.8
NF concentrate	DAF	2.9
IX brine	FF	2

Table 4.6: Enrichment factor of ∑PFAS in the foam after treating the waste streams from NF and IX with FF or DAF.

4.2.4. Adsorption data

Freundlich Isotherms

In Tables 4.7, 4.8, and 4.9 the determined Freundlich parameters are presented. These tables include the Freundlich constant (K_F) values and the adsorption intensity (n) values for the two waste streams, NF concentrate and IX brine solution, treated with different adsorbents, namely DEXSORB+ and all-silica BEA zeolites. Appendix C contains the linearised isotherm graphs for the different PFAS types with a minimum of three data points. The Freundlich parameters are listed in the tables only when the quality of the fit of the linear isotherm was sufficient (R^2 > 0.6). For the IX brine treated with DEXSORB+, there are no PFAS isotherms that meet this criteria and hence, no Freundlich parameters are given for this specific situation.

Table 4.7: Freundlich isotherm ($q_e = K_F \cdot C_e^n$) parameters from laboratory data points: K_F value and n value for NF waste stream treated with DEXSORB+. R^2, shows the quality of the fit of the linear isotherm. Linear isotherm graphs are given appendix.

Type of PFAS	K_F $[(ng/mg) \cdot (L/ng)^n]$	n [-]	R^2
PFBA (C4)	$6.3 \cdot 10^{-22}$	17.2	0.936
PFHpA (C7)	0.676	0.99	0.999
PFOA (C8)	0.1857	1.02	0.994
PFBS (C4)	0.074	0.992	0.991
PFPeA (C5)	$1.58 \cdot 10^{-24}$	14.3	0.627

Table 4.8: Freundlich isotherm ($q_e = K_F \cdot C_e^n$) from obtained laboratory data points: K_F value and n value for NF waste stream treated with all-silica BEA zeolites. R^2, shows the quality of the fit of the linear isotherm. Linear isotherm graphs are given in the appendix.

Type of PFAS	K_F $[(ng/mg) \cdot (L/ng)^n]$	n [-]	R^2
PFBA (C4)	10^{-11}	8.43	0.998
PFHpA (C7)	0.409	0.643	0.952
PFOA (C8)	0.429	2.08	0.999

Table 4.9: Freundlich isotherm ($q_e = K_F \cdot C_e^n$) from obtained laboratory data points: K_F value and n value for IX waste stream treated with all-silica BEA zeolites. Isotherm graphs are given in the appendix. R^2, shows the quality of the fit of the linear isotherm. Linear isotherm graphs are given in the appendix.

Type of PFAS	K_F $[(ng/mg) \cdot (L/ng)^n]$	n [-]	R^2
PFHxA (C6)	0.049	0.753	0.976
PFHpA (C7)	$1.07 \cdot 10^{-5}$	7.34	0.958
PFBS (C4)	$2.69 \cdot 10^{-8}$	4.13	0.896

Figure 4.5 presents the non-linear isotherm graph with a quality of fit of R^2 > 0.85. In the case of the NF waste stream treated with DEXSORB+, PFHpA, PFBS, and PFOS demonstrate nearly linear isotherms (n≈1) and PFBA adsorption was non-favorable. The linear isotherm indicates that relative absorption remained the same over all adsorbent dosages. When the NF waste stream is treated with all-silica BEA zeolites, the adsorption isotherm was favorable for PFHpA, this indicates that PFHpA is removed well at low loading and adsorption will saturate at a specific concentration. For PFBA and PFOA, the isotherm was non favorable. This suggests that a high PFBA and PFOA loading is necessary to achieve a higher equilibrium loading on the adsorbent. Regarding the treatment of the IX brine solution, only PFHxA displays a favorable adsorption isotherm, whereas PFHpA and PFBS exhibit unfavorable behavior.

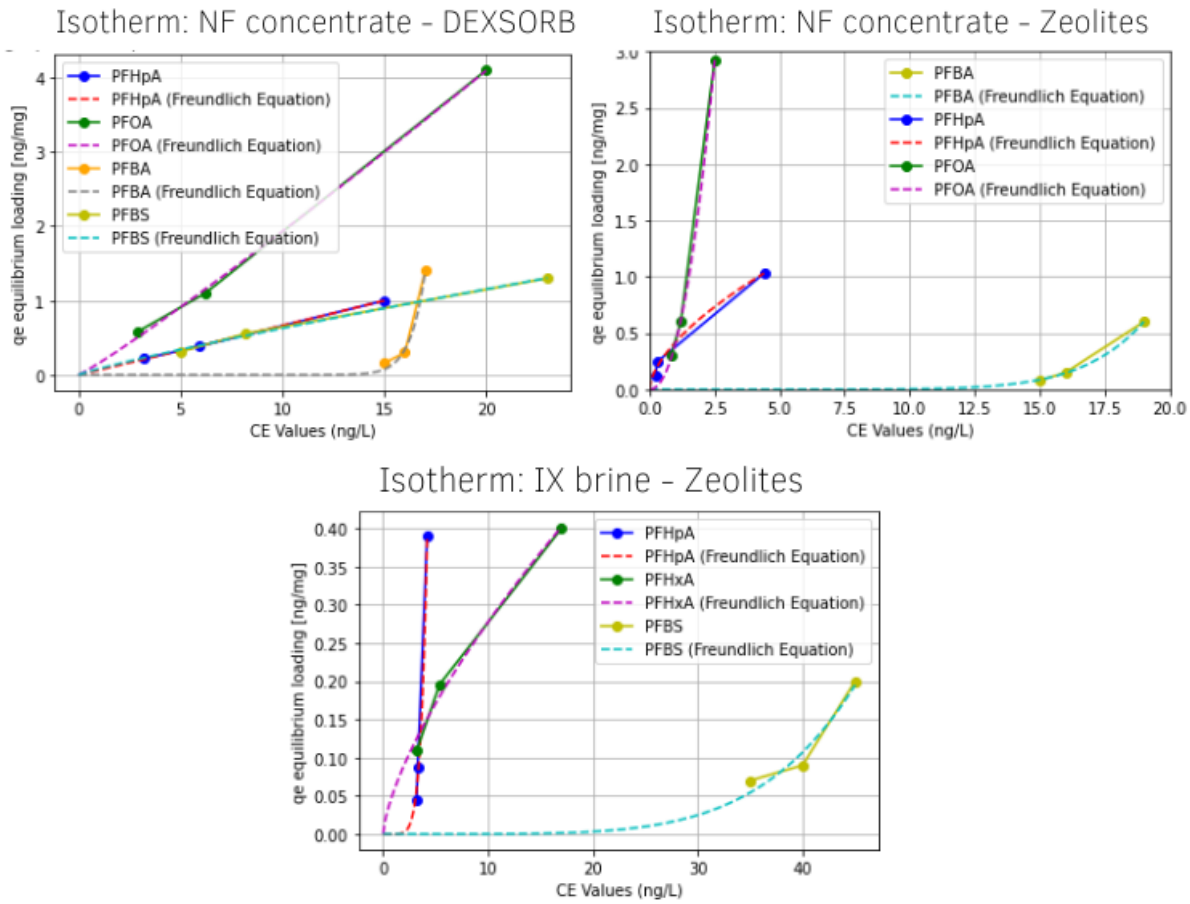

Figure 4.5: Freundlich isotherms

Regeneration efficiency

In Figure 4.6, the percentage of desorbed PFAS is shown per type of PFAS. The desorption efficiency represents the regeneration efficiency of the adsorbent materials: DEXSORB+ (100 mg/L) and all-silica BEA zeolites (200 mg/L) with the ethanol, water, and potassium sulfate mixture. The overall regeneration efficiency of DEXSORB+, which treated the NF concentrate, was 58%. When DEXSORB+ adsorbents treated the IX brine solution, the regeneration efficiency was reduced to 43%. For all-silica BEA zeolites, the regeneration efficiencies were 62% and 77% for NF concentrate and IX brine solution, respectively. For DEXSORB+ it can be observed from Figure 4.6 that PFAS with a sulfonic head were desorbed less efficiently. For all-silica BEA zeolites, the desorption of PFSA was approximately equal to the desorption efficiency of PFCA.

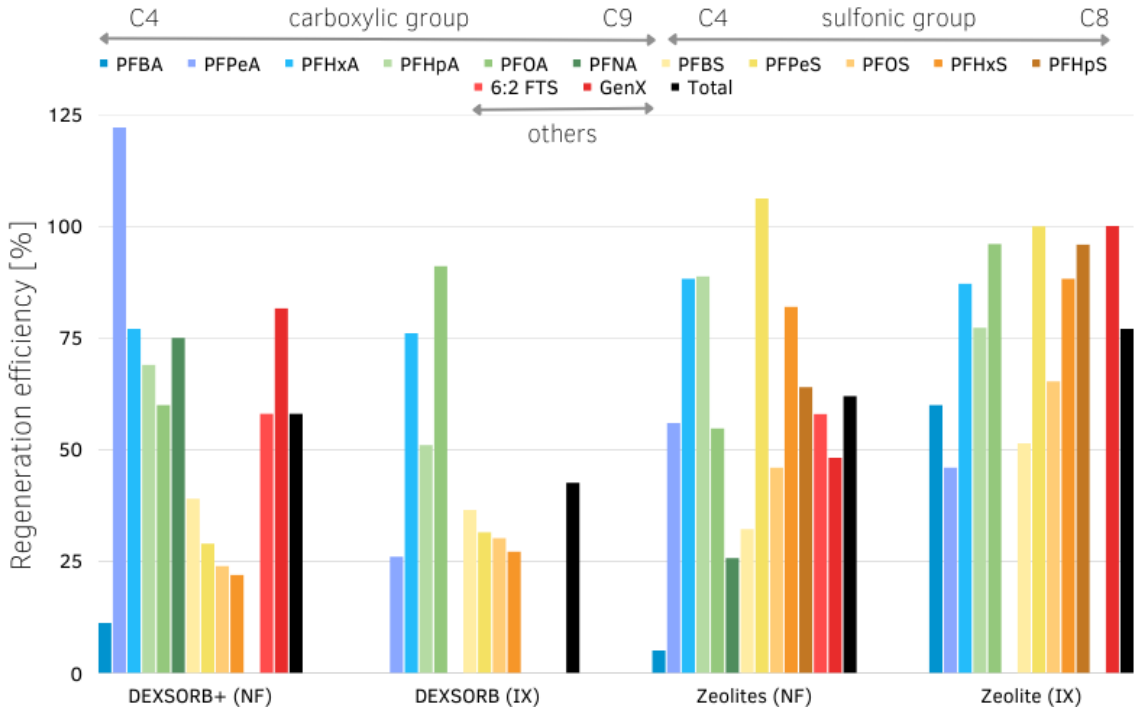

Figure 4.6: Regeneration efficiency per PFAS type for 100 mg/L DEXSORB+ that treated NF and IX waste streams and 200 mg/L all-silica BEA zeolites that treated NF and IX waste steams. Regeneration solution: ethanol and water in a ratio of 2:1, supplemented with 0.5 g/L potassium sulfate.

4.3. IMS Design modelling results

4.3.1. Nanofiltration

IMS Design was utilised to make a design of a nanofiltration membrane treatment system intended for the concentration of the IX brine solution. Figure 4.7 illustrates the obtained design of this installation, which consists of a single treatment train with four stages in parallel. The achieved permeate recovery of the NF membranes was 90%. Scaling was not an issue because there are no divalent ions (calcium and magnesium) present in the IX brine, therefore, no antiscalant or acid dosing was necessary. The energy requirement was estimated to be 1.33 kWh per cubic meter of water. Based on results from previous research, the removal efficiency of PFAS for an NF membrane, with a MWCO below 270 Da is known to be more than 90% [9].

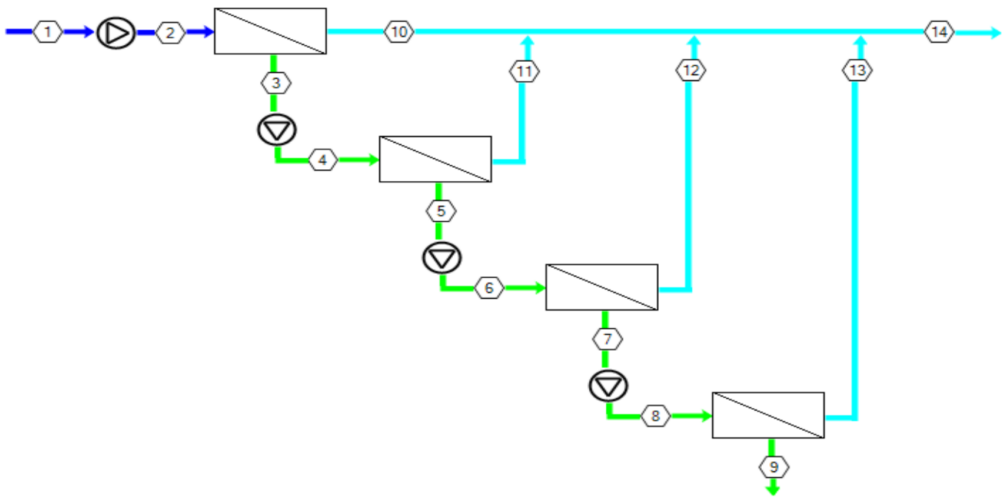

Figure 4.7: IMS Design software used to design nanofiltration treatment step for concentrating the IX brine. The input of the model is the IX brine solution characteristics measured during this research.

4.4. Costs estimations for PFAS concentration technologies

4.4.1. Adsorber filter

In Figure 4.8, the overall costs for the adsorbent filters in relation to the Empty Bed Contact Time (EBCT) are presented. The overall cost analysis takes into account construction costs, which increase with a higher EBCT due to the requirement for a larger filter volume, and regeneration costs, which decrease with a higher EBCT as less frequent regeneration is necessary. The construction costs were based on the required reactor volume and the price of the adsorbents. The breakthrough time was estimated with the Equilibrium Column model, which required isotherm data as input. The optimal EBCT concerning costs was estimated by creating a Python model that determined the regeneration and construction and the EBCT that results in minimal overall expenses.

From Figure 4.8 (1) it can be read that at an EBCT of six minutes, the overall costs (pink line) of the DEXSORB+ filter, treating the NF concentrate, would be the lowest. At this specific EBCT, regeneration of the DEXSORB+ filter should take place every ten months, resulting in an operational cost of 1.47 cents per cubic meter of produced drinking water. The construction costs for this filter were estimated at 1.2 million euros.

In the case of the all-silica BEA zeolite adsorber filter, treating the NF waste stream, the lowest overall costs were estimated at an EBCT of 4.2 minutes, as can be seen in Figure 4.8 (2). For this EBCT the filter requires approximately three regeneration cycles each year. Furthermore, the operational expenses were estimated to be 6.9 cents per cubic meter of drinking water produced. The construction cost for a filter designed to handle a flow rate of 2,000 cubic meters per hour of NF concentrate was estimated at 5 million euros.

When all-silica BEA zeolites are employed for treating the IX brine solution, minimal costs are observed at an EBCT of 13 minutes as can be seen in Figure 4.8 (3). In this scenario, PFAS breakthrough occurs approximately every 3 months, resulting in regeneration costs of 0.46 cents per cubic meter of produced drinking water. The capital expenditure for the adsorber filter, designed to treat 40 cubic meters per hour of IX brine, totals 351,000 euros.

Lastly, regarding a DEXSORB+ filter used for concentrating the IX brine, no reliable model could be developed due to the absence of isotherm data points with sufficient quality of fit. This is also visible in the results of the model in Figure 4.8 (4). Therefore, no costs were estimated based on the obtained model for the treatment of IX with a DEXSORB+ filter. However, to make a rough estimation of the costs, the Freundlich variables found for DEXSORB+ treating the NF concentrate were used. This led to an estimated operation costs of 0.16 cents per cubic meter of drinking water produced, and 125,000 euros investment costs for an adsorbent filter with a capacity to treat 40 cubic meters of brine solution per hour.

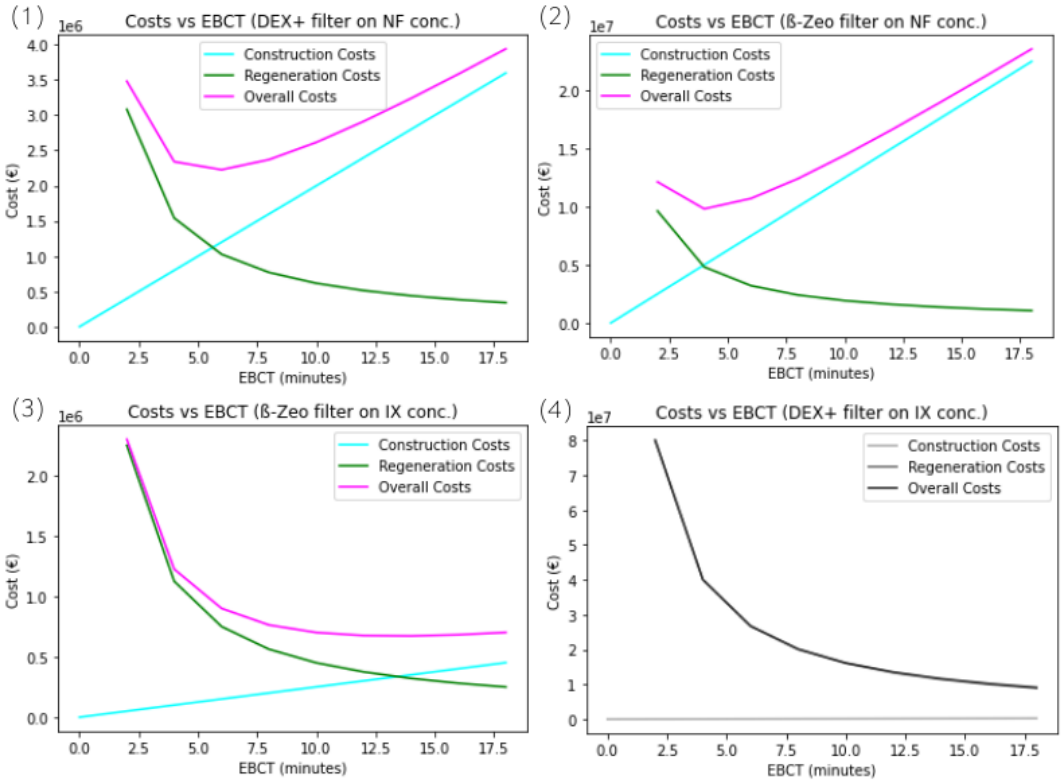

Figure 4.8: Costs variation over EBCT. The breakthrough time was determined using the Equilibrium Column Model (ECM) for PFAS types contributing most to PEQ concentration and for which a favorable isotherm was found. (1) PFOA (DEX/NF conc), (2) PFHpA (ZEO/NF conc), (3) PFHxA (ZEO/IX brine), and (4) PFBS (DEX/IX brine). Construction costs: blue line, regeneratiton costs: green line, and overall costs: pink line. Python code for generating the plot is provided in Appendix C

4.4.2. Foam fractionation

For the cost estimation of FF, it was assumed that the most significant operational expenses were energy consumption (0.55 kWh/m^3) and the required surfactant dose (1.4 mg/L for NF concentrate). The electricity rates were estimated to be €0.20/kWh. The cost of the surfactant TTAB was determined to be €7/kg [135]. Considering these factors, the operation costs per cubic meter of drinking water produced were estimated to be 3.1 cents. The construction cost for FF were assumed to be similar as those of DAF, leading to an estimated cost of 7.14 million euros for an installation that has the capacity to treat 18 million cubic meters of NF concentrate. For the treatment of the IX brine, the OPEX is slightly lower as no surfactant dose was required, resulting in an OPEX cost of 0.055 cents per cubic meter of drinking water. The construction costs for the FF plant, designed to treat 350 thousand cubic meters of brine per hour, costs 138,833 euros.

According to the 'Kostenstandaard' website, the estimated construction cost for DAF was 7.14 million euros, with an operational expenditure of 1.2 cents per cubic meter of drinking water produced. These costs include the flotation units with a water residence time of circa 10 to 15 minutes, the foam skimmer, saturated air facilities, building volume, energy supply, and general facilities such as lighting, cooling, etc. During the laboratory experiments, it was observed that the DAF requires a high surfactant dose to create stable foam in the NF concentrate, 36 mg/L. This results in an increased total operation cost of 7.5 cents per cubic meter of water.

4.4.3. Nanofiltration

The IMS Design model calculated that the operation costs would cost 54 cents per cubic meter IX brine treated. This which includes power consumption, chemical costs if required, maintenance expenses, and membrane replacement, which have a lifetime of five years. The operation costs expressed per cubic meters of drinking water produced would be 0.27 cents. The investment costs, assuming the lifetime of the installation is 15 years and membranes cost 800 euros, would be 5.95 million euros per

cubic meter of IX brine treated. Therefore the total cost of treating the IX brine with nanofiltration would cost 0.36 cents per cubic meter of produced drinking water.

4.5. Comparison

In Table 4.10, the costs of the concentration technologies, for treating the NF waste stream, are provided per cubic meter of produced drinking water. The calculation of total water costs assumes a 15-year operational lifetime for all technologies. The results indicated that a DEXSORB+ adsorber filter emerged as the most cost-effective concentration technology for the treatment of the NF concentrate. DAF (using pressurised water) was estimated to cost approximately twice as much as FF. The all-silica BEA zeolite filter proved to be the most expensive concentration technology for treating NF concentrate. The costs of treating the IX brine solution with the different concentration technologies are shown in Table 4.11. Foam fractionation was estimated to be the most economically feasible technology, followed by the DEXSORB+ adsorber filter. However, no good estimation could be made of the costs of the DEXSORB+ filter. The most expensive concentration technologies for the IX brine were nanofiltration and the all-silica BEA zeolite filter.

In the first diagram of Figure 4.9, an overview of the percentage of volume reduction and the ∑PFAS removal efficiencies achieved by various concentration technologies analysed during this research is presented. This figure shows that FF demonstrated superior performance in concentrating the NF concentrate, achieving a volume reduction of 94% while removing 75.9% of the ∑PFAS. FF, which generates air bubbles using pressurized air, outperformed Dissolved Air Flotation (DAF) where pressurised water was employed. Additionally, FF performed better when treating the NF concentrate than when the IX brine was treated, both in terms of volume reduction and ∑PFAS removal. Notably, the adsorbent exhibited a relatively consistent effect on the NF concentrate. However, for the IX brine solution, DEXSORB+ attained significantly higher removal efficiency compared to the all-silica BEA zeolite adsorbent. Nanofiltration (NF) demonstrated the highest removal efficiency for the IX brine, eliminating over 90% of the ∑PFAS while achieving a 90% volume reduction. Nonetheless, as indicated in Table 4.10, NF was estimated to be twice as expensive for treating the IX brine compared to DEXSORB+, which was found to be the second-best performing technology for the IX brine.

In the second diagram of Figure 4.9, the relationship between volume reduction and the removal efficiency for PFOA equivalent concentrations (PEQ) is depicted. Notably, all removal efficiencies exhibited an increase when considering PFOA equivalent concentrations. When treating the NF concentrate, all-silica BEA zeolites demonstrated the have the best performance in terms of PFOA equivalent removal efficiency. For the brine solution, nanofiltration remained the superior concentration technology. When comparing the two adsorbents for the IX brine, zeolites emerged as a more effective concentration technology than DEXSORB+ for the PFOA equivalent concentrations. However, it's important to acknowledge that a direct comparison between the two adsorbents is challenging due to variations in the surface/volume of the adsorbents used in the experiments.

Concentration technology	OPEX (cents/m^3 drinking water)	CAPEX (million euros)	Total costs (cents/m^3 drinking water)
ZEO	6.9	5	7.4
DEX	1.47	1.2	1.6
FF	3.1	7.14	3.8
DAF	7.5	7.14	8.2

Table 4.10: Table with an overview of the OPEX and CAPEX for the known concentration technologies when treating the NF concentrate (17.5 million m^3/year). Costs are expressed in euros per cubic meter of drinking water produced. Total costs are estimated based on the assumption that the CAPEX (investment costs) are for 15 years.

Concentration technology	OPEX (cents/m^3)	CAPEX (euros)	Total costs (cents/m^3 drinking water)
ZEO	0.46	351,000	0.49
DEX	0.16	125,000	0.17
FF	0.055	53,333	0.063
NF	0.27	893,520	0.36

Table 4.11: Table with an overview of the OPEX and CAPEX for the known concentration technologies when treating the IX brine (350 thousand m^3/year). Costs are expressed in euros per cubic meter of drinking water produced. Total costs are estimated based on the assumption that the CAPEX (investment costs) are for 15 years.)

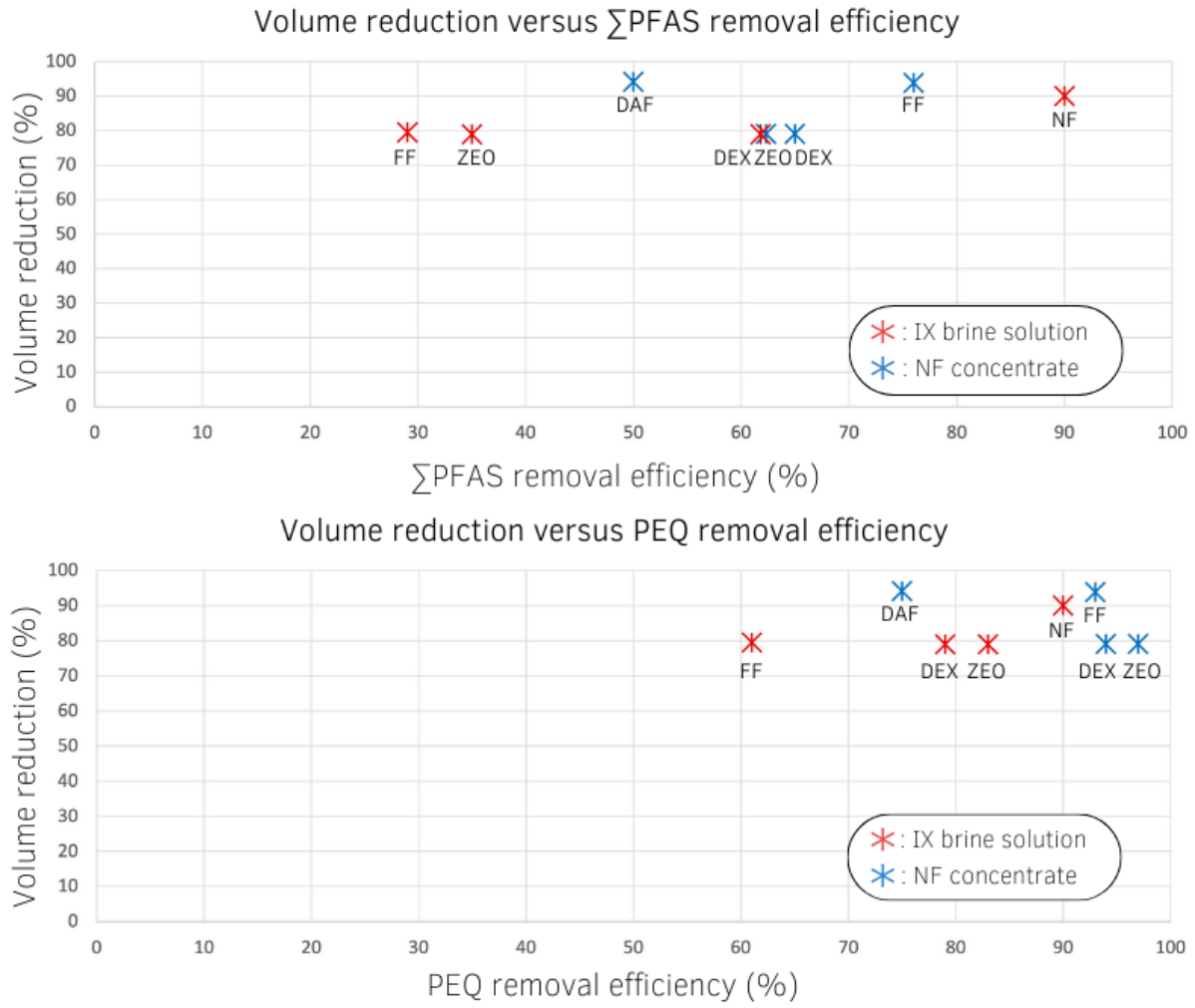

Figure 4.9: Upper Figure: volume reduction (%) versus the ∑PFAS removal efficiency (%) of the different PFAS concentration technologies treating the NF and IX waste stream. Lower Figure: volume reduction (%) versus the PEQ removal efficiency (%) of the different PFAS concentration technologies treating the NF and IX waste stream. *PEQ removal efficiency calculated based on the relative potency factors (RPF).

5 Discussion

5.1. Efficiency of PFAS removal in waste streams

5.1.1. PFAS removal with foam fractionation

During this study, two different aeration systems were tested for FF on the NF concentrate. For the first setup pressurised air was pushed through an air stone to create small air bubbles. This setup is referred to as FF. For the second setup white water, which is highly pressurised water, was injected into the wastewater-containing column which resulted in the formation of tiny air bubbles. The second setup is referred to as dissolved air flotation (DAF). During this research, it was found that the FF setup was more effective in the removal of ∑PFAS from the NF concentrate. It was expected that the smaller air bubbles of the DAF setup would lead to higher PFAS removal [77][76]. This was expected because the smaller air bubbles result in higher contact areas and lower gas flow rates [77][76][80]. However, with DAF the contact time of the air bubbles in the system was much shorter, approximately 2 minutes, than the aeration time of the FF system, which was 20 minutes. Smith et al. (2022) found that the removal of the ∑PFAS increases with increasing aeration time and airflow [75]. Higher airflow and longer aeration time result in a greater number of air bubbles carrying the PFAS to the surface, thus leading to higher removal efficiency. These two parameters were both higher with the FF setup than with the DAF setup. It is therefore hypothesised that aeration time and airflow are more dominant process variables compared to contact time and contact area. This aligns with the finding of Meng et al. who states that the aeration time is one of the most influential process variables [79]. Furthermore, when DAF is used, the waste stream is diluted with white water which also reduces the efficiency of this technology, as clean water is mixed with the polluted waste stream. Finally, the DAF system required a much higher concentration of surfactant to be able to form a stable foam layer compared to FF.

For the concentration of the NF waste stream, the highest ∑PFAS removal efficiency was achieved with foam fractionation (FF), namely 76%. Nevertheless, this removal efficiency is significantly lower than the ∑PFAS removal efficiency found by McCleaf et al. (2023). This study achieved a ∑PFAS removal efficiency of 94% from NF concentrate. The higher removal of McCleaf et al. can be explained by the fact that a higher concentration (1.6 mg/L) of surfactant was dosed and, therefore, a larger foam fraction could be collected (10%) [72]. Smith et al. (2022) state that a decreased collected foam fraction results in a decreased PFAS removal [75]. This effect is only observed at collected foam fractions ($\%_{foam}$) below 10% [75]. Therefore, increasing the collected foam fraction from 6.2% to 10% can enhance the PFAS removal efficiency. Robey et al. (2020) found that most PFAS is removed in the first 14% of collected foam volume [11]. Furthermore, the discrepancy between the two found ∑PFAS removal efficiencies can be explained even more due to the presence of more short-chained PFCA in the used NF concentrate sample compared to the NF concentrate used by McCleaf et al. (2023). Short-chain PFCA was removed by 54%, while the long-chain PFAS were all removed by more than 90%. Therefore, the share of the short-chain PFCA in the NF concentrate sample has a significant impact on the overall ∑PFAS removal efficiency.

FF performs less effectively on the IX brine solution, removing only 29% of the ∑PFAS. The differ-

ence in ∑PFAS removal efficiencies between the two different waste streams can be because the NF concentrate requires the addition of a surfactant to enhance the foamability of the waste stream, while the IX brine solution did not require the addition of a surfactant. Therefore, a cationic surfactant was only dosed for the NF concentrate treatment. According to the results of the study conducted by McCleaf et al. (2023), the addition of a cationic surfactant to the NF concentrates positively affected the ∑PFAS removal efficiency. This study showed that the removal efficiency of short-chain PFAS increased by 37% for PFPeA (C5), by 9% for PFHxA (C6), and by 34% for PFBS (C4) with the addition of the cationic surfactant. The removal efficiency of longer-chained PFAS types, namely PFOA (C8), PFHxS (C6), and PFOS (C8), remained at 99% [72]. Therefore, the addition of the surfactant might significantly influence the removal efficiency of the ∑PFAS and hence might explain the higher removal of ∑PFAS from the NF concentrate.

The study conducted by Wang et al. (2023) demonstrated that the removal efficiency increased for four tested PFAS types when natural organic matter (NOM) was present in the water matrix [56]. This might be because NOM and PFAS can bridge together due to electrostatic interactions, forming NOM-PFAS complexes [136]. Therefore, it was expected that FF removed more PFAS from the IX brine than from the NF concentrate, as the brine contains higher concentrations of NOM. This effect was not observed in the results. However, due to the addition of the surfactant in the NF waste stream, a good comparison between the ∑PFAS removal efficiency of the two different waste streams cannot be made.

Finally, based on the obtained research results, it can be concluded that the removal efficiency of long-chain PFAS is higher compared to that of short-chain PFAS. In the laboratory setup, where the NF concentrate was treated with FF, the following removal efficiencies were observed: PFBA (C4) was removed by 6.5%, PFPeA (C5) by 47.9%, PFHxA (C6) by 87%, PFHpA (C7) by 90%, and PFOA (C8) by 92%. Demonstrating the increased removal efficiency with increasing carbon chain length. The more effective removal of long-chain PFAS was already thoroughly reported by multiple studies [82][74][106][77][79]. It was stated that the removal of short-chain PFAS with FF is more challenging because of the exponentially declining partition factor with decreasing carbon chain length [106][56]. Furthermore, it was observed that the PFAS group PFSA was removed more effectively by FF than PFCA. This finding is consistent with the results reported by Dai et al. (2019) [106]. PFSA has a higher sorption affinity to the air-water interface than PFCA [137]

5.1.2. PFAS removal with DEXSORB+

50 mg/L of DEXSORB+ removed 62% of the ∑PFAS from the IX brine, which is the highest achieved removal efficiency in the laboratory for this specific waste stream. DEXSORB+ has a higher short-chain PFAS removal efficiency compared to the other laboratory-tested concentration technologies. These short-chain PFAS are mainly present in this specific waste stream sample. The higher removal of short-chained PFAS with DEXSORB+ is due to the positively charged ion added in the crosslinker that increases its efficiency to adsorb anionic PFAS, including short-chain PFAS [91]. DEXSORB+ efficiently removed 65% of the PFAS from the NF waste stream. It was discovered that the uptake of the various PFAS groups differs significantly for both waste streams. DEXSORB+ removes PFSA and long-chain PFCA better from NF concentrate than from the IX brine. On the contrary, short-chain PFCA is removed less efficiently from the NF concentrate than from the IX brine.

The concentration of natural organic matter (NOM), measured as dissolved organic carbon (DOC), is significantly higher in the IX brine solution at 358 mg/L compared to the NOM concentration in the NF concentrate at 22 mg/L. Cyclopure states that DEXSORB+ is resistant to fouling caused by NOM due to the uniform cup sizes, which enable size-exclusion of NOM. However, NOM exists in various sizes, ranging from >20,000 Da for biopolymers to <350 Da for low molecular weight (LMW) acids and LMW neutrals [138]. The molecular weight (MW) of PFAS ranges approximately from 200 to 500 Da [70], which falls within the same range as LMW-NOM. Data received from the drinking water company utilising IX, from which the IX brine sample was collected, indicates that a portion of the LMW acids and neutrals are removed from the treated water and hence may be present in the sampled IX brine solution (see Figure A.3, appendix A). Ling et al. (2020) found that micropollutants (MPs) directly compete with LMW-NOM for active sorption sites on β-cyclodextrin polymer (β-CDP), rather than higher molecular weight NOM [139]. The hypothesis is that the same competition occurs between PFAS and LMW-NOM

for DEXSORB+ as observed by Ling et al. (2020) for MPs. The study of Ching et al. (2020) reported significant inhibition of anionic and neutral PFAS adsorption from PFAS-spiked groundwater compared to spiked nano-pure water [65]. In the study of Ching et al. DEXSORB+ removed approximately 80% of four types of PFAS (PFBA, PFOA, PFBS, PFOS) from the spiked nano-pure water (pH=8.5) and around 65% from the spiked groundwater (pH=8.5, NOM = 1.1 mg/L) [65]. Ching et al. expect that this inhibition is caused by the presence of inorganic ions and LMW-NOM [65]. It is hypothesised that the reduced uptake of long-chain PFCA, short-chain PFSA, and long-chain PFSA observed in the IX brine, might be due to the competing NOM.

Furthermore, DEXSORB+ contains cationic quaternary ammonium (QA), which gives the DEXSORB+ a permanently positive charge. This enhances the adsorption affinity of β-CDP for anionic PFAS, due to the electrostatic interactions between the anionic head of the PFAS and the positive surface charge of the DEXSORB+. In the IX brine solution, the anions sulfate and chlorine are present at much higher concentrations (2,026 mg/L and 7,122 mg/L, respectively) compared to (81 mg/L and 400 mg/L, respectively) in the NF concentrate. These anions might compete with the anionic PFAS for adsorption sites. However, Wu et al. (2020) found that the influence of competing anions is not significant and that divalent cations inhibit the PFAS uptake more dominantly for β-CDP+ [140]. The electrostatic interaction between the PFAS and the positive charge of the CDP+ becomes less due to the presence of divalent cations as the anionic head groups of the PFAS bond with the cations present in the waste stream, forming neutral complexes [140]. This weakens the adsorption uptake of the CDP+ due to the reduced electrostatic interaction [140]. The divalent cations, magnesium and calcium, were present in the NF concentrate with 42 mg/L, and 202 mg/L, respectively, compared to <1 mg/L for both cations in the IX brine solution. Wu et al. (2020) also found that the inhibition due to divalent cations is more substantial for PFAS with a carboxylic head (PFCA) than for PFAS with a sulfonic head (PFSA) [140]. This study did not make a distinction between long- and short-chain PFAS, however, for long-chain PFAS, the hydrophobic interaction is the more dominant adsorption mechanism and hence, long-chain PFAS uptake might be less affected by the presence of these cations. The presence of the divalent cations in the NF waste stream might explain why DEXSORB+ removes short-chain PFCA less effectively in the NF concentrate (45%) than in the IX brine solution (55%). For the adsorbent all-silica BEA zeolites, which rely exclusively on hydrophobic interactions for the adsorption of anionic PFAS, this effect was not observed for short-chain PFCA in the NF concentrate. Wu et al. also found that hydrophobic adsorption materials exhibit lower inhibition due to divalent cations [140]

Finally, from the results, it can be observed that overall short-chain PFAS are less effective removed from both waste streams. DEXSORB+ removes PFAS primarily through the hydrophobic interaction between the fluorinated carbon chain of the PFAS and the interior of the DEXSORB+ cups [94]. The study by Yang et al. (2020) found that when the hydrophobic interaction between the PFAS chain and the adsorbent is the dominant removal mechanism, a decrease in the removal of PFAS was observed with decreasing PFAS chain length [91]. However, for DEXSORB+, the hydrophobic interaction mechanism is less dominant than for the other adsorbent due to the crosslinker chemistry of DEXSORB+. The crosslinking process allows the addition of a positively charged ion to the β-CDP, resulting in enhanced removal of PFAS, including short-chain PFAS, through the introduction of an electrostatic interaction between the anionic head of the PFAS and the added cation in the crosslinker [91]. Specifically, the PFAS group PFSA is removed more effectively which might be due to its more polar head compared to PFCA. The results of this research show the difference in short-chain PFSA removal efficiency between DEXSORB+ and all-silica BEA zeolites, DEXSORB+ removes 72% of the short-chain PFSA from the IX brine, while all-silica BEA zeolites only remove 30% of the short-chain PFSA. In the case of the NF concentrate, DEXSORB+ removes 87% of the short-chain PFSA, whereas all-silica BEA zeolites only remove 28%. This clearly demonstrates that the addition of a positively charged unit has a favorable effect on the removal of short-chain PFAS.

5.1.3. PFAS removal with all-silica BEA zeolites

All-silica BEA zeolite removed less ∑PFAS compared to the other adsorbent, DEXSORB+. However, when the PFOA equivalent concentration is considered, which takes into account the harmfulness of the individual PFAS types, all-silica BEA zeolites perform better for both waste streams. This adsorbent removes long-chain PFAS, which have a higher relative potency factor, more effectively than

DEXSORB+, resulting in a higher reduction of the PFOA equivalent concentration. The research of Li et al. (2023) concluded that the morphology, pore size, and surface functional groups of the adsorbent material play dominant roles in the adsorption of PFAS [136]. DEXSORB+ has 0.78 nm adsorbent cups, while BEA zeolites have 0.66 nm × 0.67 nm ring pores [94][141]. It can be hypothesised that the smaller pore size of the BEA zeolite or other morphological differences is slightly more effective for long-chain PFAS removal compared to the cup size and form of DEXSORB+. Van den Bergh et al. found that PFOA molecules position perfectly in the all-silica BEA zeolite. The hydrophobic chains of the PFAS go inside the channels of the zeolite, and the carboxylic heads form pairs due to hydrogen bonds that form at the intersections of these channels, leading to very favorable adsorption enthalpy [10].

All-silica BEA zeolites performs less effectively on the IX brine solution than on the NF concentrate. The concentration of NOM may again play a role in the reduced uptake of PFAS from the IX waste stream. According to Van den Bergh et al. (2020), the adsorption of PFOS (C8) on all-silica BEA zeolites decreased by 9% and 14% when the organics to PFAS ratio in the matrix was 5:1 and 15:1 (meaning a 5- or 15-time molar excess of organic competitors). However, Van den Bergh et al. did not observe a reduction of PFOA adsorption due to the presence of these organics. Further research should be conducted to investigate if there is reduced uptake of other PFAS types caused by organics in the water matrix.

Finally, the results show that all-silica BEA zeolite removes short-chain PFAS less effectively, similar as for the other laboratory-tested methods. Zeolite removes PFAS solely because it is hydrophobic. The hydrophobicity of a zeolite is determined by its silica-to-aluminium ratio (SAR). Due to the lack of the negatively charged aluminium and defects in the zeolite framework, all-silica BEA zeolites are extremely hydrophobic and can hence adsorb PFAS through the hydrophobic interaction with the PFAS chain [10]. All-silica BEA zeolites only remove PFAS through this mechanism. The lower short-chain PFAS uptake can thus be explained by the fact that the hydrophobicity of the PFAS decreases as the PFAS chain length shortens, resulting in less hydrophobic interaction between the PFAS and the zeolites [91].

5.1.4. PFAS removal with nanofiltration

According to Franke et al. (2021), nanofiltration with an MWCO lower than 270 Da removes more than 90% of the ∑PFAS [9]. This is a higher ∑PFAS removal efficiency than achieved with the laboratory-tested concentration technologies, FF, DEXSORB+, and all-silica BEA zeolites. Furthermore, after treating the PFAS-containing brine with NF, the permeate can be reused to regenerate the IX resins [98]. This is another benefit of using NF to concentrate the IX waste stream. Salehi et al. (2011) demonstrated that using a polyamide tubular NF membrane can result in a 77% reduction in salt consumption and a 90% reduction in water consumption during the regeneration process [142].

5.2. Volume reduction of the waste streams

5.2.1. Volume reduction with foam fractionation

The highest volume reduction was achieved for the NF concentrate with FF or DAF. Both technologies reduced the volume by approximately 94%, which is slightly higher than the volume reduction found during the research of McCleaf et al. (2023), who reduced the volume of the NF concentrate by 90%. For the IX brine solution, FF achieved a volume reduction of 79%. This volume reduction corresponds to the average amount of foam produced from leachate in the research of Robey et al. (2020) and McCleaf et al. (2021) which was approximately 22% and 21% of the initial volume, respectively [11] [77]. A significant difference in volume reduction was observed for FF based on the treated drinking water waste stream. The IX brine solution generated 210 mL of foam out of 1000 mL of influent (21%) without the addition of a co-surfactant, whereas 6.2% foam formation was observed from the NF concentrate with the addition of a surfactant. The IX brine did not require the addition of a surfactant to form stable foam because water with high organic carbon and high ionic strength generates foam more easily than water with lower organic matter and lower ionic strength. The higher ionic strength in the IX brine stabilizes the air bubbles which leads to the reduced likeliness of the air bubbles to break up [79]. Furthermore, the higher DOC in the brine solution leads to more foam formation. S. J. Smith et

al. (2022) found enrichment of DOC in the foam [75], indicating that DOC contributes to more foam formation. The higher concentration of DOC and ionic strength in the IX brine compared to the NF concentrate can thus explain the larger volume of foam formed from the IX brine.

The waste volumes produced by the full-scale installation of Envytech, which uses a double-stage FF treatment system, is 200-1000 liters per 30,000 cubic meters treated leachate, this corresponds with 96.7% to 99.33% volume reduction [134]. Indicating that even higher volume reduction can be achieved. This might be due to the implementation of the multi-stage FF system which, according to Wang et al. (2023), allows higher volume reduction [56].

5.2.2. Volume reduction with DEXSORB+

In the laboratory, the adsorbents were regenerated with 21 mL of the regeneration solution while treating 100 mL of the waste streams. Based on this, the volume reduction was determined. However, Cyclopure states that 19 cubic meters of, with DEXSORB+ treated water, leads to 0.34 cubic meters of regeneration solution, and hence a volume reduction of 98% [114]. This is a much larger volume reduction than determined during this research. Furthermore, the regenerant solutions of the adsorbents consist of two-thirds ethanol, which can be easily evaporated, leading to a higher volume reduction.

5.2.3. Volume reduction with all-silica BEA zeolites

The volume reduction achieved with all-silica BEA zeolites was also based on the regenerate volume used in the laboratory. On the full scale, the actual volume reduction is expected to be greater as less regeneration solution is probably required. Thermal regeneration of all-silica BEA zeolites is also feasible, after which the zeolite can be used again. Van den Bergh et al. (2020) discovered that after that the zeolites have been completely saturated with PFOA, all PFOA can be removed at 360 degrees Celsius without damaging the zeolite's framework or crystallinity [10], resulting in no new waste stream. However, it is unclear whether the PFAS is destroyed or only volatilizes at this temperature. When higher temperatures (+/- 1000 degrees Celsius) are used for regeneration, it might be possible to degrade and mineralize the PFAS on the zeolite, as it is an inorganic microporous material.

5.2.4. Volume reduction with nanofiltration

According to the IMS design modelling results, NF can effectively reduce the volume of the IX brine solution by 90%. According to the study of Korak et al. (2021), NF membranes can be used to decrease the waste brine volume by 70%. This study also states that re-use of the permeate was possible as brine for the next regeneration of the IX resins [98].

5.3. Cost of waste stream treatment

From an economic standpoint, using IX as PFAS separation technology appears to be more convenient than NF. IX generated a waste volume equivalent to 0.5% of the incoming flow, which is substantially smaller than the waste stream produced when employing NF membranes for PFAS separation. NF generates a waste stream constituting 20% of the influent flow. Consequently, the costs of the concentration technologies per cubic meter of produced drinking water are notably lower for the treatment of the IX brine than for the NF concentrate.

Among the concentration technologies, FF was identified as the least expensive for the IX brine treatment. This outcome aligns with expectations, given FF only relies on air and lacks the requirement for filter materials, chemicals, adsorbents, and regeneration solvents [75], making it a cost-effective technology. The costs of the DEXSORB+ filter for IX brine treatment could not be determined with the use of the obtained isotherm data from the conducted adsorbent experiments due to the low quality of fit, resulting in unreliable outcomes. Consequently, the Freundlich parameters of DEXSORB+ treating the NF concentrate were employed for this estimation. DEXSORB+ was estimated as the second most economically viable option. NF (as concentration technology) and all-silica BEA zeolite filters exhibited higher costs. Employing NF for IX brine concentration is expensive due to its high energy consumption and investment costs associated with NF membranes. It is hypothesised that the high operational costs of the ZEO filter compared to DEXSORB+ emerge from its low Freundlich constant (K_F). The low K_F value indicates a limited equilibrium adsorption capacity, leading to a higher likelihood of earlier PFAS

breakthrough. This results in increased operational costs due to the necessity for more frequent regenerations. Additionally, the all-silica BEA zeolite is a more costly adsorbent material than DEXSORB+, leading to higher investment costs.

As mentioned previously, PFAS separation using NF membranes leads to a larger waste stream compared to generated with IX, leading to higher costs for the concentration technologies. The most expensive technologies for concentrating the NF waste stream are DAF and again the ZEO filter. For DAF, the high cost is mainly a result of the high surfactant dose that was required to form stable foam in the NF concentrate. The high costs of the ZEO filter can once again be attributed to the lower equilibrium loading observed at the relevant concentrations of the waste stream, in comparison to the DEXSORB+ adsorbent. Overall, DEXSORB+ was the most cost-effective technology for concentrating the NF waste stream, followed by FF.

The costs determined in this study are estimations. Further research is required to establish more precise costs for each technology. For the adsorbent filter, the optimal EBCTs were determined with the goal to minimize the costs. However, it's important to note that a too-short contact time can lead to reduced PFAS removal efficiency, as there is less time for PFAS adsorption onto the material. Therefore, when determining the optimal EBCT, it is crucial to also consider this factor. The breakthrough of the adsorbent filters was estimated with the equilibrium loading (q_e), which was calculated with the Freundlich constants obtained from the conducted laboratory experiments. These experiments were only performed once due to the limit of PFAS analysis that could be carried out, and consequently, it was not possible to exclude outliers from the data. In addition, the isotherms were established with only three data points, which also makes the isotherms more prone to errors. Besides that, the reduction in adsorption efficiency of the adsorbents after multiple regeneration cycles was not examined in this study. If the adsorption capacity is reduced after only a few regeneration cycles, the adsorbent filter's cost rises considerably more. This was not incorporated into the cost estimation of this study.

5.4. Other discussion points

5.4.1. Mass balance closure

The mass balance of the NF concentrate treated with FF was found to be closed at 77% meaning 23% less ∑PFAS was measured in the foamate than was removed from the NF waste stream. Smith et al. (2022) and McCleaf et al. (2021) also had on average 41% and 30%, respectively, less ∑PFAS measured [75][77]. It was hypothesised that the incomplete PFAS mass balance could be a result of PFAS escaping into the air in the form of aerosols. However, McCleaf et al. (2023) conducted tests on a continuous FF pilot to investigate whether PFAS escaped to the air via aerosols and found no significant PFAS concentrations in the aerosols [72]. Smith et al. (2023) found that the highest loss of PFAS in aerosols corresponded to 0.3% of the total PFAS mass. However, it is expected that the actual amounts of PFAS leaving the reactor with the air is higher as not all air that exited the reactor passed through the filters [137]. Nevertheless, this does not explain the large amount of PFAS missing in the mass balance. In the case of NF treatment with DAF, the mass balance was closed at 78%, which is similar to the mass balance closure achieved with FF for NF. DAF involves more controlled air bubble formation and therefore it is assumed fewer aerosols were formed. These results thus also contradict the hypothesis that PFAS escapes through aerosols and align with the findings of McCleaf et al. (2023). To further investigate this, filters can be added on top of the column to capture aerosols that are released from the setup. The ΣPFAS, which can be desorbed from the filter with ethanol, can be measured and then included in the mass balance to verify the significance of aerosol formation for the escape of PFAS to surroundings.

Treatment of the IX brine with FF achieved a higher mass balance closure, namely 89%. McCleaf et al. (2023) discussed that an increasing dose of surfactant could lead to greater adherence of PFAS to the walls of the FF column, which may explain why the mass balance of the IX brine solution was more closed than the mass balance of the NF concentrate treatment with FF and DAF where a surfactant was dosed. To verify this, after treatment of the waste stream with FF, the walls of the column can be rinsed with ethanol. The ethanol will desorb the PFAS from the wall of the column and then the concentration of PFAS in the ethanol can be measured. This amount of PFAS, originating from the

wall of the column, can be added to the mass balance to investigate whether the mass balance is more closed.

5.4.2. Surface water quality standards

After treating the waste streams with the concentration technologies, a concentrated PFAS waste stream is produced. This waste stream can then be further treated with PFAS destruction technologies. Furthermore, a treated waste stream is formed. From this waste stream, the PFAS is removed as much as possible. It should be examined if this waste stream can be disposed of to the environment or must be treated further, including other chemicals that might still be present in the waste stream, the salinity, or the remaining PFAS. For some PFAS types, it was already found that the concentration technologies did reach the surface water quality standards set by the RIVM. However, it remains uncertain whether the surface water standards for PFOA, PFOS and GenX were met by applying the concentration technologies to the waste streams. Therefore, it is recommended that this is further investigated before discharging the treated waste stream to the surface water. The risk limit for PFOA is 0.3 ng/L, but the detection limit for measuring PFOA is 0.5 ng/L, which is higher than the risk limit set by the RIVM. The concentration of PFOA in the IX brine solution fell below the detection limit for both FF and ZEO. The detection limit for measuring PFOS is 0.2 ng/L, which is still 20 times higher than its established risk limit (10 pg/L). For GenX, the initial concentration in the IX brine solution was already below the risk limit of 10 ng/L. In the case of the NF concentrate, the initial GenX concentration was 23 ng/L. Among the laboratory-tested concentration technologies, only FF reduced the concentration of GenX below the surface water quality standard, specifically to 2.1 ng/L.

5.4.3. Freundlich Isotherms

It was difficult to obtain a good isotherms during this research due to the limited number of data points. If an experimental or analytical error occurs within this set of three data points, an isotherm could no longer be made. Furthermore, because no triplicates were made for each data point it was not possible to exclude any potential outlier from the isotherms. Therefore, the obtained Freundlich parameters should be taken with caution. For the treatment of the IX brine with DEXSORB+, no Freundlich isotherms could be made because, when the highest dose of DEXSORB+ was added to the IX waste stream, higher PFAS concentrations were measured than when a lower dose of DEXSORB+ was added. This might be due to an analytical or experimental error and makes it impossible to obtain a Freundlich isotherm with a good quality of fit.

5.4.4. Regeneration

The regeneration efficiency of the adsorbents was determined for the highest dose of DEXSORB+ (100 mg/L) and all-silica BEA zeolites (200 mg/L) after treating the NF concentrate and the IX brine. The loading on these highest doses is low, with a few ng of PFAS per mg of adsorbent. Therefore, it could be assumed that there are quite some errors in the determined regeneration efficiency. To gain a more precise insight into the desorption efficiency of the different PFAS types from the adsorbents, more tests need to be performed. Adsorbents with higher PFAS loadings should be used in these tests, with the aim of reducing the error sensitivity of the experiment.

The regeneration efficiency of DEXSORB+ was poor (43-58%). For PFOA however, 91% desorption was achieved after DEXSORB+ had treated the NF concentrate. Xiao et al. (2017) found that in the case of decafluorobiphenyl β-CD loaded with PFOA, effective desorption occurred over four regeneration cycles, as the adsorped PFAS fraction was very similar to the desorpted PFAS fraction. The authors also observed no decrease in performance for the CDP over these four cycles [92]. For the regeneration of all-silica BEA zeolites, the PFAS desorption was rather low as well (62-70%). Van den Bergh et al. (2020) found effective regeneration of all-silica BEA zeolites can be achieved by heating the zeolite to 360 degrees Celsius after which it was found that all PFOA was removed without damaging the zeolites [10],

It was observed that PFSA are desorbed less effectively from DEXSORB+ than PFCA. It is hypothesised that the positive charge of DEXSORB+ makes it more difficult to desorb PFSA due to the electrostatic interaction between the head of the PFAS and the permanent cationic compounds present in the crosslinker of DEXSORB+. For all-silica BEA zeolites, a similar removal efficiency was found for

the PFSA and PFCA. The better desorption of all-silica BEA zeolites might be because there is only a hydrophobic interaction between the PFAS and the adsorbent. For both the adsorbent materials it was observed that the type of waste stream has no significant effect on the regeneration efficiency of the adsorbents.

5.4.5. Preliminary study

It is important to note that this was a preliminary study as only a limited number of samples could be analysed. As a result, no experiments could be repeated, and no error bars were established for the data points. Furthermore, no blanks could be taken, so any PFAS leakage from the experimental setup was not researched. The results could have been influenced by PFAS leakage. Some PFAS concentrations were found to be higher after treatment compared to before the experiment. More research should be done to determine how these errors occurred. Finally, it is difficult to make an accurate comparison of concentration technologies. All concentration technologies should be further analysed. A fair comparison is only possible when all technologies have been optimized to maximize their concentration efficiency. Another important reason comparison is difficult is that the DEXSORB+ and all-silica BEA zeolites were not tested with the same adsorbent surface.

6

Conclusions

As Dutch people are currently ingesting PFAS in quantities that exceed the provisional health-based guideline, there is an urgent demand to remove PFAS from drinking water. Consequently, drinking water companies start removing PFAS from drinking water with different PFAS-separation technologies. Nanofiltration membranes and anion exchange are effective PFAS removal technologies. The disadvantage of these technologies is that they generate highly concentrated PFAS-waste streams, which are currently discharged back into the environment. This is unsustainable and maintains PFAS contamination in the environment, where it will accumulate. As a result, it is crucial to destroy PFAS before returning these drinking water waste streams to the environment. PFAS destruction methods, on the other hand, can be both energy-intensive and costly. As a result, waste volume reduction is desired in order to first concentrate the PFAS into a smaller volume before using destruction technologies. In order to save both energy and money.

In this study, the performance of different known PFAS concentration technologies were compared to each other based on their concentration efficiency, volume reduction, and cost-effectiveness for two different waste streams that were generated during drinking water treatment, which are the brine solution from anion exchange and the concentrate of nanofiltration membranes. The laboratory concentration technologies tested were foam fractionation and two different adsorption materials, DEXSORB+ and all-silica BEA zeolites. In addition, the effectiveness of concentrating the anion exchange brine solution with nanofiltration membranes was calculated using the modelling software IMS Design as it is already known that the ∑PFAS removal is ≥90% when the molecular weight cutoff is smaller than 270 Da.

According to the laboratory findings, the waste stream from nanofiltration can be treated more effectively than the anion exchange brine solution. The nanofiltration concentrate is most effectively treated by foam fractionation, achieving a removal efficiency of 76% for the ∑PFAS and concentrating it to 6.2% of the initial volume by passing pressurized air through an air stone with the addition of a cationic surfactant. Only foam fractionation was proven to be capable of removing GenX from the nanofiltration concentrate to below the RIVM's Dutch surface water quality standard of 10 ng/L. Only 50% of the PFAS was removed by dissolved air flotation, which produces smaller air bubbles than foam fractionation with the use of pressurised water. DEXSORB+ demonstrated higher ∑PFAS removal (65%) compared to the other adsorbent, all-silica BEA zeolites (62%). Both adsorbents reduced the waste volume in the laboratory by 79%.

For the concentration of the anion exchange brine solution, the ∑PFAS removal efficiencies achieved in the laboratory were 62% for DEXSORB+, 35.8% for all-silica BEA zeolites, and 29% for foam fractionation. These technologies all achieved an approximate volume reduction of 79% for the brine solution. Based on these results, it was concluded that DEXSORB+ outperformed all the other laboratory-tested technologies for the concentration of the brine solution. The IX brine solution mainly consists of short-chain PFAS, which can be most effectively eliminated by DEXSORB+. The effectiveness of this adsorbent is attributed to the presence of a cationic compound in its crosslinker, which enhances the removal of short-chain PFAS. With the use of the IMS Design software, it was determined that nanofiltration

is able to concentrate the anion exchange brine solution with 90% volume reduction while achieving ≥90% ∑PFAS removal. When considering the harmfulness of the different PFAS types, expressed as the PFOA equivalent concentration, all-silica BEA zeolites proved to be a better concentration method, for both waste streams, compared to the other laboratory-tested methods. For each concentration technology, it was observed that the removal of short-chained PFAS remains a challenge and that PFAS with a sulfonic acid head is removed more effectively compared to PFAS with a carboxylic head.

Furthermore, it can be concluded that foam fractionation is a cost-effective technology for concentrating the nanofiltration waste stream, considering the removal efficiency and volume reduction. For the concentration of the anion exchange brine solution nanofiltration is the most effective when the concentration efficiency and volume reduction are taken into account. Nevertheless, the costs are approximately two times higher than for the DEXSORB+ filter. Therefore, DEXSORB+ might be a more cost-effective concentration technology for the treatment of the IX brine solution.

Overall, it can be concluded that selecting the PFAS concentration technology with the highest removal efficiency, volume reduction, and cost-effectiveness strongly depends on the constituents in the drinking water waste stream matrix, the PFAS types within this matrix, and the PFAS regulation that must be adhered to. Accordingly, recommendations for drinking water companies must be made individually.

7

Recommendations

7.1. More than 4,000 types of PFAS

During this research, the effects of concentration technologies on a group of 25 different types of PFAS were investigated. However, more than 4,000 types of PFAS have been manufactured, and hundreds of them have been detected in environmental samples [16]. The efficiency of the investigated concentration technologies was only tested for a small group of PFAS. Further research is needed to understand the effects on other types of PFAS. To fully comprehend this problem and develop appropriate solutions, the chemical industry should report which PFAS they currently use and have used in the past and in which quantities.

7.2. Improving foam fractionation

Further research should focus on the improvement of the foam fractionation system. The effect of different co-surfactant can be further investigated. Li et al. (2021) found that the addition of a cationic surfactant, with a similar geometric shape and carbon chain length as PFOA, can enhance the removal efficiency of PFOA (C8) [81]. It might be interesting to add a mixture of different surfactants with different chain lengths (C4 and C5) and investigate whether it enhances the short-chain PFAS removal more. Furthermore, the surfactant used during this research, tetradecyltrimethylammonium bromide (TTAB), is very toxic to aquatic life and no data about its biodegradability is available. Therefore, further research should focus on finding non-toxic alternatives.

Next, the different process variables can be further optimized. For example, studies found that the enrichment factor of PFAS decreases as the airflow rate increases because a greater flow rate also led to more volume generation. However, a greater flow rate also leads to a higher PFAS removal efficiency. Therefore, an optimal should be found. Multiple studies found that a multi-stage FF system increases the enrichment factor of PFAS in the foam and higher volume reductions can be achieved, which can be further investigated to improve the efficiency of foam fractionation.

The effect of temperature on foam fractionation is unknown. Higher temperatures reduce the gas transfer rates, which can affect the air bubble formation [53]. This will be important for full-scale installation as temperatures can fluctuate depending on climate, seasons, etc.

7.3. More data of adsorption materials

Due to the limited time and samples that could be taken a great deal of data is still lacking for the adsorbent materials. First, kinetics can give more insight into the rate of adsorption, which is important in determining the applicability of the adsorbent in a treatment process. Secondly, the breakthrough time used for the cost estimations was estimated based on an Equilibrium Column Model that calculates the ideal breakthrough. Determining the exact breakthrough time would allow more precise cost estimations. Furthermore, more data points for the isotherm should be collected, now it is hard to say if a data point is an outlier, leading to a less precise isotherm. Additionally, competition data is valu-

able, measuring the ions, and DOC in the concentrated waste streams of the adsorbents to analyse if competition for adsorption sites took place. Furthermore, performing multiple regeneration cycles can give more insight on how many times the adsorbent can be re-used which also gives more insight on the sustainability of the adsorbent. These are a few points that require further research.

7.4. Blanks

Due to the limited number of PFAS analyses available during this research, no blanks were taken. However, analysis of blanks could increase the certainty of the obtained results and could explain increased PFAS concentrations after treatment. Below a few examples of blanks that should be taken are mentioned:

- Blanks from tap water that was used for producing white water. Tap water might contain background concentrations of PFAS and thus influence the initial PFAS concentrations.
- Analyse PFAS leakage for all experimental setups by using ultra-pure water (UPW) as a control for the waste streams. For example, magnetic stirrer might leak PFAS.
- Dosing DEXSORB+ and all-silica BEA zeolite to UPW. To analyse if there is PFAS leakage from the adsorbents. For DEXSORB+ as the crosslinker contains a fluorinated compound. For the all-silica BEA zeolite because for the synthesis of all-silica BEA zeolite, fluoride is used as a mineralising agent.

Except for leakage of PFAS from specific materials, some might adsorb PFAS. Therefore, it is recommended to carefully select the materials used in the laboratory.

7.5. Environmentally friendly solutions

Further research should focus on making these concentration technologies more environmentally friendly. Currently, the DEXSORB+ is crosslinked with a fluorinated compound that is acutely toxic when swallowed, all-silica BEA zeolites are synthesised using fluoride as mineralising agent [10], and foam fractionation and DAF require a dosage of toxic surfactant.

8

Reflection

8.1. Responsibility

Even though water companies have to guarantee the safety of the drinking water they provide, they are not the only ones that can be held responsible for removing PFAS from drinking water. Also, other stakeholders are involved. In this section, the aim is to answer the question: ”Who is responsible for the PFAS problems humanity is facing today?” Chemical companies, that have been producing PFAS since 1950, already knew about the harmful health effects arising from PFAS exposure. This group actively suppressed this information. They refused to take responsibility to inform the public, regulators, and their own employees about the potential health effects. This industry handles high concentrations and large volumes of highly toxic chemicals and failed to take responsibility. On the contrary, these companies discharge PFAS directly into the surface water. Hence, their acts are deteriorating the current situation, instead of solving it.

Moreover, the voluntary phase-out of PFOS and PFOA by the chemical companies resulted in the growing use of GenX and short-chain PFAS [5]. Nonetheless, these compounds cannot yet be effectively removed from the water. Further, the Environmental Protection Agency (EPA) found that GenX has even higher risks at much lower levels than PFOA and PFOS [28]. Similarly, the European Chemical Agency (ECHA) recognised PFBS (C4) as a substance of high concern. Furthermore, short-chain PFAS has higher mobility in water and soil and is already detected in very remote regions, such as Antarctica [143]. It should be questioned if the switch from long-chain PFAS to short-chain PFAS and GenX was ethical and not solely for their economic benefits. The chemical industry again did not take responsibility. Once more, new PFAS types were introduced on the market without considering their toxic effects on humans and the environment even though PFOA and PFOS were already phased out due to toxicity. I believe that the polluters should pay for the damage they have caused. In this way, the chemical companies producing, or having produced PFAS in the past, should cover the costs and reverse the damage they have created on the environment, which arose from their lack of responsibility.

PFAS does not fall in the group of chemicals added to REACH. This while REACH was established in 2007 to ensure all chemicals would be tested before entering the European market, protecting European citizens against toxic chemicals. Yet, the chemical industry lobbied within the European Union and stated that REACH would increase unemployment in the EU. PFAS was not added to REACH and the production of these toxic chemicals continued. Governments play an influential role in setting standards, regulations, and guidelines for PFAS, which in turn should motivate drinking water companies to remove PFAS from their water, forbid the discharge of toxic chemicals into the environment, or even ban the production of these chemicals. Nonetheless, the governments licensed these companies, allowing them to dispose of PFAS in surface water, without ever conducting any toxicity tests. Therefore, it can be stated that also the government did not take responsibility and is responsible. In the future, toxic chemical pollution should be prevented by reinforcing REACH.

Also wastewater treatment plans discharge PFAS into the environment, which makes them likewise

responsible for polluting the water bodies. Currently, wastewater treatment plants are not able to effectively remove PFAS and other chemicals from the wastewater. Via this route, PFAS can enter the water and contaminates both the environment and drinking water source. Moreover, also companies that utilise PFAS in their production processes can be seen as liable. A lot of consumer products contain PFAS, as mentioned in Chapter 2. These companies should also investigate the toxic effects that can arise from the ingredients they use in their products. For example, a cosmetic brand should become aware and transparent towards its clients regarding the potential health risks associated with the utilisation of its products.

Nevertheless, the chemical industry is the party that must be held accountable for the ongoing PFAS pollution and consequently should pay for it. This group was already aware of the harmful effects PFAS has and actively did not communicate this with other actors/ stakeholders as they suppressed this information.

8.2. Benefits distribution of concentrating PFAS waste streams

It is crucial that the solution for PFAS in drinking water does not lessen the urgency of finding an environmentally friendly replacement for PFAS or postpone the prohibition of PFAS. If PFAS can be removed from drinking water, it could provide temporary relief, as it directly tackles the immediate health impacts PFAS has on our health. This can alleviate the urgency of prohibiting PFAS. Furthermore, when the public sees that there are solutions being found for the polluted drinking water, they might believe that the stakeholders are making significant progress in resolving the issue. This may result in less public pressure and consequently this might slow down the actual process. Moreover, it might give people new perspectives, making the ongoing PFAS pollution seem less problematic. It is critical that finding ways to remove, concentrate and destroy PFAS from drinking water does not interfere with solving the fundamental cause of the problem, which is prohibiting the production, use, and discharge of PFAS.

Furthermore, new risks arise from concentrating the PFAS-containing drinking water waste streams. Because of the high PFAS concentrations arising from the concentration technologies, the correct safety measures must be taken at drinking water treatment plants to ensure the health of their employees. More research should be conducted on the possible risks of treating these waste streams. It was already found that foam fractionation can lead to high PFAS emissions into the air [137]. Other risks of concentrating the drinking water waste streams can be the leakage of the regeneration solution or the foamate, which contains very high concentrations of PFAS, posing a threat to the employees and the direct environment.

During this research the aim was to compare the removal efficiency, the achieved volume reduction, and the cost-effectiveness of the four known concentration technologies. However, more criteria should be considered when selecting a concentration technology, such as environmental impact, effectiveness for removal of other harmful chemicals, durability, robustness, resilience to water quality variables, etc. It can be discussed that these criteria are more important than cost-effectiveness. DEXSORB+ uses a fluorinated compound to crosslink the cyclodextrin cups to form polymers, all-silica BEA zeolites are synthesised using fluoride as mineralising agent, and for foam fractionation and dissolved air flotation, a surfactant was dosed which can be toxic to the aquatic environment. These technologies solve one problem but, also create new ones. The environmental impact of these concentration technologies should therefore be a more dominant design criterion than the costs.

8.3. What can I do

The first and significantly important step is raising people's understanding of the health risks associated with the usage of PFAS-containing products in everyday life and informing people of the alternatives and efforts they can take to limit their PFAS exposure. In this way, people can make educated decisions for themselves about which products they use on a daily basis. Not to forget, it is also very important that people understand the environmental impact of utilizing PFAS. In this way, people will understand why they should not only avoid products that contain PFAS for their personal benefit but also for the environment.

Secondly, it is critical that governmental decision-makers understand the issue of toxic chemical pollution in the aquatic environment. I will stay informed about local and national PFAS regulations and advocate for stronger regulations. I want to do this by conducting more research that can help politics to make good informed decisions for new law-making.

Finally, research can be conducted on how these concentration technologies can be used on industrial waste. In this way, chemical companies can clean their own waste streams and take their own responsibility.

References

[1] Van Dale. *PFAS*. 2022. URL: https://www.vandale.nl/gratis-woordenboek/nederlands/betekenis/PFAS#.Yx2SRi2QlQI (visited on 09/24/2022).

[2] Suman Das and Avner Ronen. “A Review on Removal and Destruction of Per- and Polyfluoroalkyl Substances (PFAS) by Novel Membranes”. In: *Membranes* 12 (2022). DOI: https://doi.org/10.3390/membranes12070662.

[3] National Institute of Environmental Health Sciences. *Perfluoroalkyl and Polyfluoroalkyl Substances (PFAS)*. 2022. URL: https://www.niehs.nih.gov/health/topics/agents/pfc/index.cfm (visited on 10/11/2022).

[4] RIVM. *pfas*. 2022. URL: https://www.rivm.nl/pfas (visited on 09/24/2022).

[5] Busra Sonmez Baghirzade et al. “Thermal Regeneration of Spent Granular Activated Carbon Presents an Opportunity to Break the Forever PFAS Cycle”. In: *Environ. Sci. Technol.* 55 (2021). DOI: https://doi.org/10.1021/acs.est.0c08224.

[6] European Chemicals Agency. *Perfluoralkyl bevattende chemische stoffen (PFAS)*. 2022. URL: https://echa.europa.eu/nl/hot-topics/perfluoroalkyl-chemicals-pfas (visited on 11/14/2022).

[7] Shanshan Liu et al. “Perfluoroalkyl substances (PFASs) in leachate, fly ash, and bottom ash from waste incineration plants: Implications for the environmental release of PFAS”. In: *Science of the Total Environment* 795 (2021). DOI: https://doi.org/10.1016/j.scitotenv.2021.148468.

[8] Fuhar Dixit et al. “PFAS removal by ion exchange resins: a review”. In: *Chemosphere* 272 (2021). DOI: 10.1016/j.chemosphere.2021.129777",keywords="Adsorption,Brinetreatment,EmergingPFAS,Long-andshort-chain,PFAS,Organicmatter,Regeneration.

[9] Vera Franke et al. “Efficient removal of per- and polyfluoroalkyl substances (PFASs) in drinking water treatment: nanofiltration combined with active carbon or anion exchange”. In: 1 (2021). DOI: https://dx.doi.org/10.1021/acsestwater.0c00141.

[10] Matthias Van den Bergh et al. “Highly Selective Removal of Perfluorinated Contaminants by Adsorption on All-Silica Zeolite Beta”. In: *Aangewandte Chemie* 59 (2020). DOI: https://doi-org.tudelft.idm.oclc.org/10.1002/ange.202002953.

[11] Nicole M. Robey et al. “Concentrating Per- and Polyfluoroalkyl Substances (PFAS) in Municipal Solid Waste Landfill Leachate Using Foam Separation”, journal = ”Environ. Sci. Technol.” In: 54 (2020). DOI: https://dx.doi.org/10.1021/acs.est.0c01266.

[12] European Environmetnal Agency. *Emerging chemical risks in Europe — ‘PFAS’*. 2023. URL: https://www.eea.europa.eu/publications/emerging-chemical-risks-in-europe (visited on 06/09/2023).

[13] Dushanthi M. Wanninayake. “Comparison of currently available PFAS remediation technologies in water: A review”. In: *Journal of Environmental Management* 283 (2021). DOI: https://doi.org/10.1016/j.jenvman.2021.111977.

[14] Utah Department of Environmental Quality. *Sources of PFAS*. 2022. URL: https://deq.utah.gov/pollutants/sources-of-pfas (visited on 11/19/2022).

[15] Vlaams Parlement. *SCHRIFTELIJKE VRAAG nr. 1172*. 2021. URL: https://docs.vlaamsparlement.be/pfile?id=1735596 (visited on 11/10/2022).

[16] Elsie M. Sunderland et al. “A review of the pathways of human exposure to poly- and perfluoroalkyl substances (PFASs) and present understanding of health effects”. In: *Journal of Exposure Science and Environmental Epidemiology volume* 29 (2019). DOI: https://doi.org/10.1038/s41370-018-0094-1.

[17] Fauconier G. et al. “Perfluorinated compounds in the aquatic food chains of two subtropical estuaries”. In: *The Science of the total environment* 719 (2020). DOI: https://doi.org/10.1016/j.scitotenv.2019.135047.

[18] Nadia Barbo et al. “Locally caught freshwater fish across the United States are likely a significant source of exposure to PFOS and other perfluorinated compounds”. In: *Environmental Research* 220 (2023). DOI: https://doi.org/10.1016/j.envres.2022.115165.

[19] Steven Lasee et al. “Targeted analysis and Total Oxidizable Precursor assay of several insecticides for PFAS”. In: *Journal of Hazardous Materials Letters* 3 (2022). DOI: https://doi.org/10.1016/j.hazl.2022.100067.

[20] RIVM. *Vragen en antwoorden over te veel blootstelling aan PFAS*. 2021. URL: https://www.rivm.nl/pfas/vraag-antwoord/efsa (visited on 01/18/2023).

[21] RIVM. *vraag en antwoord: zijn pfas schadelijk voor mijn gezondheid*. 2022. URL: https://www.rijksoverheid.nl/onderwerpen/pfas/vraag-en-antwoord/zijn-pfas-schadelijk-voor-mijn-gezondheid (visited on 09/24/2022).

[22] Swedish Chemicals Agency. *Per- and polyfluoroalkyl substances (PFAS)*. 2022. URL: https://www.kemi.se/en/chemical-substances-and-materials/highly-fluorinated-substances (visited on 12/15/2022).

[23] ITRC. *2.2 Chemistry, Terminology, and Acronyms*. 2022. URL: https://pfas-1.itrcweb.org/2-2-chemistry-terminology-and-acronyms/#2_2_2_1 (visited on 12/16/2022).

[24] Targol Teymourian et al. “A review of emerging PFAS contaminants: sources, fate, health risks, and a comprehensive assortment of recent sorbents for PFAS treatment by evaluating their mechanism”. In: *Research on Chemical Intermediates* 47 (2021). DOI: https://doi-org.tudelft.idm.oclc.org/10.1007/s11164-021-04603-7.

[25] Duning Li et al. “Functionalized bio-adsorbents for removal of perfluoroalkyl substances: A perspective”. In: *AWWA water science* (2021). DOI: https://doi.org/10.1002/aws2.1258.

[26] Emiliano Panieri et al. “PFAS Molecules: A Major Concern for the Human Health and the Environment”. In: *Toxics* 10 (2022). DOI: https://doi.org/10.3390/toxics10020044.

[27] US EPA. *Fact Sheet: 2010/2015 PFOA Stewardship Program*. 2022. URL: https://www.epa.gov/assessing-and-managing-chemicals-under-tsca/fact-sheet-20102015-pfoa-stewardship-program (visited on 12/28/2022).

[28] The Environmental Working Group. *‘Forever chemical’ GenX more toxic than previously acknowledged, says EPA*. 2021. URL: https://www.ewg.org/news-insights/statement/2021/10/forever-chemical-genx-more-toxic-previously-acknowledged-says-epa (visited on 12/28/2022).

[29] HEAL. *Another “forever chemical” – PFBS – added to Europe’s list of substances of very high concern*. 2019. URL: https://www.env-health.org/another-forever-chemical-pfbs-added-to-europes-list-of-substances-of-very-high-concern/ (visited on 12/28/2022).

[30] Fenton SE et al. “Per- and Polyfluoroalkyl Substance Toxicity and Human Health Review: Current State of Knowledge and Strategies for Informing Future Research.” In: *Environ Toxicol Chem.* 40 (2021). DOI: 10.1002/etc.4890.

[31] Erinc A et al. “Considering environmental exposures to per- and polyfluoroalkyl substances (PFAS) as risk factors for hypertensive disorders of pregnancy.” In: *Environ Res.* 197 (2021). DOI: 10.1016/j.envres.2021.111113.

[32] Olsen G. W. et al. “Half-life of serum elimination of perfluorooctanesulfonate,perfluorohexanesulfonate, and perfluorooctanoate in retired fluorochemical production workers.” In: *Environmental health perspectives* 115 (2007). DOI: https://doi.org/10.1289/ehp.10009.

[33] Katarzyna H. Kucharzyk et al. “Novel treatment technologies for PFAS compounds: A critical review”. In: *Journal of Environmental Management* 204 (2017). DOI: https://doi.org/10.1016/j.jenvman.2017.08.016.

[34] Ali Mahmoudnia. “The role of PFAS in unsettling ocean carbon sequestration”. In: *Environ. Monit. Assess.* 195 (2023). DOI: https://doi.org/10.1007/s10661-023-10912-8.

[35] National Geographic. *Plankton revealed*. 2023. URL: https://education.nationalgeographic.org/resource/plankton-revealed/ (visited on 04/24/2023).

[36] Ashley Morrow. *NASA Study Shows Oceanic Phytoplankton Declines in Northern Hemisphere*. 2017. URL: https://www.nasa.gov/feature/goddard/nasa-study-shows-oceanic-phytoplankton-declines-in-northern-hemisphere (visited on 05/29/2021).

[37] N.G.F.M. van der Aa, J. Hartmann, and C.E. Smit (RIVM). "PFAS in Nederlands drinkwater vergeleken met de nieuwe Europese Drinkwaterrichtlijn en relatie met gezondheidskundige grenswaarde van EFSA". In: *Rijksinstituut voor Volksgezondheid en Milieu* (2022). DOI: DOI10.21945/RIVM-2022-0149.

[38] Monique van der Aa, Julia Hartmann, Jan Dirk te Biesebeek. *Analyse bijdrage drinkwater en voedsel aan blootstelling EFSA-4 PFAS in Nederland en advies drinkwaterrichtwaarde*. 2021. URL: https://open.overheid.nl/repository/ronl-96b58f2a-ff24-4fdc-9f69-f8163be00e87/1/pdf/Bijlage\%201\%20RIVM\%20Advies\%204-PFAS.pdf (visited on 12/15/2022).

[39] Vereniging van Rivierwaterbedrijven. "Annual Report 2020 The Rhine". In: *Chemical engineering journal* 262 (2020).

[40] RIVM. *Risicogrenzen voor PFAS in oppervlaktewater. Doorvertaling van de gezondheidskundige grenswaarde van EFSA naar concentraties in water*. 2022. URL: https://www.rivm.nl/publicaties/risicogrenzen-voor-pfas-in-oppervlaktewater-doorvertaling-van-gezondheidskundige#:~:text=Voor%20de%20drie%20PFAS%20waarvoor,HFPO%2DDA%20(GenX). (visited on 07/06/2023).

[41] Lise M. Møller. *Danish EPA more tough on PFAS in drinking water*. 2021. URL: https://tox.dhi.dk/en/news/news/article/danish-epa-more-tough-on-pfas-in-drinking-water/ (visited on 12/15/2022).

[42] ECHA. *REACH begrijpen*. 2023. URL: https://echa.europa.eu/nl/regulations/reach/understanding-reach#:~:text=REACH\%20stands\%20for\%20Registration\%2C\%20Evaluation,force\%20on\%201\%20June\%202007. (visited on 06/11/2023).

[43] Irish Times. *Will the new EU chemicals strategy make our world less toxic?* 2021. URL: https://www.irishtimes.com/news/science/will-the-new-eu-chemicals-strategy-make-our-world-less-toxic-1.4527407 (visited on 04/08/2022).

[44] Rijksinstituut voor Volksgezondheid en Milieu. *Wat is REACH?* unknown. URL: https://www.rijksoverheid.nl/onderwerpen/gevaarlijke-stoffen/vraag-en-antwoord/wat-is-reach (visited on 04/08/2022).

[45] Groenlinks. *Chemische industrie aan banden*. 2005. URL: https://eenvandaag.avrotros.nl/item/chemische-industrie-aan-banden/ (visited on 04/08/2022).

[46] Marta Kucharska en Dziennik Gazeta Prawna. *Lobbyisten regeren in Brussel*. 2010. URL: https://voxeurop.eu/nl/lobbyisten-regeren-in-brussel/ (visited on 04/08/2022).

[47] Arjen Dijkgraaf. *Greenpeace: chemische industrie maakt REACH kapot*. 2006. URL: https://www.sciencelink.net/nieuws-and-verdieping/greenpeace-chemische-industrie-maakt-reach-kapot/5563.article (visited on 04/08/2022).

[48] European Environmental Agency. "Chemische stoffen." In: *Het milieu in Europa: de tweede balans* (unknown), pp. 109–127.

[49] Susan Lamontagne. *University of California San Francisco: Makers of PFAS 'Forever Chemicals' Covered up the Dangers*. 2023. URL: https://www.ucsf.edu/news/2023/05/425451/makers-pfas-forever-chemicals-covered-dangers (visited on 06/11/2023).

[50] Schrenk D et al. "Scientific Opinion on the risk to human health related to the presence of perfluoroalkyl substances in food." In: *EFSA Journal* 18 (2020). DOI: https://doi.org/10.2903/j.efsa.2020.6223.

[51] M.A.A. Schepens et al. "Risk assessment of exposure to PFAS through food and drinking water in the Netherlands." In: *National Institute for Public Health and the Environment* (2023). DOI: DOI10.21945/RIVM-2023-0011.

[52] USEPA. *Reducing PFAS in Drinking Water with Treatment Technologies*. 2018. URL: https://www.epa.gov/sciencematters/reducing-pfas-drinking-water-treatment-technologies (visited on 02/22/2023).

[53] Kees Roest, Thomas L. ter Laak, Hans Huiting, Wolter Siegers, Nienke Meekel (KWR), Coen de Jong, Martijn de Jong, Martijn van Houten, Tessa Pancras, Wim Plaisier, Joost Dalmijn. *Performance of water treatment systems for PFAS removal*. 2021. URL: https://www.concawe.eu/wp-content/uploads/Rpt_21-5.pdf (visited on 11/21/2022).

[54] Nadine Belkouteb et al. "Removal of per- and polyfluoroalkyl substances (PFASs) in a full-scale drinking water treatment plant: Long-term performance of granular activated carbon (GAC) and influence of flow-rate". In: *Water Research* 182 (2020). DOI: https://doi.org/10.1016/j.watres.2020.115913.

[55] Marcel Riegel, Brigitte Haist-Gulde, and Frank Sacher. "Sorptive removal of short-chain perfluoroalkyl substances (PFAS) during drinking water treatment using activated carbon and anion exchanger". In: *Environmental Sciences Europe* 35 (2023). DOI: https://doi.org/10.1186/s12302-023-00716-5.

[56] Yifei Wang et al. "Removing per- and polyfluoroalkyl substances (PFAS) in water by foam fractionation". In: *Chemosphere* 311 (2022). DOI: https://doi.org/10.1016/j.chemosphere.2022.137004.

[57] Rebecca DiStefano et al. "Thermal destruction of PFAS during full-scale reactivation of PFAS-laden granular activated carbon". In: *Remediation* 32 (2022). DOI: https://doi.org/10.1002/rem.21735.

[58] A. Alsbaiee et al. "Rapid removal of organic micropollutants from water by a porous β-cyclodextrin polymer." In: *Nature* 529 (2016). DOI: https://doi.org/10.1038/nature16185.

[59] Nobuhisa Watanabe et al. "Residual organic fluorinated compounds from thermal treatment of PFOA, PFHxA and PFOS adsorbed onto granular activated carbon (GAC)". In: *Journal of Material Cycles and Waste* 18 (2016). DOI: 10.1007/s10163-016-0532-x.

[60] Tasha Stoiber, Sydney Evans, and Olga V. Naidenko. "Disposal of products and materials containing per- and polyfluoroalkyl substances (PFAS): A cyclical problem". In: *Chemosphere* 260 (2020). DOI: https://doi.org/10.1016/j.chemosphere.2020.127659.

[61] Du Pont Chemical company. *TECHNICAL GUIDANCE FOR REMOVAL OF PFAS USING ION EXCHANGE RESINS*. 2020. URL: https://www.dupont.com/content/dam/dupont/amer/us/en/corporate/PFAS/Guide\%20for\%20PFAS\%20Removal\%20Using\%20Ion\%20Exchange\%20ResinsFIN.pdf (visited on 01/03/2023).

[62] Fuhar Dixit, Shadan Ghavam Mostafavi Benoit Barbeau, and Madjid Mohseni. "Removal of legacy PFAS and other fluorotelomers: Optimized regeneration strategies in DOM-rich waters". In: *Water Research* 183 (2020). DOI: https://doi.org/10.1016/j.watres.2020.116098.

[63] Chao Zeng et al. "Removing per- and polyfluoroalkyl substances from groundwaters using activated carbon and ion exchange resin packed columns". In: *AWWA Wat Sci.* 1172 (2020). DOI: https://doi.org/10.1002/aws2.1172.

[64] Steve Woodard, John Berry, and Brandon Newman. "Ion exchange resin for PFAS removal and pilot test comparison to GAC". In: *Remediation Journal* 27 (2017). DOI: 10.1002/rem.21515.

[65] Casey Ching et al. "β□Cyclodextrin Polymers with Different Cross-Linkers and Ion- Exchange Resins Exhibit Variable Adsorption of Anionic, Zwitterionic, and Nonionic PFASs". In: *Environ. Sci. Technol.* 54 (2020). DOI: https://dx.doi.org/10.1021/acs.est.0c04028.

[66] Treavor H. Boyer et al. "Anion exchange resin removal of per- and polyfluoroalkyl substances (PFAS) from impacted water: A critical review". In: *Water Research* 200 (2021). DOI: https://doi.org/10.1016/j.watres.2021.117244.

[67] Minnesota Pollution Control Agency. *Evaluation of Current Alternatives and Estimated Cost Curves for PFAS Removal and Destruction from Municipal Wastewater, Biosolids, Landfill Leachate, and Compost Contact Water*. 2023. URL: https://www.pca.state.mn.us/sites/default/files/c-pfc1-26.pdf (visited on 06/22/2023).

[68] Dr. ir. Kim Maren Lompe and Prof.dr.ir. Doris van Halem. *Ion exchange and biological IEX*. 2020. URL: https://brightspace.tudelft.nl/d2l/le/content/399357/viewContent/2290461/View (visited on 02/22/2023).

[69] Zhen Liu et al. “Alleviating the burden of ion exchange brine in water treatment: From operational strategies to brine management”. In: *Water Research* 205 (2021). DOI: https://doi.org/10.1016/j.watres.2021.117728.

[70] Vera Franke et al. “The Price of Really Clean Water: Combining Nanofiltration with Granular Activated Carbon and Anion Exchange Resins for the Removal of Per- And Polyfluoralkyl Substances (PFASs) in Drinking Water Production”. In: *Environmental science Water Research and Technology* (2019). DOI: 10.1039/C9EW00286C.

[71] Bas Heijman. *Micropollutants removal*. 2020. URL: https://brightspace.tudelft.nl/d2l/le/content/399357/viewContent/2543795/View (visited on 02/23/2023).

[72] Philip McCleaf, William Stefansson, and Lutz Ahrens. “Drinking water nanofiltration with concentrate foam fractionation—A novel approach for removal of per- and polyfluoroalkyl substances (PFAS)”. In: *Water Research* 232 (2023). DOI: https://doi.org/10.1016/j.watres.2023.119688.

[73] I. Kamalanathan. *Foam Fractionation of surfactant-protein mixtures*. 2015. URL: https://pure.manchester.ac.uk/ws/portalfiles/portal/54575628/FULL_TEXT.PDF (visited on 04/03/2023).

[74] David J. Burns, Paul Stevenson, and Peter J.C. Murphy. “PFAS removal from groundwaters using Surface Active Foam Fractionation”. In: *Remedation* 31 (2021). DOI: 10.1002/rem.21694.

[75] Sanne J. Smith et al. “Pilot-Scale Continuous Foam Fractionation for the Removal of Per- and Polyfluoroalkyl Substances (PFAS) from Landfill Leachate”. In: *ACS EST Water* 2 (2022). DOI: https://doi.org/10.1021/acsestwater.2c00032.

[76] J. Merz et al. “Purification and identification of a novel cutinase from Coprinopsis cinerea by adsorptive bubble separation”. In: *Separation and Purification Technology* 69 (2009). DOI: https://doi.org/10.1016/j.seppur.2009.06.021.

[77] Philip McCleaf, Ylva Kjellgren, and Lutz Ahrens. “Foam fractionation removal of multiple per- and polyfluoroalkyl substances from landfill leachate”. In: *AWWA Water Science* 3 (2021). DOI: fhttps://doi.org/10.1002/aws2.1238.

[78] Mark L. Brusseau. “The influence of molecular structure on the adsorption of PFAS to fluid-fluid interfaces: Using QSPR to predict interfacial adsorption coefficients”. In: *Water Research* 152 (2019). DOI: https://doi.org/10.1016/j.watres.2018.12.057.

[79] Pingping Meng et al. “Efficient removal of perfluorooctane sulfonate from aqueous film-forming foam solution by aeration-foam collection”. In: *Chemosphere* 203 (2018). DOI: https://doi.org/10.1016/j.chemosphere.2018.03.183.

[80] Jinfeng Chai et al. “Effect of Bubble Velocity and pH Step Changes on the Foam Fractionation of Sporamin”. In: *Agricultural food chemistry* 46 (1998). DOI: https://doi.org/10.1021/jf970929b.

[81] Yueh-Feng Li et al. “Perfluorooctanoic acid (PFOA) removal by flotation with cationic surfactants”. In: *Chemosphere* 266 (2021). DOI: https://doi.org/10.1016/j.chemosphere.2020.128949.

[82] Thomas Buckley et al. “Effect of different co-foaming agents on PFAS removal from the environment by foam fractionation”. In: *Water Research* 230 (2022). DOI: https://doi.org/10.1016/j.watres.2022.119532.

[83] William Stefansson. “Thesis. Evaluation of PFAS removal from nanofiltration membrane concentrate using foam fractionation”. In: *Uppsala Universiteit* (2022).

[84] Madjid Delkash, Babak Ebrazi Bakhshayesh, and Hossein Kazemian. “Using zeolitic adsorbents to cleanup special wastewater streams: A review”. In: *Microporous and Mesoporous Materials* 214 (2015). DOI: https://doi.org/10.1016/j.micromeso.2015.04.039.

[85] Sanny Verma, Rajender S. Varma, and Mallikarjuna N. Nadagouda. “Remediation and mineralization processes for per- and polyfluoroalkyl substances (PFAS) in water: A review”. In: *Science of the Total Environment* 794 (2021). DOI: https://doi.org/10.1016/j.scitotenv.2021.148987.

[86] James J. Licato, Gregory D. Foster, and Thomas B. Huff. “Zeolite Composite Materials for the Simultaneous Removal of Pharmaceuticals, Personal Care Products, and Perfluorinated Alkyl Substances in Water Treatment”. In: 2 (2022). DOI: https://doi.org/10.1021/acsestwater.2c00024.

[87] Yousheng Tao et al. “Mesopore-Modified Zeolites: Preparation, Characterization, and Applications”. In: *Chem. Rev.* 106 (2006). DOI: https://doi.org/10.1021/cr040204o.

[88] American Chemical Society. *Cyclodextrins*. 2022. URL: https://www.acs.org/molecule-of-the-week/archive/c/cyclodextrins.html (visited on 12/31/2022).

[89] Barinya Seresirikachorn and Maliheh Ghadiri. *Targeting Chronic Inflammatory Lung Diseases Using Advanced Drug Delivery Systems*. Elsevier & Academic Press, 2020.

[90] C.Y. de Jong MSc and T.P.M. Spit BSc and A. Veldhoen and P.T. Li MSc. *Stowa: HAALBAARHEIDSSTUDIE DEXFILTER: INNOVATIE IN ADSORBENTIA*. 2021. URL: https://www.stowa.nl/publicaties/haalbaarheidsstudie-dexfilter-innovatie-adsorbentia-ipmv (visited on 02/13/2023).

[91] A. Yang et al. “Cyclodextrin polymers with nitrogen-containing tripodal crosslinkers for efficient PFAS adsorption”. In: *ACS Materials Letters* 2 (2020). DOI: DOI:10.1021/acsmaterialslett.0c00240.

[92] Leilei Xiao et al. “β□Cyclodextrin Polymer Network Sequesters Perfluorooctanoic Acid at Environmentally Relevant Concentrations”. In: *Journal of the American Chemical Society* 139 (2017). DOI: https://doi-org.tudelft.idm.oclc.org/10.1021/jacs.7b02381.

[93] Syeda S.E.Z. et al. “Recent Advancements in Cyclodextrin-Based Adsorbents for the Removal of Hazardous Pollutants from Waters.” In: *Polymers* 14 (2022). DOI: https://doi.org/10.3390/polym14122341.

[94] Cyclopure. *DEXSORB® Environmental Applications for Engineered Treatment Systems*. 2021. URL: https://cyclopure.com/wp-content/uploads/2022/05/2022-05-31_Handout_DEXSORB-in-Engineered-Systems-v3.pdf (visited on 01/18/2023).

[95] Damian E. Helbling and William R. Dichtel. “Rational Design and Implementation of Novel Polymer Adsorbents for Selective Uptake of PFAS from Groundwater”. In: *SERDP* (2022).

[96] Barin Gokhan. “Novel cyclodextrin adsorbents for selective removal of PFAS”. In: *American Chemical Society.* ().

[97] National Library of Medicine. *Tetrafluoroterephthalonitrile*. 2023. URL: https://pubchem.ncbi.nlm.nih.gov/compound/Tetrafluoroterephthalonitrile#datasheet=LCSS&section=Identifiers (visited on 06/09/2023).

[98] Julie A. Korak, Leah C. Flint, and Miguel Arias-Paić. “Decreasing waste brine volume from anion exchange with nanofiltration: implications for multiple treatment cycles”. In: *Environ. Sci.: Water Res. Technol.* 7 (2021). DOI: 10.1039/d1ew00001b.

[99] CDM Smith. *PFAS destruction*. 2022. URL: https://www.cdmsmith.com/en/Client-Solutions/Insights/PFAS-Destruction (visited on 11/29/2022).

[100] Feng Xiao et al. “Thermal Stability and Decomposition of Perfluoroalkyl Substances on Spent Granular Activated Carbon”. In: *Environmental Science Technology* 7 (2020). DOI: 10.1021/acs.estlett.0c00114.

[101] USEPA. *Per- and Polyfluoroalkyl Substances (PFAS): Incineration to Manage PFAS Waste Streams*. 2020. URL: https://www.epa.gov/sites/default/files/2019-09/documents/technical_brief_pfas_incineration_ioaa_approved_final_july_2019.pdf (visited on 12/01/2022).

[102] Parimal Pal. “Chapter 6 - Industry-Specific Water Treatment: Case Studies”. In: *Industrial Water Treatment Process Technology* (2017), pp. 243–511. DOI: https://doi.org/10.1016/B978-0-12-810391-3.00006-0..

[103] Paul M. Dombrowski et al. “Technology review and evaluation of different chemical oxidation conditions on treatability of PFAS”. In: *Remediation* 28 (2018). DOI: https://doi.org/10.1002/rem.21555.

[104] Blossom Nwedo Nzeribe et al. “Physico-Chemical Processes for the Treatment of Per- And Polyfluoroalkyl Substances (PFAS): A review”. In: *Critical Reviews in Environmental Science and Technology* 49 (2019). DOI: https://doi-org.tudelft.idm.oclc.org/10.1080/10643389.2018.1542916F.

[105] Dushanthi M. Wanninayake. “Comparison of currently available PFAS remediation technologies in water: A review”. In: *Journal of Environmental Management* 283 (2021). DOI: https://doi.org/10.1016/j.jenvman.2021.111977.

[106] Xiaodong Dai et al. “Comparative study of PFAS treatment by UV, UV/ozone, and fractionations with air and ozonated air”. In: *Environmental Science: Water Research Technology* 5 (2019). DOI: https://doi-org.tudelft.idm.oclc.org/10.1039/C9EW00701F.

[107] ITRC. *PFAS: Treatment Technologies*. 2022. URL: https://pfas-1.itrcweb.org/12-treatment-technologies/ (visited on 11/29/2022).

[108] A. van Nieuwenhuijzen and B. Bloks and A. Essed and C. de Jong. *Verkenning Technologische mogelijkheden voor verwijdering van geneesmiddelen uit afvalwater*. 2017. URL: https://www.stowa.nl/sites/default/files/assets/PUBLICATIES/Publicaties%202017/STOWA%202017-36%20%20defversie.pdf (visited on 12/13/2022).

[109] Yean Ling Pang, Ahmad Zuhairi Abdullah, and Subhash Bhatia. “Review on sonochemical methods in the presence of catalysts and chemical additives for treatment of organic pollutants in wastewater”. In: *Desalination* 277 (2011). DOI: https://doi.org/10.1016/j.desal.2011.04.049.

[110] Huimin Caoa, Weilan Zhang Cuiping Wang, and Yanna Liang. “Sonochemical degradation of poly- and perfluoroalkyl substances – A review”. In: *Ultrasonics-Sonochemistry* 69 (2020). DOI: https://doi.org/10.1016/j.ultsonch.2020.105245.

[111] Clean Water Wave CIC. *Environmental impact of wastewater on marine ecosystems, and decentralised water treatment systems that bring power and responsibility back to local communities for cost effective and efficient water treatment.* 2022. URL: https://www.goesfoundation.com/media/2130/eden-circle.pdf (visited on 11/29/2022).

[112] Zhiming Zhang et al. “Biodegradation of per- and polyfluoroalkyl substances (PFAS): A review”. In: *Bioresource Technology* 344 (2022). DOI: https://doi.org/10.1016/j.biortech.2021.126223.

[113] PressPacs. *Farewell to ‘forever’ – Destroying PFAS by grinding it up with a new additive*. 2023. URL: https://www.acs.org/pressroom/presspacs/2023/january/farewell-to-forever-destroying-pfas-by-grinding-it-up-with-new-additive.html (visited on 06/13/2023).

[114] Poonam Kulkarni et al. “TURNKEY MOBILE TREATMENT OF PFAS: USING A CYCLODEXTRIN SORBENT AND MECHANOCHEMISTRY FOR SEQUESTRATION, CONCENTRATION, AND DESTRUCTION”. In: *GSI Environmental Inc. andd Cyclopure* ().

[115] USEPA. *POTENTIAL PFAS DESTRUCTION TECHNOLOGY: ELECTROCHEMICAL OXIDATION*. 2021. URL: https://www.epa.gov/sites/default/files/2021-01/documents/pitt_research_brief_electrochemical_oxidation_final_jan_25_2021_508.pdf (visited on 12/04/2022).

[116] Jelena Radjenovic and David L. Sedlak. “Challenges and Opportunities for Electrochemical Processes as Next-Generation Technologies for the Treatment of Contaminated Water”. In: *Environ. Sci. Technol.* 49 (2015). DOI: https://doi-org.tudelft.idm.oclc.org/10.1021/acs.est.5b02414.

[117] Vital Fluid. *Plasma activated water*. 2021. URL: https://vitalfluid.nl/plasma-activated-water/ (visited on 12/06/2022).

[118] John van Winkle. *Air Force tests plasma reactor to degrade, destroy synthetic chemical compounds in groundwater*. 2019. URL: https://www.af.mil/News/Article-Display/Article/2009997/air-force-tests-plasma-reactor-to-degrade-destroy-synthetic-chemical-compounds/ (visited on 12/06/2022).

[119] Hannah Thomasy. *Innovators Tackle Toxic "Forever Chemicals"*. 2022. URL: https://eos.org/articles/innovators-tackle-toxic-forever-chemicals (visited on 12/06/2022).

[120] Muhammad Jehanzaib Khan et al. "Effectiveness of Non-Thermal Plasma Induced Degradation ofPer- and Polyfluoroalkyl Substances from Water". In: *Water* 14 (2022). DOI: 10.3390/w14091408.

[121] Gunnar R. Stratton et al. "Plasma-Based Water Treatment: Efficient Transformation of Perfluoroalkyl Substances in Prepared Solutions and Contaminated Groundwater". In: *Environ. Sci. Technol.* 51 (2017). DOI: https://doi-org.tudelft.idm.oclc.org/10.1021/acs.est.6b04215.

[122] Olga S.Arvaniti et al. "Reductive degradation of perfluorinated compounds in water using Mg-aminoclay coated nanoscale zero valent iron". In: *Chemical engineering journal* 262 (2015). DOI: https://doi.org/10.1016/j.cej.2014.09.079.

[123] Sanny Verma et al. "Recent Advances on PFAS Degradation via Thermal and Nonthermal Methods". In: *Chemical Engineering Journal Advances* 100421 (2022). DOI: https://doi.org/10.1016/j.ceja.2022.100421.

[124] Viktor Polishchuk et al. "Investigation of the Efficiency of Wet Biodiesel Purification". In: *EPD Sciences* 154 (2020). DOI: https://doi.org/10.1051/e3sconf/202015402006.

[125] Bharat Chandramouli et al. "Sorption of per- and polyfluoroalkyl substances (PFASs) on filter media: Implications for phase partitioning studies". In: *Environmental Chemistry* 34 (2014). DOI: https://doi-org.tudelft.idm.oclc.org/10.1002/etc.2751.

[126] Alan Gabelman - Amercian Institute of Chemical Engineering (AIChE. *Adsorption Basics: Part 1*. 2017. URL: https://www.aiche.org/sites/default/files/docs/pages/adsorption_basics_part_1.pdf (visited on 06/28/2023).

[127] T. Guleria. "Investigating Critical Parameters of Dissolved Air Flotation for Solid-Liquid Separation with Different Influents". In: *Tu Delft repository* (2019).

[128] Carl Roth. *Safety data sheet Tetradecyltrimethylammonium bromide ≥ 96%, extra pure*. 2022. URL: https://www.carlroth.com/medias/SDB-7452-GB-EN.pdf?context=bWFzdGVyfHNlY3VyaXR5RGF0YXNoZWV0c3wyODU5NjB8YXBwbGljYXRpb24vcGRmfHNlY3VyaXR5RGF0YXNoZWV0cy9oN2IvaDEzLzkwODQwMzU0NjUyNDYucGRmfGJmNWNkOGNiNTQxNmE2N2MzOWM3NGMxYzU0OWQxY2Q4ZDdiN2Y2ZTJmNDkyODdiMGNiZmEzZmNjNWU2YWQwZTA (visited on 06/28/2023).

[129] Waternet:Amsterdamse Waterleidingduinen. *Waterzuivering Hoe de Amsterdamse Waterleidingduinen het water zuiveren.* 2023. URL: https://awd.waternet.nl/beleef/waterzuivering/#:~:text=Tegenwoordig%20zuiveren%20we%20jaarlijks%20maar,een%20natuurlijke%20manier%20verder%20gezuiverd. (visited on 07/03/2024).

[130] Eckhard Worch. *Adsorption Technology in Water Treatment. Fundamentals, processes, and modeling.* De Gruyter, 2012. ISBN: 978-3-11-024022-1.

[131] Cyclopure. *DEXSORB+® A High Affinity Adsorbent for the Removal of PFAS from Water*. 2021. URL: https://cyclopure.com/wp-content/uploads/2020/07/2020-06-25_DEXSORB_ProductSheet.pdf (visited on 06/08/2023).

[132] GlobalPetrolPrices. *Ethanol prices, litre, 07-Aug-2023*. 2023. URL: https://www.globalpetrolprices.com/ethanol_prices/ (visited on 08/07/2023).

[133] Intratec. *Potassium Sulfate Price by country*. 2018. URL: https://www.intratec.us/chemical-markets/potassium-sulfate-price (visited on 06/16/2022).

[134] Envytech. *PFAS Treatment and remediation – water*. 2023. URL: https://envytechsolutions.com/pfas-treatment-and-remediation-water/ (visited on 06/19/2023).

[135] EChemi.com. *Tetradecyltrimethylammonium Bromide*. 2023. URL: https://www.echemi.com/searchGoods/pid_Seven6037-cetrimide.html (visited on 07/03/2023).

[136] Huarui Li et al. “A recent overview of per- and polyfluoroalkyl substances (PFAS) removal by functional framework materials”. In: *Chemical Engineering Journal* 452 (2023). DOI: https://doi.org/10.1016/j.cej.2022.139202.

[137] Sanne J. Smith et al. “Foam fractionation for removal of per- and polyfluoroalkyl substances: Towards closing the mass balance”. In: *Science of The Total Environment* 871 (2023). DOI: https://doi.org/10.1016/j.scitotenv.2023.162050.

[138] Simon Francesc Xavier et al. “NOM characterization by LC-OCD in a SWRO desalination line.” In: *Desalination and water treatment.* 51 (2013). DOI: 10.1080/19443994.2012.704693.

[139] Yuhan Ling et al. “Evaluating the effects of water matrix constituents on micropollutant removal by activated carbon and β-cyclodextrin polymer adsorbents”. In: *Water Research* 173 (2020). DOI: https://doi.org/10.1016/j.watres.2020.115551.

[140] Congyue Wu et al. “Exploring the factors that influence the adsorption of anionic PFAS on conventional and emerging adsorbents in aquatic matrices”. In: *Water Research* 182 (2020). DOI: https://doi.org/10.1016/j.watres.2020.115950.

[141] Ueno K et al. “Hydrophobic *BEA-Type Zeolite Membranes on Tubular Silica Supports for Alcohol/Water Separation by Pervaporation”. In: *Membranes (Basel)* 9 (2019). DOI: 10.3390/membranes9070086.

[142] Fakhreddin Salehi, Seyed M.A. Razavi, and Mohammad Elahi. “Purifying anion exchange resin regeneration effluent using polyamide nanofiltration membrane”. In: *Desalination* 278 (2011). DOI: https://doi.org/10.1016/j.desal.2011.04.067.

[143] William F. Hartz et al. “Levels and distribution profiles of Per- and Polyfluoroalkyl Substances (PFAS) in a high Arctic Svalbard ice core”. In: *Science of the total environment* 871 (2023). DOI: https://doi.org/10.1016/j.scitotenv.2023.161830.

A

Data separation technologies

PFAS separation performance

PFAS concentrations in influent

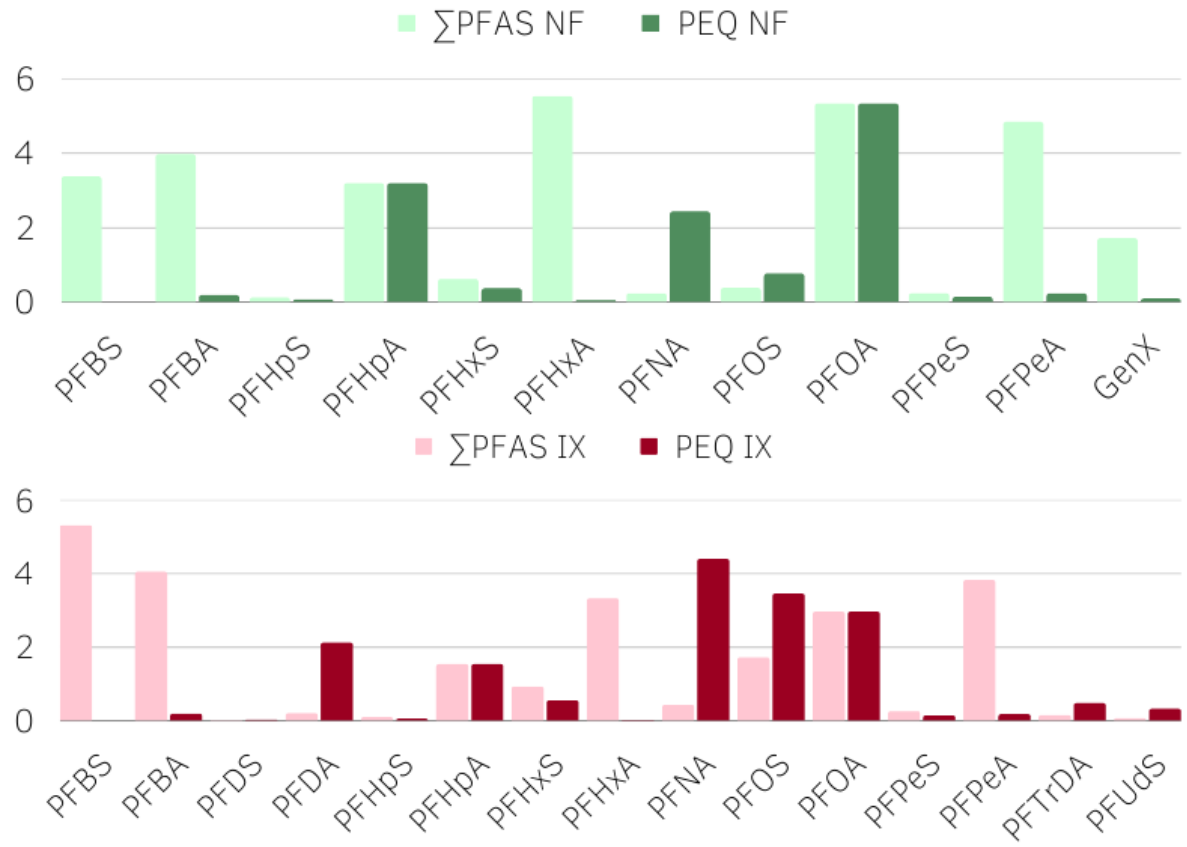

Figure A.1: PFAS concentrations [ng/L] and PFOA equivalent concentrations [ng PEQ/L] in NF and IX influent. Data obtained from companies. PFOA equivalent concentrations are determined with the relative potency factors (RPFs).

Figure A.1 illustrates the incoming PFAS concentrations for both drinking water treatment technologies: NF and IX. In the NF influent, the most prevalent PFAS types were PFHxA, PFOA, and PFPeA. Among these, PFOA itself was the primary contributor to the PFOA equivalent concentration. The influent for anion exchange primarily contains PFBS. However, the significant contributors to the PFOA equivalent concentration are PFNA, PFOS, and PFOA. The influent concentrations of the NF membranes is 30.3

ng/L for the sum of all PFAS which corresponds to a PFOA equivalent concentration of 12.8 ng/L. For anion exchange the sum of PFAS influent concentration is 23.7 ng/L, and the PFOA equivalent concentration is 16.4 PEQ/L.

Table A.1: Measured PFAS concentrations (∑PFAS) and PFOA equivalent concentrations (PEQ) in the influnet of nanofiltration (green) and anion exchange (red).

Influent	∑PFAS [ng/L]	PFOA eq. [ng PEQ/L]
Nanofiltration	30.3	12.8
Anion exchange	23.7	16.4

Mass balances

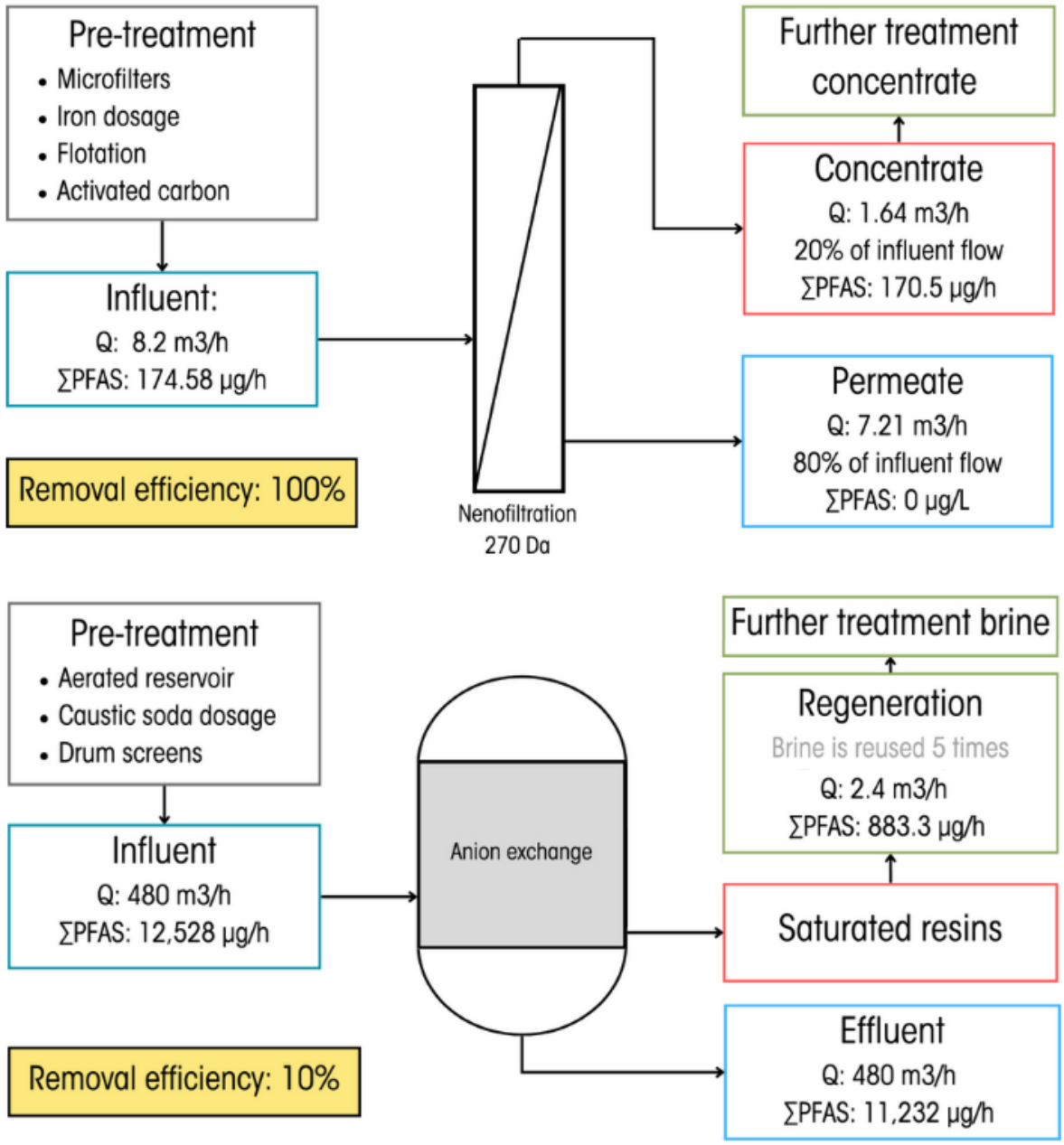

Figure A.2: Mass balances of nanofiltration and anion exchange. Data for specific influent water matrices. Data concentrations and volume of water treated per day obtained from drinking water company.

In Figure A.2, the mass balances of the separation technologies, based on data from water companies, are depicted. NF generates a waste stream equivalent to 20% of the incoming volume, which contains approximately ten times more PFAS than the influent. The PFAS removal efficiency of NF is 100%. However, the anion exchange reactor only removes 10% of the PFAS, but it generates a significantly smaller waste stream compared to NF. A brine solution is used for the regeneration of the saturated resins, this brine solution can be reused five times after the polluted brine is discharged. The volume of the IX brine formed from the influent of the IX is 0.5%.

Figure A.3, shows the removal of the different types of NOM by the anion exchange reactor from which the IX brine solution was collected. This figure indicates that LMW acids and neutrals are removed with IX and hence will be present in the brine solution. Due to their LWM these types of NOM will compete for sorption sites with PFAS.

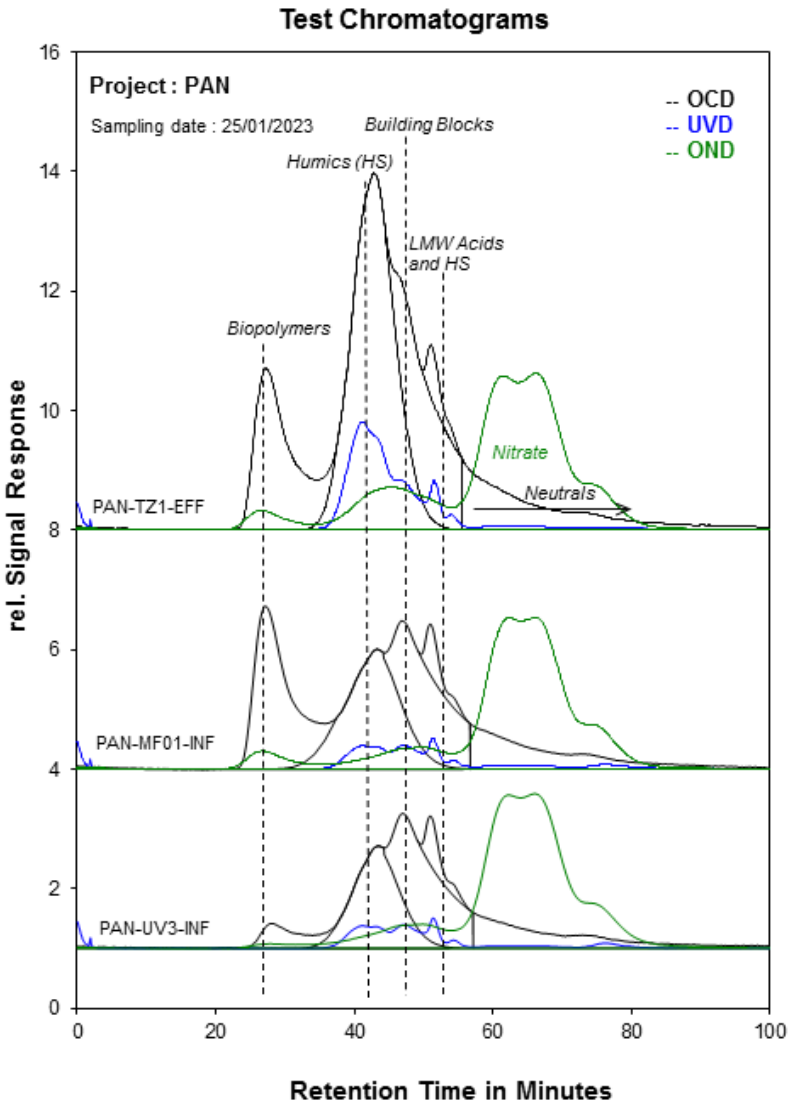

Figure A.3: Data from drinking water company that uses IX and from which the IX sample is collected. Graph shows the removal of the specific types of NOM with the IX. Graph one shows the influent NOM concentrations, and graph two shows the effluent of the IX reactor.

B

Laboratory data

Initial tests with octanoic acid

Initial tests were conducted with octanoic acid to analyse the performance of DEXSORB+ and all-silica BEA zeolites adsorbents. Demiwater spiked with octanoic acid was treated with different dosages of DEXSORB+ and all-silica BEA zeolites. The final concentration was analysed after 24 hours.

Table B.1: Removal efficiency of octanoic acid with DEXSORB+ and all-silica BEA zeolites adsorbents

Adsorbent	Dosage [mg/L]	Initial DOC concentration	Final DOC concentration	Removal efficiency [%]	Equilibrium loading (mg/g)
DEXS	10	25.91	25.05	3.3	86
DEXS	20	25.91	24.62	5	64.5
DEXS	50	25.91	21.77	19	82.8
Zeo	10	25.91	24.46	5.6	145
Zeo	20	25.91	23.82	8.1	104.5
Zeo	50	25.91	23.36	9.8	51
DEXS	10	23.44	22.21	5.2	
DEXS	20	23.44	22.15	5.5	
DEXS	50	23.44	20.90	10.8	
DEXS	100	23.44	21.11	9.9	
Zeo	10	23.44	21.46	8.45	
Zeo	20	23.44	20.89	10.9	
Zeo	50	23.44	18.60	20.65	
Zeo	100	23.44	14.82	36.77	

Experimental setups

Figure B.1 shows the different foam layers formed for the different waste streams and for the air stone compared to the dissolved air flotation that utilises white water.

Air stone
Anion exchange brine
No surfactant

Air stone
Nanofiltration concentrate
Surfactant dose: 1.4 mg/L

DAF
Nanofiltration concentrate
Surfactant dose: 36 mg/L

Figure B.1: Figures of the foam formation in laboratory setups for different waste streams and different aeration technologies.

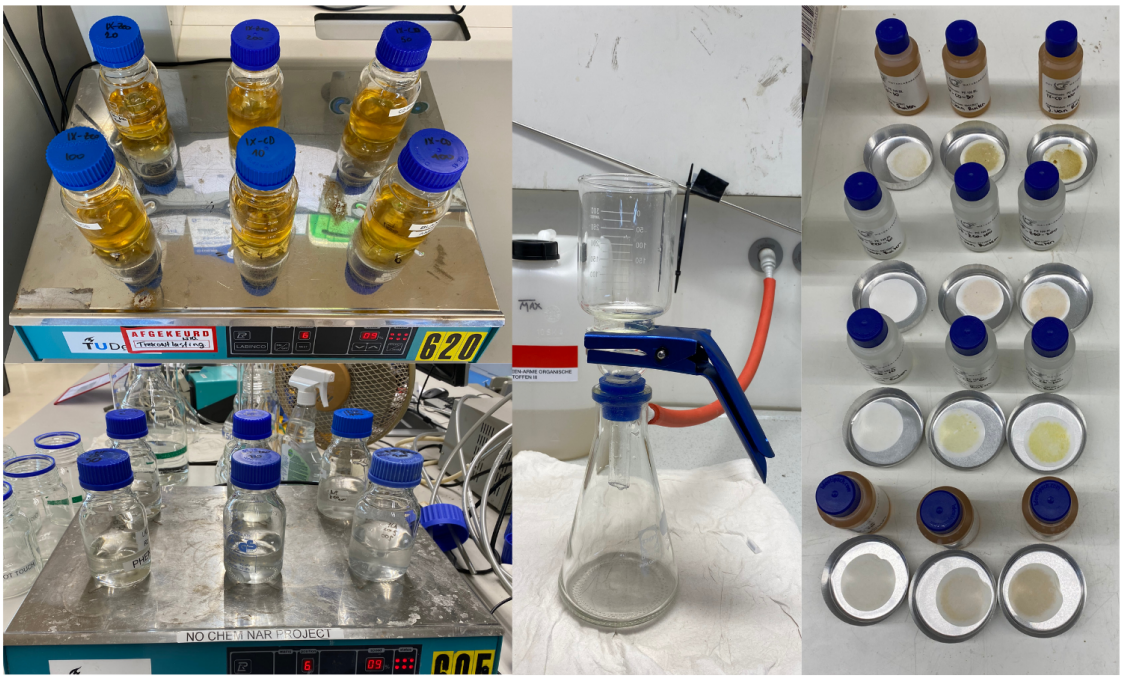

Magnetic stirrer
Equilibrium tests - 24h

Glass filter holder with
glass fiber filter paper

Filtered samples
Adosrbents on filter paper

Figure B.2: Figures of the adsorbents tests in laboratory for different waste streams.

C

Isotherm graphs

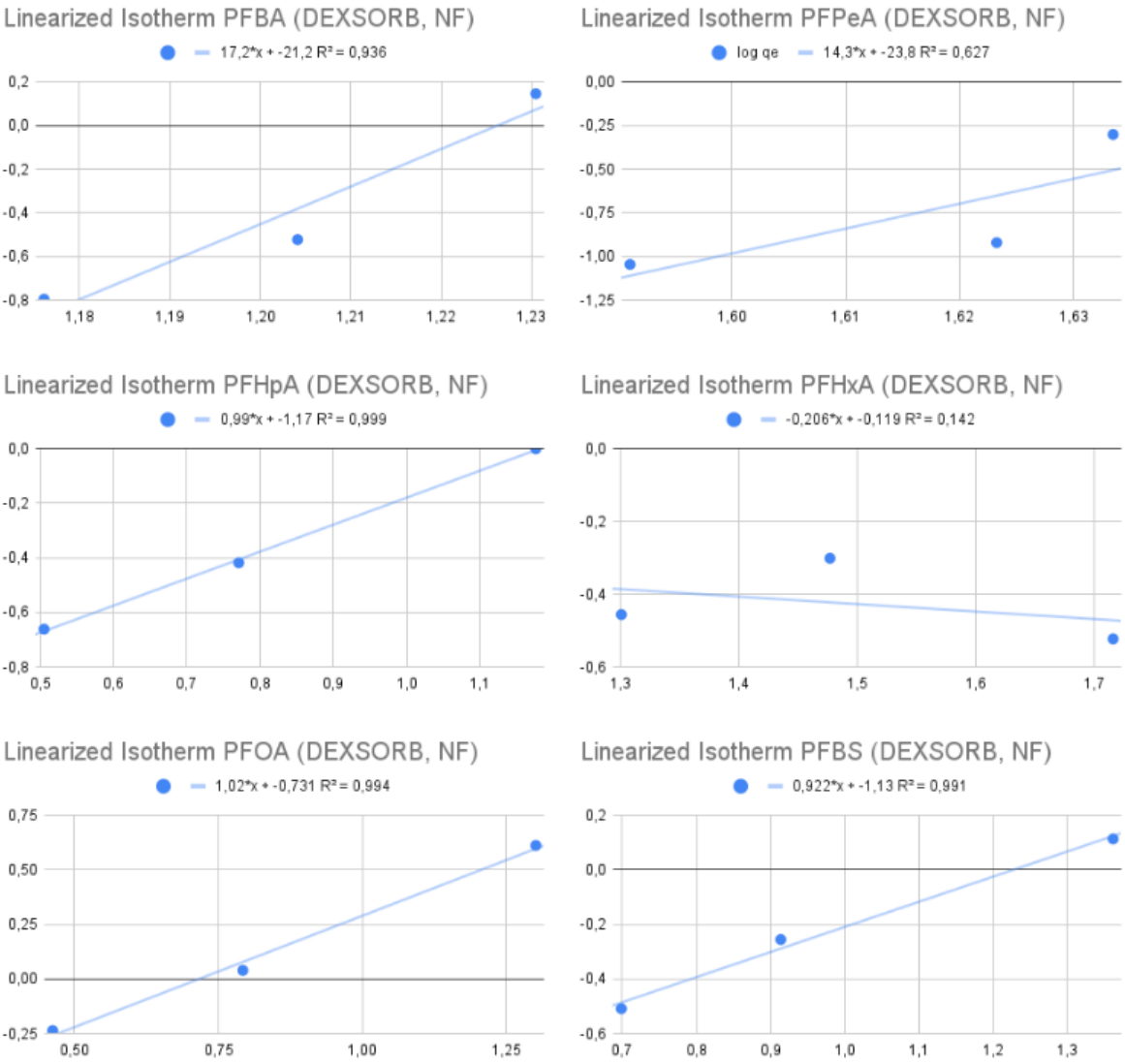

Figure C.1: Linear isotherm graphs for NF waste stream treated with DEXSORB+ for PFAS removal. Isotherms were only made for PFAS with three data points.

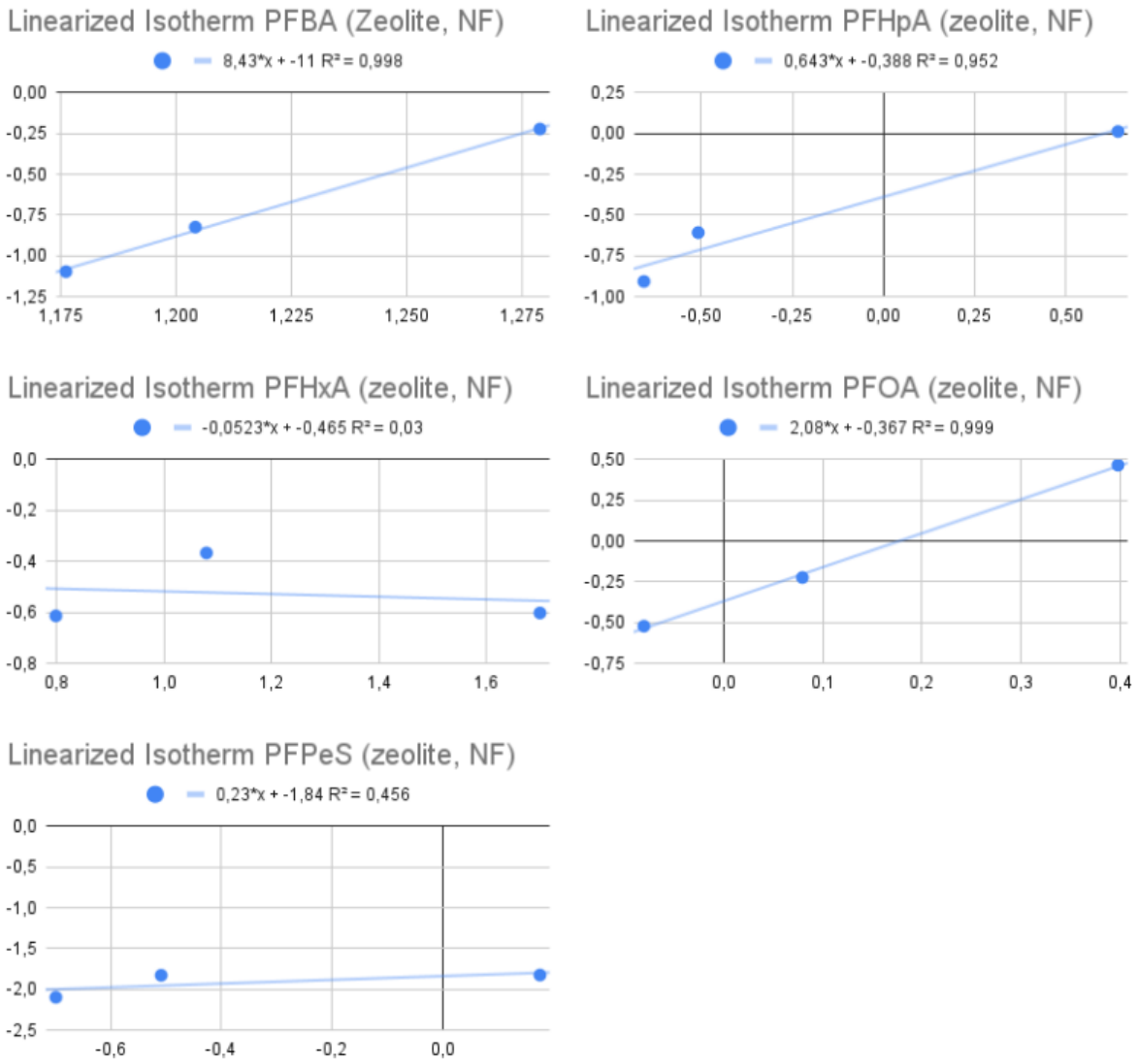

Figure C.2: Linear isotherm graphs for NF waste stream treated with all-silica BEA zeolites for PFAS removal. Isotherms were only made for PFAS with three data points.

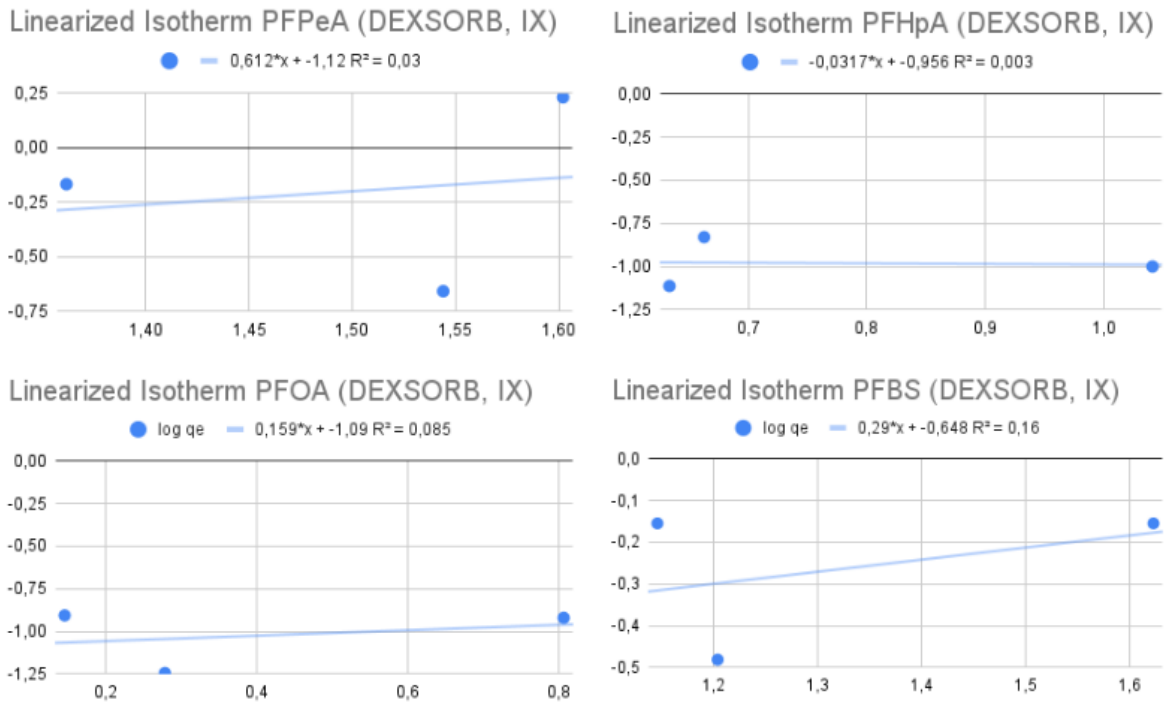

Figure C.3: Linear isotherm graphs for IX waste stream treated with DEXSORB+ for PFAS removal. Isotherms were only made for PFAS with three data points.

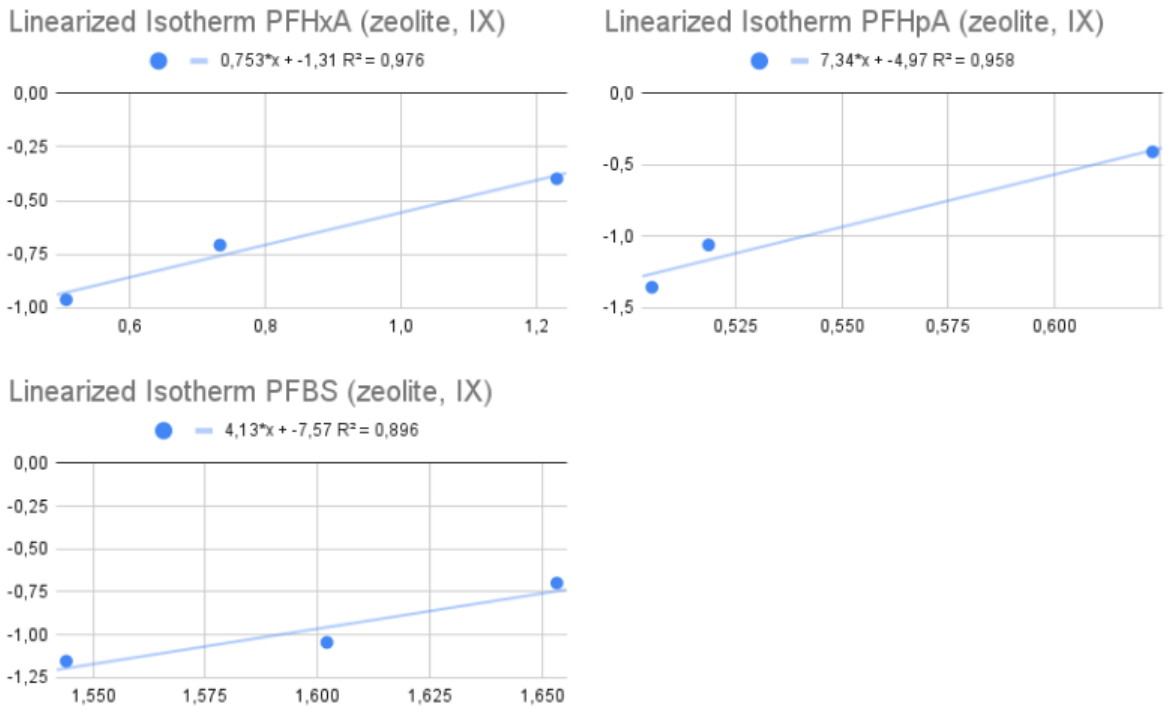

Figure C.4: Linear isotherm graphs for IX waste stream treated with all-silica BEA zeolites for PFAS removal. Isotherms were only made for PFAS with three data points.

D

Python codes

Cost estimation adsorber filters

Listing D.1: Python code: cost estimation DEXSORB+ adsorber filter.

```
import matplotlib.pyplot as plt
import numpy as np

#NF concentrate treated with DEX

#PFOA:
c0 = 300  # PFAS inlet concentration (in ng/L) #PEQ (PFOA EQUIVALENT CONC.)
Kf = 0.1857 #(ng/mg)*(L/ng)*n
n = 1 #[-]
qe = Kf*c0**n #ng/mg


#DEXSORB+
rho_B = 400 #kg/m3  # kg/m3 Bulk density filter bed
#Variable:
EBCT = np.linspace(0, 0.3, 10)  #hours

#reactor:
Q = 1998 #m3/h (17.5*10^6 m3/year)
V = EBCT*Q
tb = (qe * EBCT * rho_B*1000) / (c0)

#COSTS
CC = (15 * rho_B ) #euros/kg DEX*kg/m3 = euro/m3 DEXSORB+
RC = (2/3 * 2000 + 1/3*2.5 + 0.5*0.45)*3*223 #euros/regeneration cycle
#cyclopure states 3BV of regeneration solution is required for regeneration of the DEXSORB+
#223 is the mean filter volume
#ethanol-water (2:1) + 0.5 kg/m3 potassium sulfate
#ethanol prijs €2000/m3 (density ethanol)
#water: 2.5 euros/m3
#potassium sulfate: €0.45/kg and required dose: 0.5 kg/m3


#Construction cost function
def construction_cost(EBCT):
    return CC * EBCT * Q # Costs per volume x volume = costs


#Regeneration cost function
def regeneration_cost(EBCT):
    return (356*24)/(qe * EBCT * rho_B*1000/(c0))*RC#€

#overall cost function
def overall_cost(construction_cost, regeneration_cost):
    return construction_cost + regeneration_costs

```

```

#Construction costs calculation
construction_costs = construction_cost(EBCT)

#Regeneration costs calculation
regeneration_costs = regeneration_cost(EBCT)

#Overall costs calculation
overall_costs = overall_cost(construction_costs, regeneration_costs)

# Plotting
plt.plot(EBCT*60, construction_costs, color='cyan', label='Construction Costs')
plt.plot(EBCT*60, regeneration_costs, color='green', label='Regeneration Costs')
plt.plot(EBCT*60, overall_costs, color='magenta', label='Overall Costs')

plt.xlabel('EBCT (minutes)')
plt.ylabel('Cost €()')
plt.title('Costs vs EBCT (DEX+ filter on NF conc.)')
plt.legend()

plt.show()



# Find the the minimum overall cost
min_index = np.argmin(overall_costs)

# Get the corresponding EBCT value and breakthrough time
min_ebct = round(EBCT[min_index], 2)
min_tb = round(tb[min_index], 2)


# Get the corresponding overall costs, regeneration costs, and construction costs
min_overall_costs = round(overall_costs[min_index], 2)
min_regeneration_costs = round(regeneration_costs[min_index], 2)
min_construction_costs = round(construction_costs[min_index], 2)



print("Breakthrough time at the minimum overall cost:", min_tb/(24*30), "months")

print("EBCT at the minimum overall cost:", min_ebct*60, "minutes" )
print("Overall Costs for the minimum EBCT:", min_overall_costs)
print("Regeneration Costs for the minimum EBCT:", min_regeneration_costs, "for one year")
print("Construction Costs for the minimum EBCT:", min_construction_costs)
```

Listing D.2: Python code: cost estimation all-silica BEA zeolite adsorber filter.

```

import matplotlib.pyplot as plt
import numpy as np

#NF concentrate treated with zeo

#PFHpA:
c0 = 300   # PFAS inlet concentration (in ng/L) #PEQ (PFOA EQUIVALENT CONC.)
Kf = 0.409 #(ng/mg)*(L/ng)*n
n = 0.643 #[-]
qe = Kf*c0**n #ng/mg

#All-silica BEA zeolites
rho_B = 800 #kg/m3  # kg/m3 Bulk density filter bed
#Variable:
EBCT = np.linspace(0, 0.3, 10)  #hours

#reactor:
Q = 1998 #m3/h (6132 m3/year)
V = EBCT*Q

mPFAS = c0*Q*24*365 #
mZEO = mPFAS/(qe/1000)/rho_B
```

```

#COSTS
CC = (47 * rho_B )#euros/kg DEX  * kg/m3 = euro/m3 DEXSORB+
RC = (2/3 * 2000 + 1/3*2.5 + 0.5*0.45)*3*400 #euros/regeneration cycle/year
#cyclopure states 3BV of regeneration solution is required for regeneration of the DEXSORB+, assumed same for zeo
#400 is the mean filter volume
#ethanol-water (2:1) + 0.5 kg/m3 potassium sulfate
#ethanol prijs €2000/m3 (density ethanol)
#water: 2.5 euros/m3
#potassium sulfate: €0.45/kg and required dose: 0.5 kg/m3
tb = (qe * EBCT * Q * rho_B*1000) / (Q * c0)

#Construction cost function
def construction_cost(EBCT):
    return CC * EBCT * Q # Costs per volume x volume = costs


#Regeneration cost function
def regeneration_cost(EBCT):
    return (356*24)/(qe * EBCT * rho_B*1000/(c0))*RC#€

#overall cost function
def overall_cost(construction_cost, regeneration_cost):
    return construction_cost + regeneration_costs

#Construction costs calculation
construction_costs = construction_cost(EBCT)

#Regeneration costs calculation
regeneration_costs = regeneration_cost(EBCT)

#Overall costs calculation
overall_costs = overall_cost(construction_costs, regeneration_costs)

# Plotting
plt.plot(EBCT*60, construction_costs, color='cyan', label='Construction Costs')
plt.plot(EBCT*60, regeneration_costs, color='green', label='Regeneration Costs')
plt.plot(EBCT*60, overall_costs, color='magenta', label='Overall Costs')

plt.xlabel('EBCT (minutes)')
plt.ylabel('Cost €()')
plt.title('Costs vs EBCT (ß-Zeo filter on NF conc.)')
plt.legend()

plt.show()


# Find the index of the minimum overall cost
min_index = np.argmin(overall_costs)

# Get the corresponding EBCT value and breakthrough time
min_ebct = round(EBCT[min_index], 2)
min_tb = round(tb[min_index], 2)

# Get the corresponding overall costs, regeneration costs, and construction costs
min_overall_costs = round(overall_costs[min_index], 2)
min_regeneration_costs = round(regeneration_costs[min_index], 2)
min_construction_costs = round(construction_costs[min_index], 2)

print("volume zeo required", mZEO)

print("Breakthrough time at the minimum overall cost:", min_tb/(24*30), "months")
print("EBCT at the minimum overall cost:", min_ebct*60, "minutes" )
print("Overall Costs for the minimum EBCT:", min_overall_costs)
print("Regeneration Costs for the minimum EBCT:", min_regeneration_costs, "for one year")
print("Construction Costs for the minimum EBCT:", min_construction_costs)
```

E

Results: individual PFAS types

The tables E.1, E.2, E.3, E.4, E.5, E.6, E.7 show the PFAS removal efficiencies from both waste streams with each laboratory tested concentration technology for each individual PFAS type.

Table E.1: IX brine solution treated with all-silica BEA zeolites with dose 20, 100, and 200 mg/L. *GenX removal efficiency between dose 20 mg/L and 200 mg/L

	c_0	c_e (20 mg/L)	c_e (100 mg/L)	c_e (200 mg/L)	PFAS RE% for dose 200 mg/L
PFBA	10	12	10	11	-10%
PFPeA	57	64	56	52	9%
PFHxA	25	17	5.4	3.2	87%
PFHpA	12	4.2	3.3	3.2	73%
PFOA	7.6	0.92	0.87	<0.50	100%
GenX*	0.58	8.5	7.8	7	8.2%
PFBS	49	45	40	35	29%
PFHxS	5.1	<0.20	<0.20	<0.20	100%
PFOS	4.6	0.35	<0.20	<0.20	100%
PFPeS	1.3	0.47	<0.20	<0.20	100%
PFHpS	0.24	<0.20	<0.20	<0.20	100%

Table E.2: IX brine solution treated with DEXSORB+ with dose 10, 50, and 100 mg/L. *GenX removal efficiency between dose 10 mg/L and 50 mg/L

	c_0	c_e (10 mg/L)	c_e (50 mg/L)	c_e (100 mg/L)	PFAS RE% for dose 50 mg/L
PFBA	10	8.3	6	10	40%
PFPeA	57	40	23	35	59.7%
PFHxA	25	26	12	16	52%
PFHpA	12	11	4.6	4.3	61.7%
PFOA	7.6	6.4	1.4	1.9	81.6%
GenX*	0.58	7.5	4.6	8.1	38.7%
PFBS	49	42	14	16	71.4%
PFHxS	5.1	2.2	0.26	0.32	94.9%
PFOS	4.6	0.85	<0.20	0.30	99%
PFPeS	1.3	0.68	<0.20	<0.20	99%
PFHpS	0.24	<0.20	<0.20	<0.20	99%

Table E.3: IX brine solution treated with FF.

	c_0	c_e	PFAS RE%
PFBA	10	19	-90%
PFPeA	57	47	17.5%
PFHxA	25	14	44%
PFHpA	12	11	8.33%
PFOA	7.6	<0.20	99%
GenX*	0.58	<	%
PFBS	49	31	36.7%
PFHxS	5.1	<	%
PFOS	4.6	<0.20	99%
PFPeS	1.3	<0.20	99%
PFHpS	0.24	<0.20	99%

Table E.4: NF concentrate treated with all-silica BEA zeolites with dose 20, 100, and 200 mg/L. *GenX removal efficiency between dose 20 mg/L and 200 mg/L

	c_0	c_e (20 mg/L)	c_e (100 mg/L)	c_e (200 mg/L)	PFAS RE% for dose 200 mg/L
PFBA	31	19	16	15	52%
PFPeA	48	58	40	43	10.4%
PFHxA	55	50	12	6.3	89%
PFHpA	25	4.4	0.31	0.22	99%
PFOA	61	2.5	1.2	0.83	99%
PFNA	2.6				99%
PFDA	2.6				99%
GenX*	23	33	25	22	33.3%
PFBS	36	36	29	27	25%
PFHxS	7.8	1.5	0.27	<0.20	99%
PFOS	8.9	<0.20	<0.20	<0.20	99%
PFPeS	1.8	1.5	0.31	0.20	89%
PFHpS	0.34	<0.20	<0.20	<0.20	99%

Table E.5: NF concentrate treated with DEXSORB+ with dose 10, 50, and 100 mg/L. *GenX removal efficiency between dose 10 mg/L and 100 mg/L

	c_0	c_e (10 mg/L)	c_e (50 mg/L)	c_e (100 mg/L)	PFAS RE% for dose 100 mg/L
PFBA	31	17	16	15	52%
PFPeA	48	42	42	39	18.8%
PFHxA	55	52	30	20	63.6%
PFHpA	25	15	5.9	3.2	87%
PFOA	61	20	6.2	2.9	95%
PFNA	2.6	0.71	<0.50	<0.50	99%
PFDA	2.6	<0.50	<0.50	<0.50	99%
GenX*	23	27	25	21	22.2%
PFBS	36	23	8.2	5	86%
PFHxS	7.8	1.2	0.25	<0.20	99%
PFOS	8.9	0.50	<0.20	<0.20	99%
PFPeS	1.8	0.73	<0.20	<0.20	99%
PFHpS	0.34	<0.20	<0.20	<0.20	99%

Table E.6: NF concentrate treated with FF (pressurised air)

	c_0	c_e	PFAS RE% for dose 100 mg/L
PFBA	31	29	6.5%
PFPeA	48	25	48%
PFHxA	55	7.1	87%
PFHpA	25	2.5	90%
PFOA	61	4.9	92%
PFNA	2.6	0.2	92%
PFDA	2.6	0.2	80%
GenX*	23	2.1	91%
PFBS	36	2.6	93%
PFHxS	7.8	0.2	97%
PFOS	8.9	0.20	98%
PFPeS	1.8	<0.20	99%
PFHpS	0.34	<0.20	99%

Table E.7: NF concentrate DAF with FF (pressurised water)

	c_0	c_e	PFAS RE% for dose 100 mg/L
PFBA	31	27	12.5%
PFPeA	48	37	23%
PFHxA	55	32	42%
PFHpA	25	10	60%
PFOA	61	18	70.5%
PFNA	2.6	0.51	80.4%
PFDA	2.6	<0.2	99%
GenX*	23	12	48%
PFBS	36	13	64%
PFHxS	7.8	1	87%
PFOS	8.9	0.25	97%
PFPeS	1.8	0.53	70.6%
PFHpS	0.34	<0.20	99%